Increased Hexosamine Biosynthetic Pathway Flux Impairs Myocardial GLUT4 Translocation

By
Gordon Williams

Thesis presented in partial fulfillment of the degree of Masters of Physiological Sciences at the University of Stellenbosch

Supervisor: Prof. M. Faadiel Essop

January 2009

Declaration

I, Gordon Williams, hereby declare that this thesis is my own original work and that all sources have been accurately reported and acknowledged, and that this document has not previously been submitted at any university in order to obtain an academic qualification.

Signature : _____

Date : _____

Abstract

Aims and Background: According to the World Health Organization type 2 diabetes will constitute a major global burden of disease within the next few decades. In agreement, reports show that rapid urbanization and lifestyle changes in South Africa are major factors responsible for these projections. Therefore, any perturbations that alter the regulatory steps that control myocardial glucose uptake by the cardiac-enrich glucose transporter, GLUT4, will lead in the development of diabetic cardiomyopathy and cardiac hypertrophy. Although considerable efforts are been put into unraveling molecular mechanisms underlying this process, less is known regarding the spatio-temporal regulation of GLUT4. In light of this, our specific aim was to establish *in vitro* fluorescence microscopy- and flow cytometry-based models for visualization and assessment of myocardial GLUT4 translocation using H9c2 cardiac-derived myoblasts. After successful establishment of our *in vitro*-based model for myocardial GLUT4 translocation, our second aim was to determine the role of the hexosamine biosynthetic pathway (HBP) in this process. Here, we employed HBP modulators to alter flux and subsequently evaluate its effect on myocardial GLUT4 translocation. To further strengthen our hypothesis, we also investigated the role of the HBP in hearts of an *in vivo* type 2 diabetes mouse model.

Hypothesis: We hypothesize that increased flux through the HBP impairs myocardial GLUT4 translocation by greater O-linked glycosylation of the insulin signaling pathway, ultimately leading to myocardial insulin resistance.

Methods: Rat cardiac-derived H9c2 myoblasts were cultured until ~ 80-90 % confluent for 3 days and thereafter subcultured in Lab-Tek chamber slides (~ 15, 000 cells per well) for 24 hours. Cells were then serum starved for 3 hours by insulin administration of 100 nM for 0, 5 and 30 minutes, respectively. We employed a method to quantify the relative proportion of GLUT4 at the sarcolemma using immunofluorescence microscopy- and flow cytometry-based models for visualization and assessment of myocardial GLUT4 translocation. Using these methods we investigated the role HBP have during GLUT4 translocation. The HBP were then activated through the following: a) high glucose and glutamine concentrations; b) low glucose and glucosamine stimulation; and c) over-expression of the HBP rate-limiting enzyme, i.e. GFAT. Subsequently, cardiac-derived myoblasts were fixed and probed for ~ 24 hours with antibodies specific for intracellular- and membrane-bound GLUT4, anti-myc GLUT4 (9E10) and O-GlcNAc. To assess GLUT4 translocation and O-GlcNAcylation we employed the following secondary antibodies: FITC Green for intracellular-bound GLUT4; and b) Texas Red for membrane-bound GLUT4 (immunofluorescence microscopy) and Phycoerythrin for flow cytometry-based model. Cells were thereafter viewed by multi-dimension imaging using an inverted system microscope (Olympus IX81) and a BD FACS Aria cell sorter for flow cytometric analysis. We also assessed HBP in an *in vivo* context by probing heart tissue - from insulin resistant db/db mice - with a GFAT monoclonal antibody.

Results: The db/db mouse represents an ideal model to confirm our hypothesis in an *in vivo* context. In agreement, our preliminary results show increased GFAT expression versus heterozygous db/+ controls. Our *in vitro* model show myocardial GLUT4 translocation at 5 minute peak response when H9c2 cardiac-derived myoblasts were stimulated with 100 nM insulin, and GLUT4 vesicles return to normal after longer insulin stimulatory times (10, 15 and 30 minutes. Myocardial Glut4

translocation was impaired when cells were stimulated with 100 nM wortmannin. Our transfection based model (immunofluorescence microscopy- and flow cytometry-based models) confirms 5 minute peak response under real time conditions. High glucose concentration (25 mM glucose), glucosamine concentrations (2.5 mM, 5 mM, and 10 mM) and over-expression of GFAT led to an impairment of myocardial GLUT4 translocation. Employment of an HBP activator (50 μM PUGNAc) also caused impairment of myocardial GLUT4 translocation. Myocardial GLUT4 translocation was restored when cells were treated with an HBP inhibitor (40 μM DON). High glucose concentrations (25 mM glucose), glucosamine concentrations (2.5 mM, 5 mM, and 10 mM) and over-expression of GFAT resulted in an increase in O-GlcNAcylation. HBP activation (50 μM PUGNAc) showed an increase in O-GlcNAcylation, while administration of 40 μM DON reversed this effect.

Discussion and conclusion: We successfully established an *in vitro* experimental system to assay myocardial GLUT4 translocation. Our data show that dysregulated flux through the HBP impairs myocardial GLUT4 translocation. It is likely that the HBP becomes dysregulated during the pre-diabetic/early diabetic state and that O-GlcNAcylation of members of the insulin signaling pathway occurs during this stage. This will lead to myocardial insulin resistance, and in the long term, will contribute to the onset of the diabetic cardiomyopathy. Investigations to find unique inhibitors of this maladaptive pathway should therefore result in the development of novel therapeutic agents that will lead to a reduction in the growing global burden of disease for type 2 diabetes and associated cardiovascular diseases.

Opsomming

Doelwitte en agtergrond: Volgens die Wêreld Gesondheidsorganisasie sal tipe 2 diabetes ‘n groot deel uitmaak van siekte wêreldwyd binne die volgende paar dekades. Ooreenkomstig toon navorsing dat versnelde verwestering en lewenstyl veranderinge in Suid Afrika hooffaktore is wat verantwoordelik kan wees vir hierdie projeksies. Dus, enige versteurings wat die regulatoriese stappe om miokardiale glukose opname kan wysig te beheer deur die kardiale-ryke glukose draer, GLUT 4, aanleiding kan gee tot die ontwikkeling van diabetiese kardiomiopatie en kardiale hipertrofie. Alhoewel verskeie pogings aangewend is om die molekulêre weg te ontsyfer in hierdie onderliggende prosesse, is weinig bekend in die “spatio-temporale” regulering van GLUT 4. In die lig hiervan, is ons spesifieke doelstelling om *in vitro* fluoresensie mikroskopie- en vloeisitometriesgebaseerde modelle vir die visualisering en evaluering van miokardiale GLUT 4 translokasie, deur van afgestamde hartmioblaste H9c2 gebruik te maak. Na suksesvolle vestiging van ons *in vitro* gebaseerde model vir miokardiale GLUT 4 translokasie, is ons tweede doelwit om die rol van die heksosamienbiosinteseweg (HBW) in hierdie proses te bepaal. Hier is HBW, moduleerders met die doel om fluks te wysig, en gevolglik die effek op miokardiale GLUT 4 translokasie te evalueer. Om die hipotese verder te versterk, het ons ook die rol van HBW in harte van ‘n *in vivo* tipe 2 diabetes muismodel ondersoek.

Hipotese: Ons hipotetiseer dat verhoogde fluks deur die HBW, miokardiale GLUT 4 translokasie inperk deur verhoogde O-gebonde glikosilering van die insulienweg, wat uiteindelik tot miokardiale insuilienweerstand lei.

Metodes: Rothartmioblaste, H9c2, is gekweek to ~80-90% konfluensie vir drie dae en daarna sub-gekweek in Lab-Tek kamerskyfies (~15 000 selle per kamer) vir 24 uur. Die selle is gevolglik vir drie uur serumverhonger deur 100nM insulien vir 0.5 en 30 minute onderskeidelik toe te dien. Ons het ‘n metode aangewend om die relatiewe deel van GLUT 4 by die sarkolemma te visualiseer en te evalueer deur van immunofluoresensie mikroskopie en vloeisitometrie modelle gebruik te maak. Deur hierdie metodes te gebruik, het ons die rol van HBW tydens GLUT 4 translokasie ondersoek. Die HBW is gevolglik geaktiveer soos volg: a) hoë glukose- en glutamienkonsentrasies; b) lae glukose en glukosamienstimulering; en c) ooruitdrukking van die HBW tempo beperkende ensiem i.e. GFAT. Gevolglik is hartmioblaste gefikseer en vir 24 uur ondersoek met spesifike teenliggame vir

intrasellulêre en membraangebonde GLUT 4, anti-myc GLUT 4 (9E10) en O-GlcNAc. Om GLUT 4 translokasie en O-GluNAc te evalueer het ons die volgende sekondêre teenliggame gebruik: a) FITC groen vir intrasellulêrgebonde GLUT 4; b) Texas rooi vir membraangebonde GLUT 4 (immunofluoresensie mikroskopie) en c) phycoerythrin vir die vloeisitometriegebaseerde model.

Selle is na afloop deur multi-dimensionele beelding ondersoek met behulp van ‘n omgekeerde mikroskoopsisteem (OlympusIX81) en ‘n BD FACS Aria selsorteerder vir vloeisitometrie analise. Ons het verder HBW evalueer in ‘n *in vivo* konteks deur hartweefsel te ondersoek – van insulienweerstandige db/db muise – met ‘n GFAT monoklonale teenliggaam.

Resultate: Die db/db muis verteenwoordig ‘n ideale model om ons hipotese in ‘n *in vivo* konteks te bevestig. Ons voorlopige resultate toon ‘n verhoogde GFAT uitdrukking teenoor heterosigotiese db/+ kontrole. Ons *in vitro* model toon miokardiale GLUT 4 translokasie by 5 minute piekrespons wanneer H9c2 hartmioblaste met 100nM insulin gestimuleer is, en GLUT 4 vesikels terugkeer na normaal na langer insulien stimulasie intervalle (10, 15 en 30 minute). Miokardiale GLUT 4 translokasie is ingeperk wanneer die selle met 100nM wortmannin gestimuleer is. Ons transfeksie gebaseerde model (immunofluoresensie mikroskopie en vloeisitometriese modelle) bevestig die 5 minuut piekrepsons onder ware tydstip toestande. Hoë glukosekonsentrasie (25mM glukose), glukosamienkonsentrasie (2.5mM, 5mM en 10mM) en ooruitdrukking van GFAT het tot ‘n vertraging in miokardiale GLUT 4 translokasie gelei. Die gebruik van ‘n HBW (50µM PUGNAc) het ook vertraging van miokardiale GLUT 4 translokasie gelei. Miokardiale GLUT 4 translokasie is herstel na selle met ‘n HBW inhibeerder (40uM DON) behandel is. Hoë glukosekonsentrasie (25mM glukose), glukosamienkonsentrasie (2.5mM, 5mM en 10mM) en ooruitdrukking van GFAT het tot ‘n toename in O-GlycNAsiellering gelei. HBW aktivering (50µM PUCNAc) het ‘n toename in O-GlcNAsiellering getoon terwyl 40µM DON toediening hierdie effek omgekeer het.

Bespreking en gevolgtrekking: Ons het suksesvol ‘n *in vitro* eksperimentele stelsel om miokardiale GLUT 4 translokasie aan te toon, beskryf. Ons data toon disregulerende fluks deur die HBW lei tot miokardiale inperking van GLUT 4 translokasie. Dit is moontlik dat die HBW disregulerend raak tydens die pre-diabetiese/vroeë diabetiese toestand en dat die O-GlcNAsiellering van lede van die insulienseinweg tydens hierdie stadium onstaan. Dit het miokardiale insulienweerstand tot gevolg en op die langtermyn kan dit bydra tot die ontwikkeling

van diabetiese kardiomiopatie. Ondersoek om unieke inhibeerders van hierdie wanaanpassingsweg te vind behoort daartoe te lei dat nuwe terapeutiese middels ontwikkel kan word wat sal lei tot ‘n verlaging in die groeiende wêreldlas van siekte vir tipe 2 diabetes en geassosieërde kardiovaskulêre siektes.

Acknowledgements

I first off all would like to thank the LORD Jesus Christ for His strength, knowledge and wisdom to allow me to do this project. I specially thank Him for giving me the passion not just for this project, but for pursuing my life time dream that is now firmly in sight.

Special thanks to my grand parents for passing your life experiences torches onto me. Special thanks to my late grandfather who taught me that nothing is impossible and to take the‘t’ of the word ‘’can’t’’ and shaft it elsewhere to form the word ‘’can’’. To my brother Vincent Harris Williams thanks for comradeship, brotherly love and sometimes for just being a father figure to me. To my immediate family Evellyn Louw (mother), Charlene (sister) and Mario (brother), special thanks for your love and patience.

My sincere thanks to my best friend, companion, and rock of life, Mrs Diana Williams - for your patience, perseverance, attitude and your soft and gentle spirit. Thank you for being the best wife any man would dare to have.

Also special thanks to the following people: the late true prophet of the LORD, Oom Dawid Tieties, Simon Lepedi (prophet), the late Maria Lehman, Pastor Lehman, Pastor Phielander, the late Aunty Nella (prophetess), Pastor Barker and his wife, special women prayer groups in Mitchells Plain (women with a vision), Bishop Lavis, Upington, Athlone, Pastor Morkel and wife, and finally Pastor Pieter Stevenson and his wife for passing your spiritual torches onto me.

Special thanks to the following people who played an important role during my academic career: Mrs Jansen (Grade 1 teacher), Mr. Marshall (Grade 6 teacher), Mr. LC De Wet (Grade 12 teacher), Prof. Jan Persens (UWC), Prof. Loyiso Nongxa (Wits), Prof. Mervin Shear (Wits), Prof. Harneker (UWC), Prof. Johnson (UWC), Prof. Gerard v/d Horst (UWC), and the late Prof. Cedric Wannenburg (UCT) for passing your academic torches onto me.

Finally, thanks to Stellenbosch academic staff and non academic staff (Katriena Martin and Johnifer Isaacs) for making this manuscript possible. My sincere thanks to Benjamin Loos for your patience and time to make these beautiful fluorescence microscopy images a possibility. I definitely will miss the Friday morning sessions in the Live Cell Imaging Lab, especially the non academic discussions we also had.

Special thanks to the Essop Cardiometabolic Research Group for your academic input. Here, I would like to thank Mrs Urthra Rajamani for spicing my life up with endless conversations and support. To Dr. James Meiring special thanks for assisting with this thesis and for being a positive role model in my life. I will definitely miss your sincere friendship. Thanks to Dr Theo Nell for editing and helpful advice.

Finally, my sincere gratitude to a life-changing friend, leader, teacher, supervisor, role model and father figure who taught me that the true value of a great team player is to sacrifice yourself for the good of the team - Prof. Mohammed Faadiel Essop. Remember Prof, you do not meet people through consequences in life, but rather through divine appointments.

Remember he who wants to succeed in life, should learn how to fight, strive, and (most importantly) how to suffer, because only through suffering will one know the true meaning of the word ***happiness****, which is an indescribable inner peace that cannot be bought or found in any text books.*

Table of Index

List of Tables and Figures

Chapter 1

Chapter 1

Introduction

1. Epidemiology

The prevalence of type 2 diabetes and obesity has rapidly increased and remain a large and global health concern (Fig. 1; Seidell *et al.,* 2002; Passa *et al.,* 2002; Riste *et al.,* 2001; Engelgau *et al.,* 2004; Strumpf *et al.,* 2004). It is estimated that the world wide incidence of diabetes will increase from 135 million in 1995 to 300 million by 2025 (King *et al.,* 1998). In agreement, the World Health Organization estimates that ~ 366 million people will be afflicted with diabetes by 2030 (Garcia *et al.,* 1974). Insulin resistance is the essential etiological factor of both type 2 diabetes and obesity and is the common denominator of multiple diseases in Western societies (Reaven 1988; DeFronzo 1991). For example, cardiovascular diseases are the major cause of death for obese/type 2 diabetic individuals (Wild *et al.,* 2004).

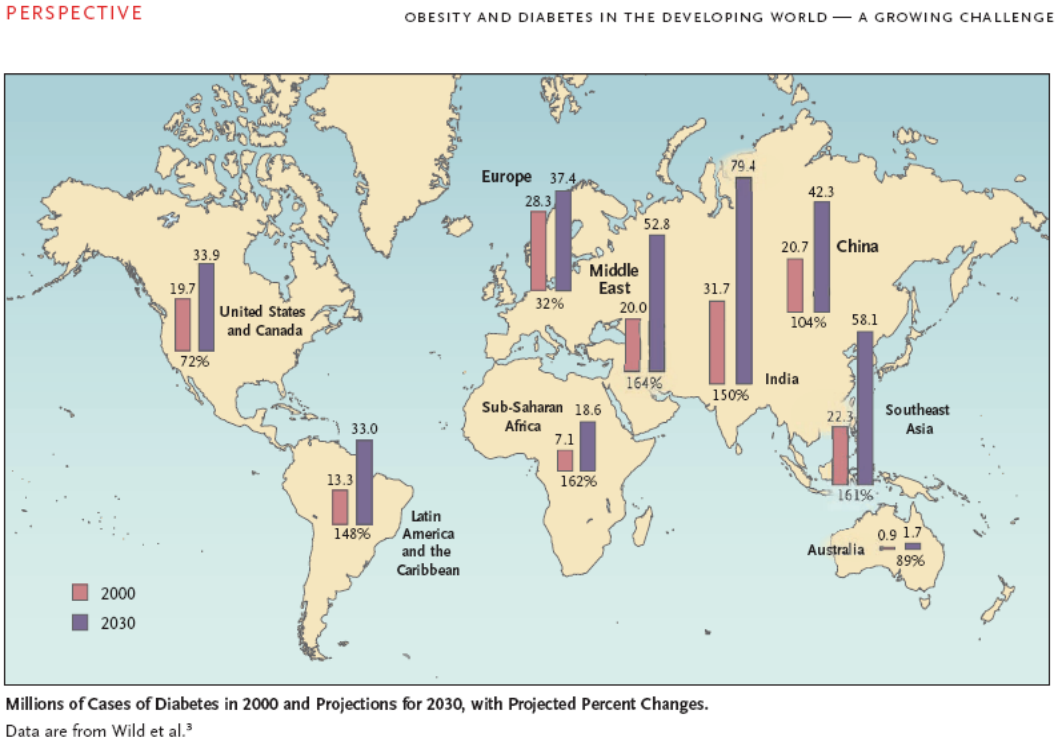

Figure 1: Schematic representation of the number of reported cases world wide and its projections until 2030 (from Wild et al., 2004).

2. The phenomenon of insulin resistance

Insulin resistance was first described in the 1930's when Himsworth (1936) described diabetic patients who did not respond to insulin treatment. Insulin resistance is defined as the state of reduced responsiveness to normal circulating levels of insulin (Kahn 1978). This is distinct from clinical insulin resistance that is defined as the reduced ability of insulin to lower plasma glucose (Maria Buse G. 2006). Although insulin resistance is well characterized, the underlying mechanisms driving this phenomenon are poorly understood.

It is well established that chronic exposure of plasma fuel substrates such as glucose and lipids can lead to cellular insulin resistance. This includes chronic hyperglycemia, characterized by “glucose toxicity”, and chronic hyperlipidemia characterized by “lipotoxicity” (Rossetti *et al.,* 1990; Yki-Jarvinen *et al.,* 1987). Insulin resistance is usually associated with decreased glucose transport, abnormalities in insulin signaling and an increase in intramyocellular triglycerides (Shulman 2000; Ruderman 2006). Moreover, it is coupled with impaired insulin action on both glucose transport and intracellular glucose metabolism (Garvey 1992; Freymond *et al.,* 1988; Beck-Nielsen *et al.,* 1992). Ruderman (2006) proposes that insulin resistance and related intracellular dysfunction develop when long chain fatty acyl-CoAs (LCFA-CoA) accumulate in the cytosol. This leads to an increase in diacylglycerol (DAG), a fatty acid derivative, and subsequent activation of protein kinases e.g. PKCβ, PKCδ, PKCθ and nuclear factor-κB (NF-κB; Itani *et al.,* 2002). Moreover, increased triglycerides, ceramide and oxidative stress, are all implicated in the onset of insulin resistance (Itani *et al.,* 2002). However, insulin resistance may also happen in the absence of increased intracellular LCFA-CoAs and is accompanied by alterations in lipid metabolism (Burant *et al.,* 1984; Heydrick *et al.,* 1991). Since the focus of my thesis is on impaired insulin-mediated glucose transport, I will now review some basic aspects of this process.

3. Glucose transport

3.1 Insulin-mediated glucose transport

Glucose transport is the rate limiting step for glucose metabolism in normal glucose-tolerant (Fink *et al.,* 1992; Ki-Jarvinen *et al.,* 1992) and diabetic (Ki-Jarvinen *et al.,* 1992; Butler *et al.,* 1990) individuals. In support, several nuclear magnetic resonance spectroscopy (NMR) studies show that glucose transport is the rate limiting step for glucose metabolism (Cline 1999; Shulman 2000). The question then arises: how does glucose actually enter a cell? Glucose enters cells via two mechanisms:

i) An energy dependent Na^+/glucose co-transporter which is located in polarized epithelial cells in the lumen of the small intestine and in the proximal tubules of the kidney (Fig. 2; 67; 68). Here in the presence of ATP, glucose is pumped against a concentration gradient across the cellular membrane.

ii) Due to the hydrophilic nature of glucose it cannot pass through the lipid bilayer by simple diffusion and requires specific carrier proteins to facilitate its transport into the cytosol. These proteins are known as the glucose transporters (GLUTs; Mueckler 1994; Fig. 2). GLUTs are found in all cell types and are responsible for glucose uptake.

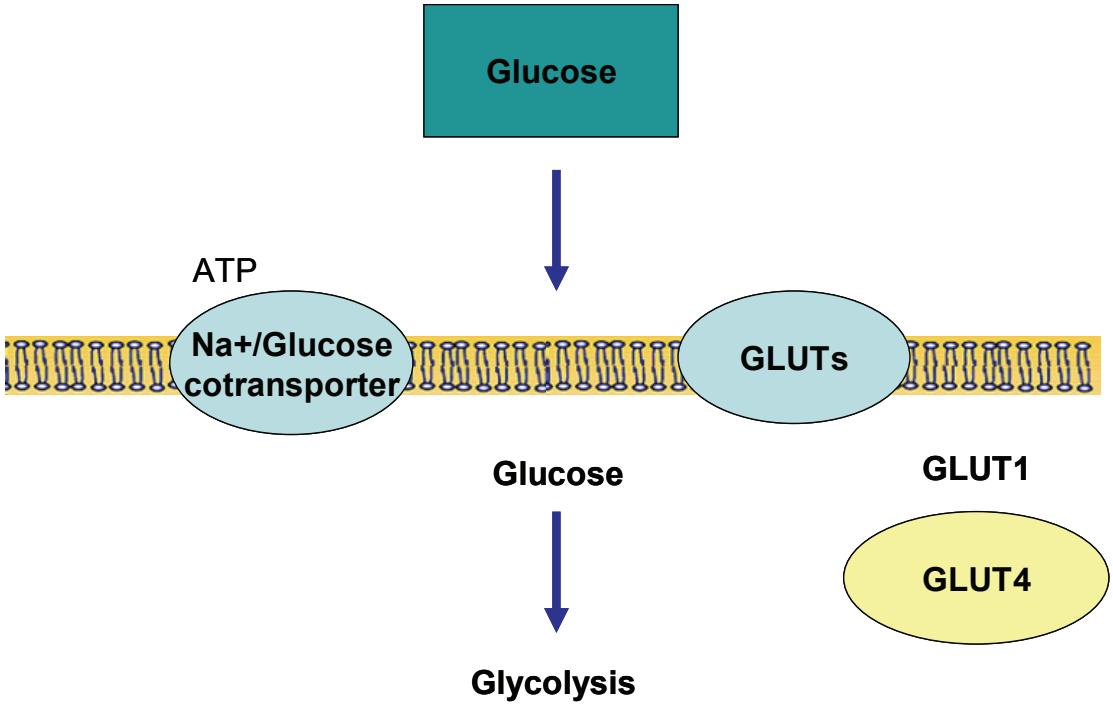

Figure 2. Schematic representation showing the mechanism of entrance of glucose across the lipid bilayer. GLUTs – glucose transporters.

3.2 Glucose transporters (GLUTs)

Glucose transporters (GLUTs) are integral membrane proteins with 12 membrane-spanning-helices that differ in tissue distribution and response to metabolic and hormonal regulation (James *et al.,* 1994; Mueckler 1994; Stephen and Pilch 1995; Fig. 3). Both the N- and C- terminals of the protein structure are predicted to be in the cytoplasm. There are up 13 different GLUT isoforms currently identified (Table 1). GLUT1 is expressed in most tissues and is responsible for the basal uptake of glucose across the lipid bilayer. GLUT4 is the major insulin responsive glucose transporter in muscle, adipose tissue and the heart. Besides GLUT4, a few novel members of the GLUT family have also recently been identified in the heart (GLUT11 and GLUT12; Doege *et al.,* 2001; Rogers *et al.,* 1998).

Isoform	Expression	Function	Function
GLUT1	All tissues (abundant in brain and erythrocytes	Basal uptake	Mueckler *et al.* 1985
GLUT2	Liver, pancreatic islet cells, retina	Glucose sensing	Fukumoto *et al.* 1988 Watanabe *et al.* 1999
GLUT3	Brain	Basal transport and uptake from cerebral fluid	Kayano *et al.* 1988
GLUT4	Muscle, fat, heart	Insulin responsive	Fukumoto *et al.* 1988
GLUT5	Intestine, testis, kidney, erythrocytes	Fructose transport	Kayano *et al.* 1990, Concha *et al.* 1997
GLUT6	Spleen, leukocytes, brain	ND	Doege *et al.* 2000
GLUT7	Liver	Release of glucose from gluconeogenesis from ER	Joost &Thorens 2001
GLUT8	Testis, brain	ND	Doege *et al.* 2000a
GLUT9	Liver, kidney	ND	Phay *et al.* 2000
GLUT10	Liver, pancreas	ND	McVie-Wyli *et al.* 2001
GLUT11	Heart, muscle	ND	Doege *et al.* 2001
GLUT12	Heart, prostate	ND	Rogers *et al.* 1998
GLUT13	Brain	ND	Kayano *et al.* 1990

Table 1. Tissue specific expression of GLUT family. ND–Not determined.

3.3 GLUT4 and insulin resistance

Since GLUT1 and GLUT4 are the most essential GLUTs in response to whole body glucose disposal (Lienhard 1992), our focus for this thesis will be mainly on GLUT4. As described, GLUT4 is an integral membrane protein that consists of a 12-span helix across the cell membrane and plays an essential role in myocardial glucose uptake.

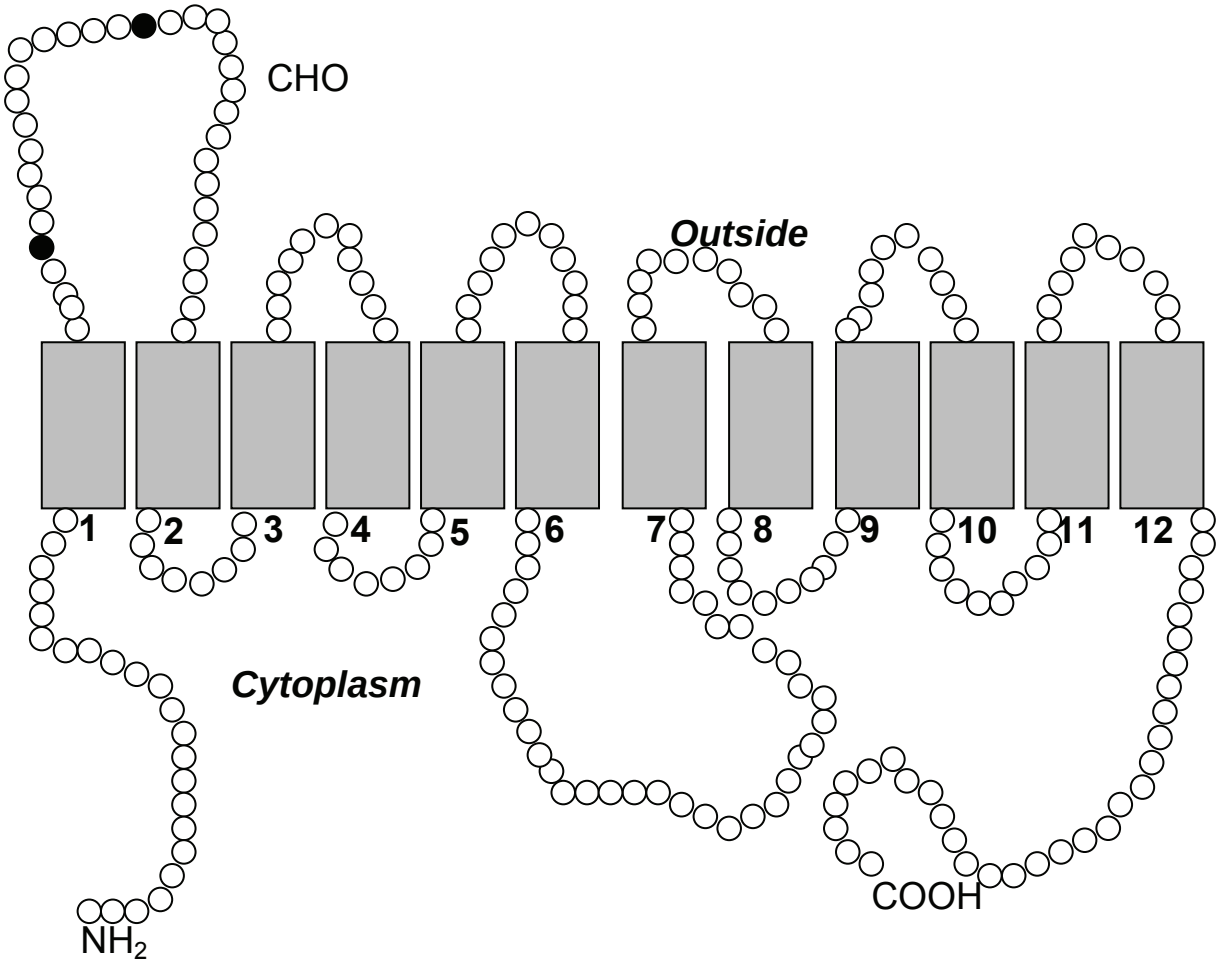

Figure 3. Image portraying the structure of GLUT4 and its possible immunological binding sites. Indicated are the 12 membrane spanning-helices (1-12), the N-terminus (left) and C—terminus (right) both in the cytoplasm (Adapted from Czech et al., 2007).

GLUT4 is an inducible transporter also known as the insulin-responsive transporter. It is highly expressed in the heart, skeletal and adipose tissue (Fukumoto *et al.,* 1988). Before insulin stimulation, GLUT4 proteins are primarily localized to specialized intracellular vesicular compartments known as GLUT4 storage vesicles (GSV) (Stephens and Pilch 1995) (Fig. 4). Embedded in the GSV is an abundant cargo protein termed the insulin responsive amino peptidase (IRAP; Kandror and Pilch 1994; Kandror *et al.,* 1994; Mastick *et al.,* 1994; Keller *et al.,* 1995; Malide *et al.,* 1997; Martin *et al.,* 1997; Ross *et al.,* 1997; Fig. 4). It is essentially the only major cargo constituent of GSV that traffic through the insulin-regulated pathway (Gross *et al.,* 2004). This makes IRAP the only known *bona fide* marker of GSV. In the basal state GLUT4 and IRAP are more intracellular concentrated, while insulin induces a large increase (5-20-fold) in GLUT4 and IRAP at the sarcolemma. The transferrin receptor (TR) is another protein that is also associated with GSV that traffics by the

general recycling pathway, by at most twofold (Zeigerer *et al.,* 2002).The extracellular and transmembrane domains of the TR displays IRAP- and GLUT4-like trafficking in 3T3-L1 adipocytes (Subtil *et al.,* 2000; Fig. 4).

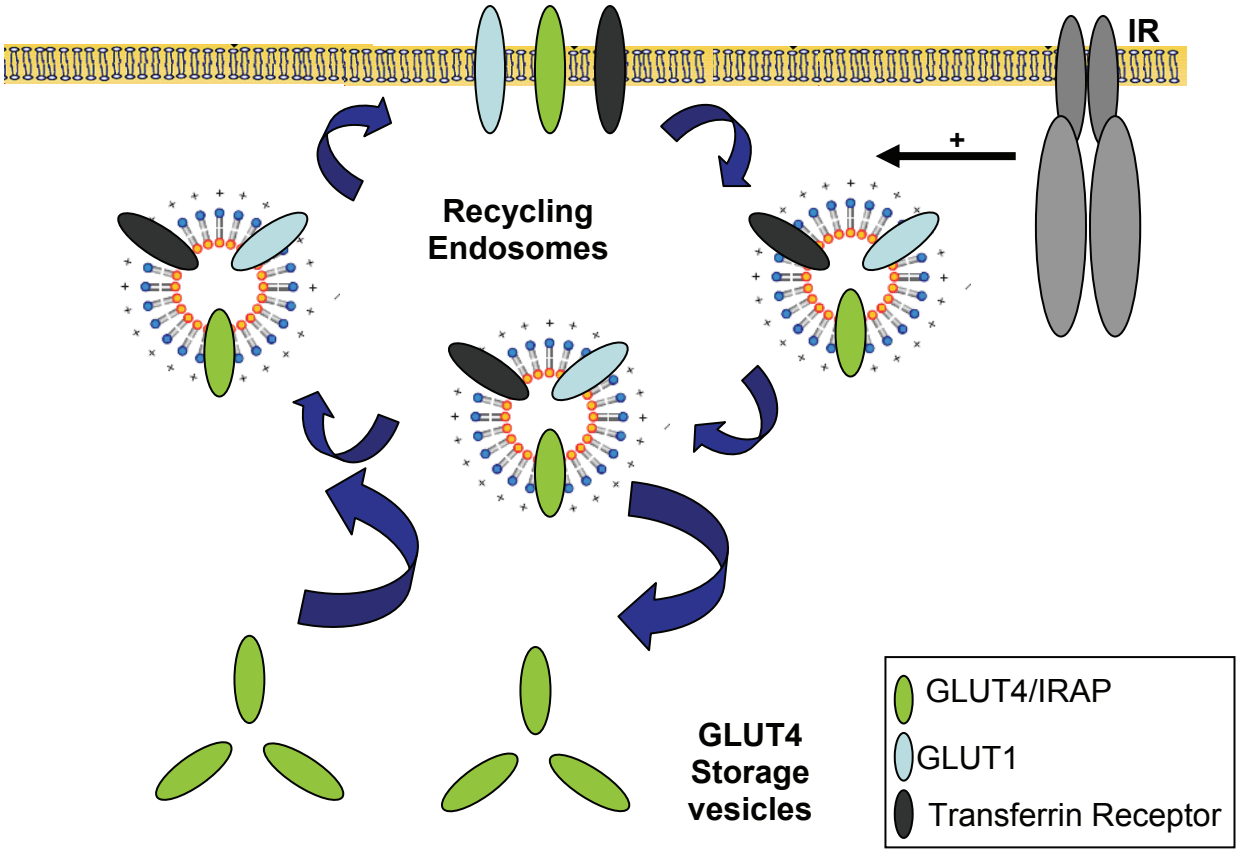

Figure 4. In the resting phase, GLUT4 proteins are primarily localized to specialized intracellular vesicular compartments known as GLUT4 storage vesicles (GSV).Upon insulin stimulation, GLUT4 rapidly translocates from the storage pools to the sarcolemma (Ducluzeau (2002). Both transferrin and IRAP have been associated with GLUT4 translocation (Adapted from Subtil et al., 2000).

The GSV is divided into two pools, i.e. an endosomal compartment that contains TR, and a "specialized" pool that contains GLUT4 and IRAP but is devoid of TR. It is still unclear, however, how GLUT4 is retained within endosomes and specialized pools. Upon insulin stimulation GLUT4 rapidly translocates from cytosolic storage pools to the sarcolemma (Czech and Buxton 1993; Juhn *et al.,* 1992; Satoh *et al.,* 1993; Yang and Holman 1993). However, the mechanism how GLUT4/IRAP compartments and the general endosomal pools operate is still unknown (Elmendorf *et al.,* 1999; Inoue *et al.,* 2003) Semiz *et al.,* 2003). In addition to insulin, numerous other stimuli can also lead to GLUT4 translocation, including hypoxia, ethanol, muscle contraction and myocardial ischemia (Slot *et al.,* 1991; Fischer *et al.,* 1997). Impaired GLUT4 translocation is associated with insulin, obesity and ultimately type 2 diabetes (Stephens and Pilch 1995). For example, both homozygous GLUT4 $^{-/-}$ (Rosetti *et al.,*

1997; Stenbit *et al.,* 1997; Li *et a,l* 2000) and heterozygous GLUT4$^{+/-}$ mice (Tsoa *et al.,* 1999) display insulin resistance. Also, transgenic mice over-expressing GLUT4 in adipose (Shepard *et al.,* 1993) or skeletal muscle tissue (Tsoa *et al.,* 2001) are highly insulin sensitive and glucose tolerant.

3.4 Insulin signaling mechanisms

Insulin binds to the α-subunit of the insulin receptor and activates the tyrosine kinase within the β-subunit. The tyrosine kinase phosphorylates the insulin receptor substrates (IRS) proteins, i.e. IRS1 and IRS2, and phosphotyrosine residues on IRS proteins become good targets for the p85 regulatory subunit of phosphatidylinositol (PI) 3-kinase (Eriksson *et al.,* 1989; Kahn *et al.,* 1989; Sun *et al.,* 1991; Wang *et al.,* 1993; Myers *et al.,* 1994; Sun *et al.,* 1993). The latter catalyzes phosphatidylinositol 4,5 diphosphate into phosphatidylinositol 3,4,5 triphosphate. Downstream regulators such as phosphatidylinositol-dependant kinase (PDK) and protein kinase B (PKB)/AKT have a pleckstrin homology domain that enables these molecules to migrate toward the plasma membrane (Kanai *et al.,* 1994; Okada *et al.,* 1994; Clark *et al.,* 1994; Cheatham *et al.,* 1994; Hara *et al.,* 1994). Here AKT reacts with the intracellular tubulovesicular structures of GLUT4 clustered in the *trans*-Golgi region (Slot *et al.,* 1991), releasing it and causing translocation to the sarcolemma (Lund *et al.,* 1995; Kolter *et al.,* 1992; Fig. 5).

A PI3-kinase independent pathway also mediates GLUT4 translocation (Saltiel and Kahn 2001). Here, insulin receptor activation leads to the phosphorylation of c-Cbl, that is associated with the adaptor c-Cbl associated protein (CAP; Ribon *et al.,* 1998). Following phosphorylation, the c-Cbl-CAP complex translocates to lipid rafts within the plasma membrane. Cbl then reacts with the adaptor protein Crk, that is constitutively associated with the Rho-family guanine nucleotide exchange factor, C3G. C3G in turn activates TC10, a member of the GTP-binding protein family (Chiang *et al.,* 2001).

While the molecular target(s) of TC10 are currently unknown, its activation seems to be required for insulin-stimulated GLUT4 translocation from the GSV pool to the plasma membrane (Fig. 6).

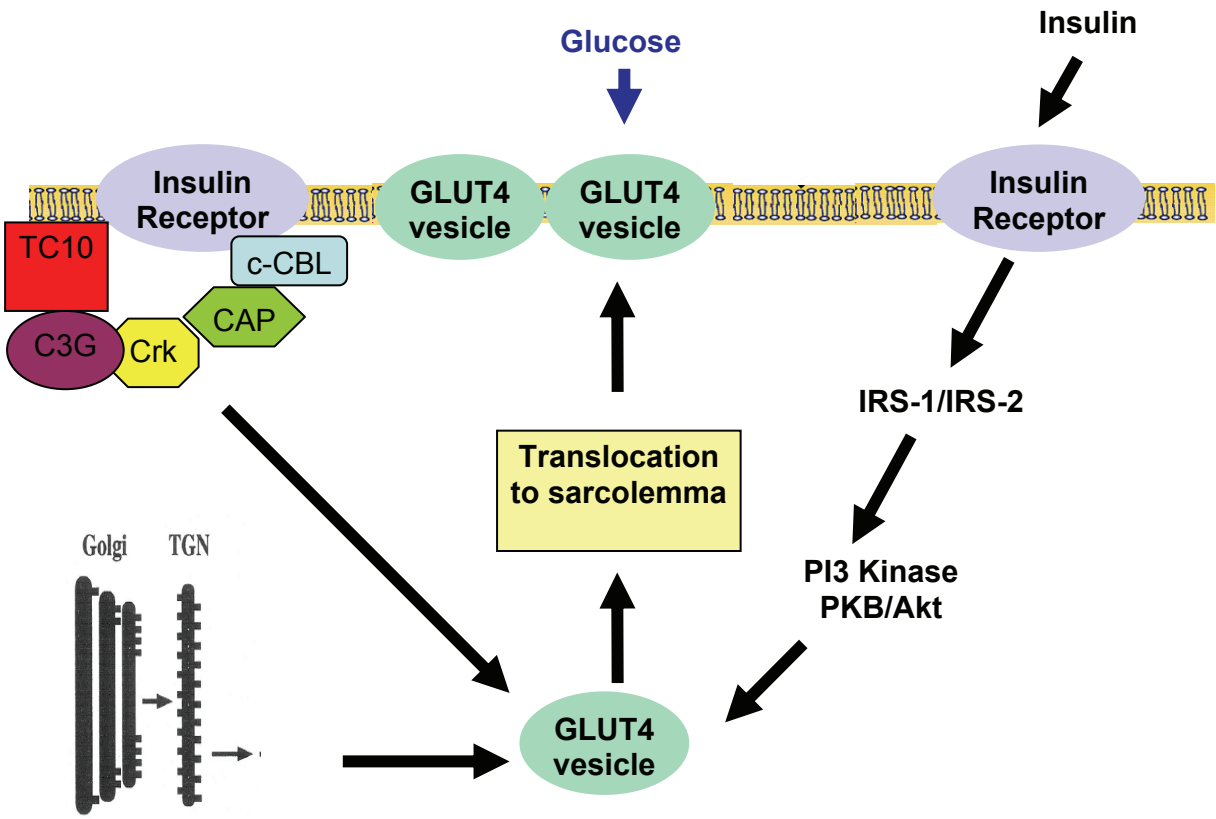

Figure 5. Insulin signaling pathway involving the PI-3 kinase-dependent and PI-3 kinase-independent pathways, leading to GLUT4 translocation. The insert indicates the origin of GLUT4 (Adapted from Sten Lund 2003).

3.5 Non-insulin dependent signaling mechanism

There are other mechanisms that also impact on GLUT4 translocation (Fig. 6). For example, both activation of 5'-AMP activated protein kinase (AMPK) and excitation-contraction of rat cardiomyocytes result in GLUT4 translocation (Fig. 6; Winder and Hardie 1999; Kurth-Kraczek *et al.,* 1999). Substantial evidence also indicates that atypical PKCλ/ζ acts downstream of PI3-kinase to relay insulin signals for GLUT 4 translocation (Farese *et al.,* 2005). Another regulatory protein, AKT substrate 160 (AS160) also plays an essential role during GLUT4 translocation. AS160 seems to do its regulatory work in adipocytes (Eguez *et al.,* 2005; Larance *et al.,* 2005) and skeletal muscle (Brus *et al.,* 2005; Karlsson *et al.,* 2005; Plogaard *et al.,* 2005) in response to insulin, exercise, and AICAR treatments (Fig. 6). Muscle contraction seems to induce AS160 phosphorylation through the AMPK pathway (Krammer *et al.,* 2006; Treebak *et al.,* 2006). Therefore any disruption of AMPK and AKT results in inhibition of contraction-induced AS160 phosphorylation and leads to insulin resistance. Interestingly, insulin-stimulated AS160 phosphorylation is impaired in

skeletal muscle of type 2 diabetic patients (Karlsson *et al.,* 2005) and in response to TNF-α (Plomgaard *et al.,* 2005).

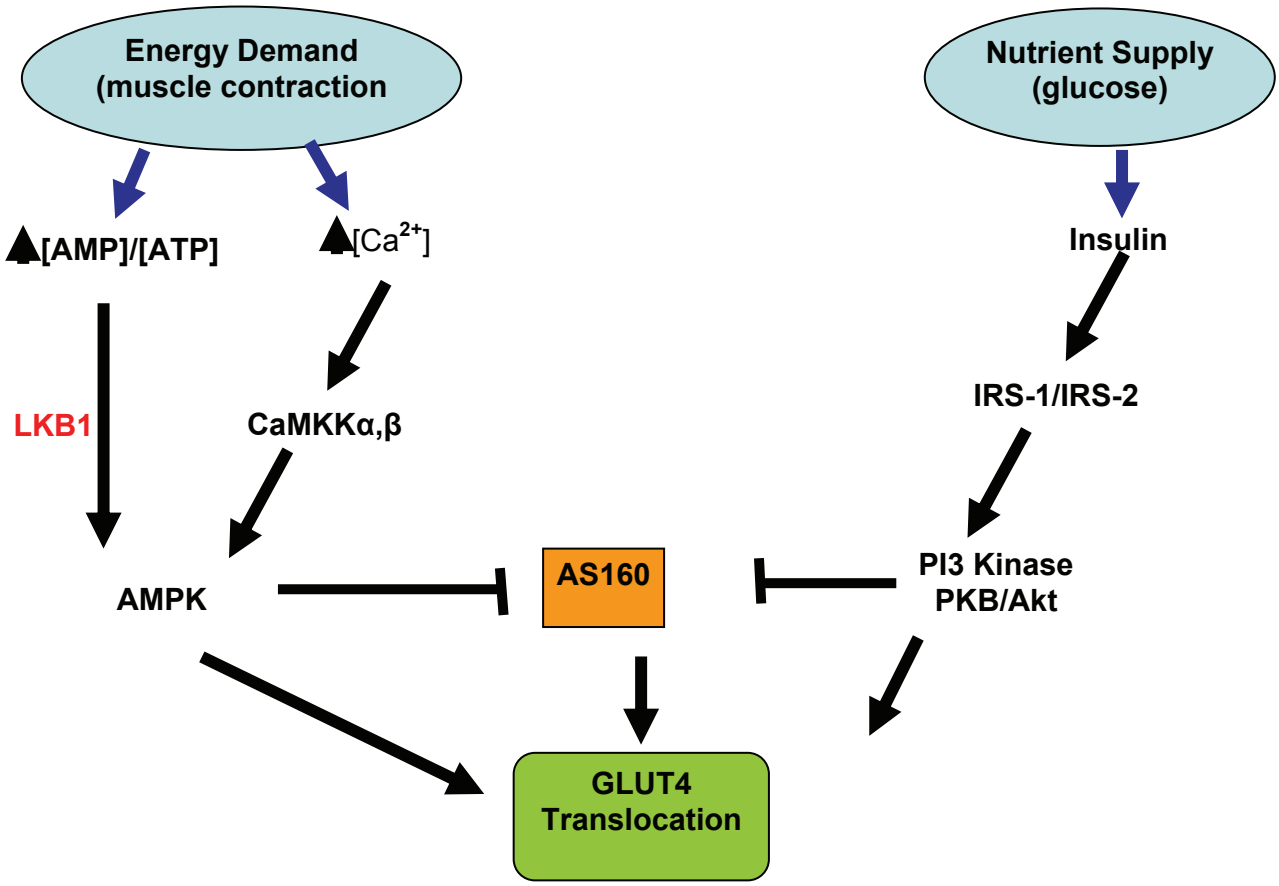

Figure 6. Schematic representation of pathways mediating GLUT4 translocation (Adapted from Shoahui Huang and Michael Czech 2007).

3.6 GLUT4 translocation: docking and fusion

Another important step in GLUT4 translocation is the docking and fusion of the GLUT4 storage vesicle within the plasma membrane (Cushman 1980; Birnbaum 1992). Significant understanding of docking/fusion of GLUT4 vesicles is due to delineation of synaptic vesicle trafficking in the regulation of neurotransmitter release from the presynaptic membrane (Calakos and Scheller 1996; Sollner 1995). Here two cytosolic proteins were identified, i.e. the N-ethylmaleimide (NEM)-sensitive fusion protein (NSF) and the soluble NSF attachment proteins (SNAPs; Calakos and

Scheller, 1996). With the identification of the soluble components, their membrane-bound partners were identified, i.e. the SNARES (SNAP receptors).

The SNARE family of proteins is divided into two groups, i.e. vesicle-associated SNARE (v-SNARE) and target-membrane SNARE (t-SNARE). The v-SNARE family of proteins consists of another peptide family known as the vesicle-associated membrane proteins (VAMP), that are associated with GSV. Several VAMP isoforms have now been identified, i.e. VAMP1, VAMP2 and VAMP3 (Randhawa *et al.,* 2000). The VAMP2 family of the v-SNARE proteins is associated with GLUT4 storage vesicles (Martin *et al.,* 1998; Sevilla *et al.,* 1997).

The t-SNARE family of proteins consists of the syntaxin peptide family that is associated with the plasma membrane. Numerous syntaxin isoforms have been identified, including syntaxin 1, syntaxin 2, syntaxin 3 and syntaxin 4 (Calakos *et al.,* 1994; Pevsner *et al.,* 1994). Syntaxin 4 and SNAP23 are associated with GLUT4 translocation (Volchuk *et al.,* 1996; Olson *et al.,* 1997; Yang *et al.,* 2001). Another membrane-associated protein that plays an essential role in the docking/fusion steps has also been identified, i.e. Munc 18a family of proteins (Harrison *et al.,* 1994; Hosono *et al.,* 1992; Novick and Schekman 1979). Two additional isoforms have been identified, i.e. Munc 18b and Munc 18c. The accessory proteins Munc 18c and Synip also play an important role in GLUT4 translocation (Pessin *et al.,* 1999).

Since I have now discussed proteins associated with docking/fusion, I will now focus on the mechanism underlying GLUT4 translocation. During the basal state (no insulin), VAMP 2 is embedded in the GLUT4 storage vesicle (Cain *et al.,* 1992; Volchuk *et al.,* 1995). VAMP 2 contains a coiled spring. Moreover, Munc 18c, a membrane-associated protein, binds to syntaxin 4 with high affinity at the plasma membrane, thereby preventing its interaction with VAMP 2-GSV. Interestingly, syntaxin 4 also contains a series of coiled springs. Upon insulin stimulation, Munc 18c undergoes a conformational change that allows interactions between syntaxin 4 and VAMP 2 to occur. The two springs coiled up together (VAMP2 and syntaxin 4) allows fusion of the two lipid membranes (GSV and sarcolemma; Fig 7a). This model is further strengthened by overexpression studies, i.e. Munc 18c expression inhibits GLUT4 vesicle translocation. This likely occurs by Munc 18c binding to syntaxin 4,

thereby preventing its interaction with VAMP 2 (Tellam *et al.,* 1997; Thurmond *et al.,* 1998, 2000; Fig . 7b).

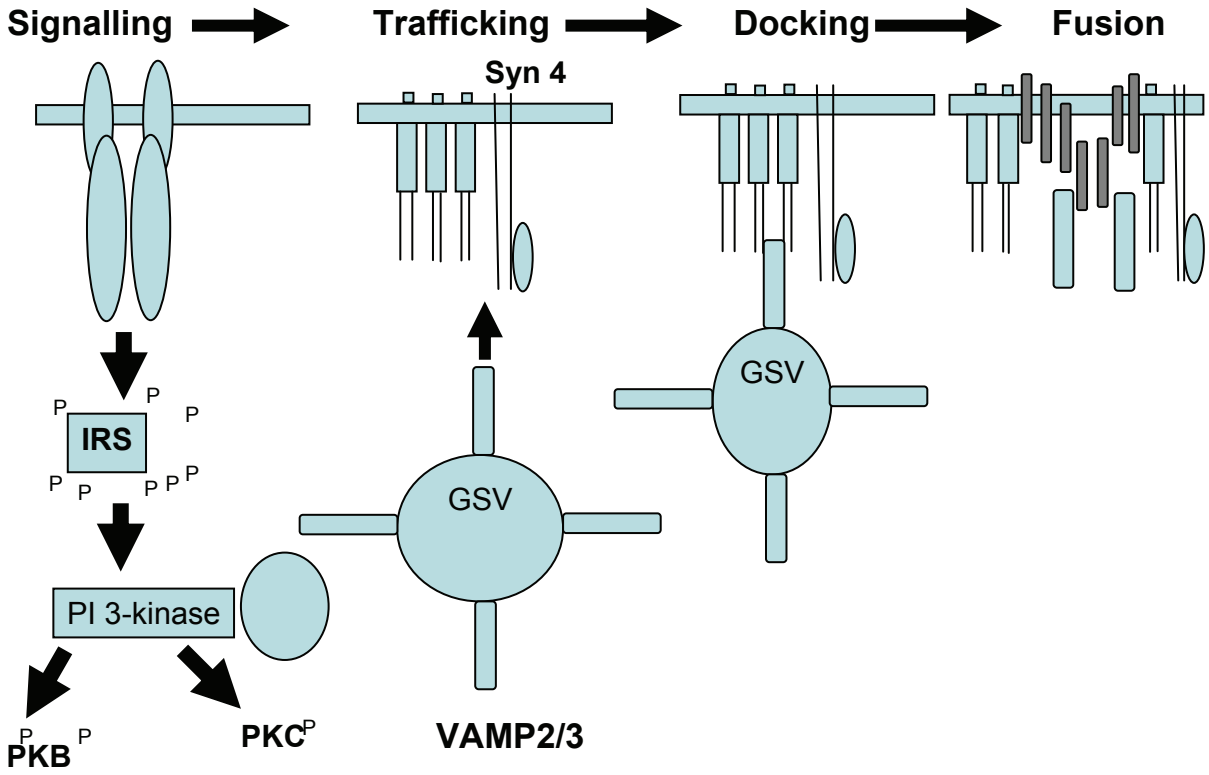

Figure 7a. Image showing the insulin signalling events during GLUT4 translocation (Adapted from Thurmond Pessin 2000).

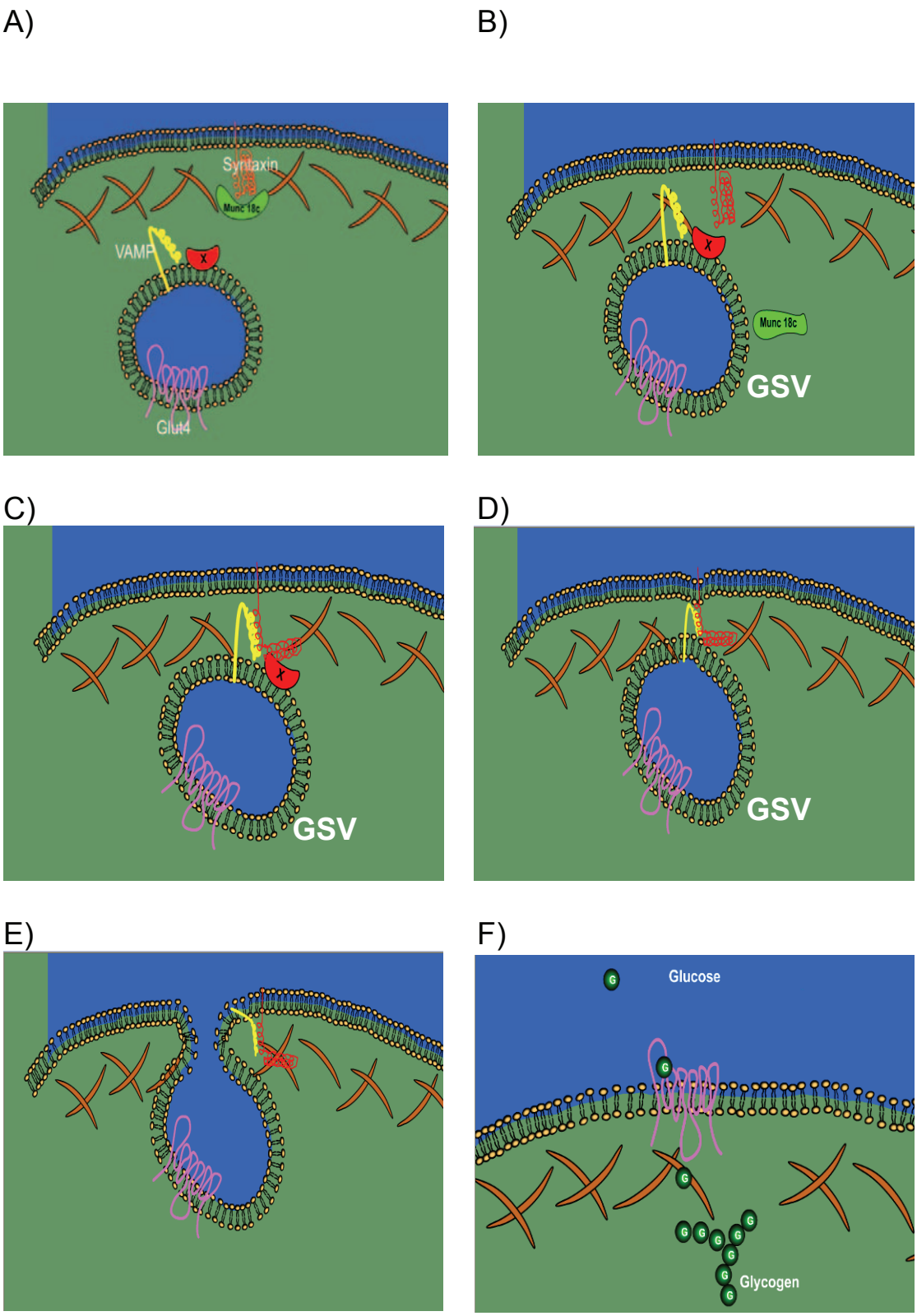

Figure 7b. Schematic representation of the docking and fusion events during GLUT4 translocation (David E James 2001).

4. Nutrient sensors and insulin resistance

Initiation of insulin resistance as a response to excessive nutrient flux requires a nutrient sensor, i.e. the concept being that once activated the sensor initiates adaptive mechanisms. This results in a decline in insulin's ability to mediate nutrient uptake and breakdown/metabolism. In the late 1970's McGarry (2002) first identified malonyl-CoA as a biochemical sensor that regulates the switch from fatty acid to glucose oxidation (Fig. 8). It was further proposed (Ruderman *et al.,* 2006) that a malonyl-CoA fuel-sensing and signaling mechanism existed in which acetyl-CoA carboxylase acts as a sensor and malonyl-CoA as the signal in such a nutrient sensing system (Saha *et al.,* 1995; Ruderman *et al.,* 1999).

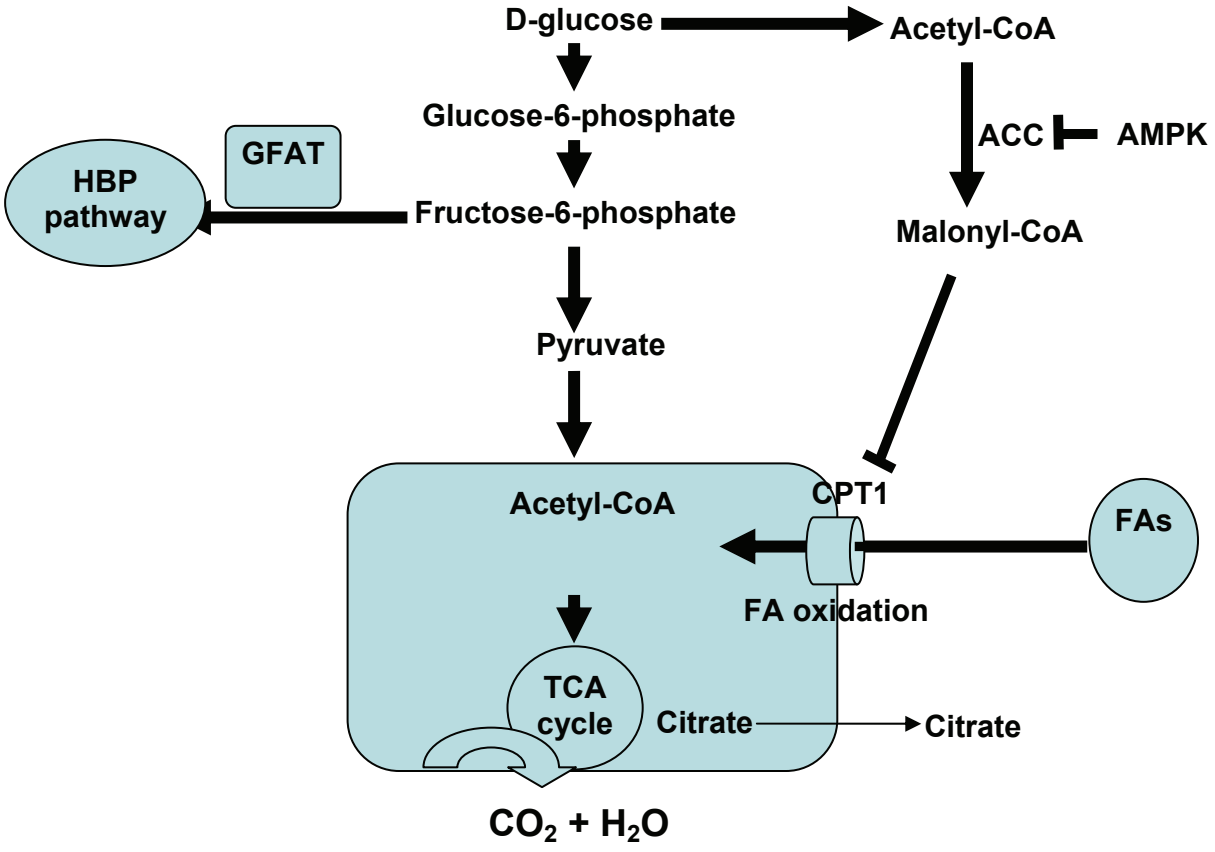

Figure 8. Schematic representation showing malonyl-CoA and the hexosamine biosynthetic pathway (HBP) acting as fuel sensors, which play an important role in the regulation of cellular glucose uptake.

Interestingly, another nutrient sensing mechanism was also identified, i.e. the hexosamine biosynthetic pathway (HBP) that is the focus of this thesis (Fig. 8; Brownlee 2001; Brownlee 2005; Hammes *et al.,* 2003) McClain 2002; Rossetti 2000).

4.1 Hexosamine biosynthetic pathway (HBP)

Insulin normalizes elevated plasma glucose levels mainly by increasing glucose uptake into muscle and fat cells. Upon entry into the cell, glucose is rapidly converted to glucose-6-phosphate. The latter has multiple "fates" in terms of its catabolism (Fig 9). The majority enters the glycolytic pathway, where it is further metabolized for the generation of ATP. However, lesser pathways also contribute to its metabolism, e.g. the pentose phosphate pathway, glycogen synthesis and the hexosamine biosynthetic pathway.

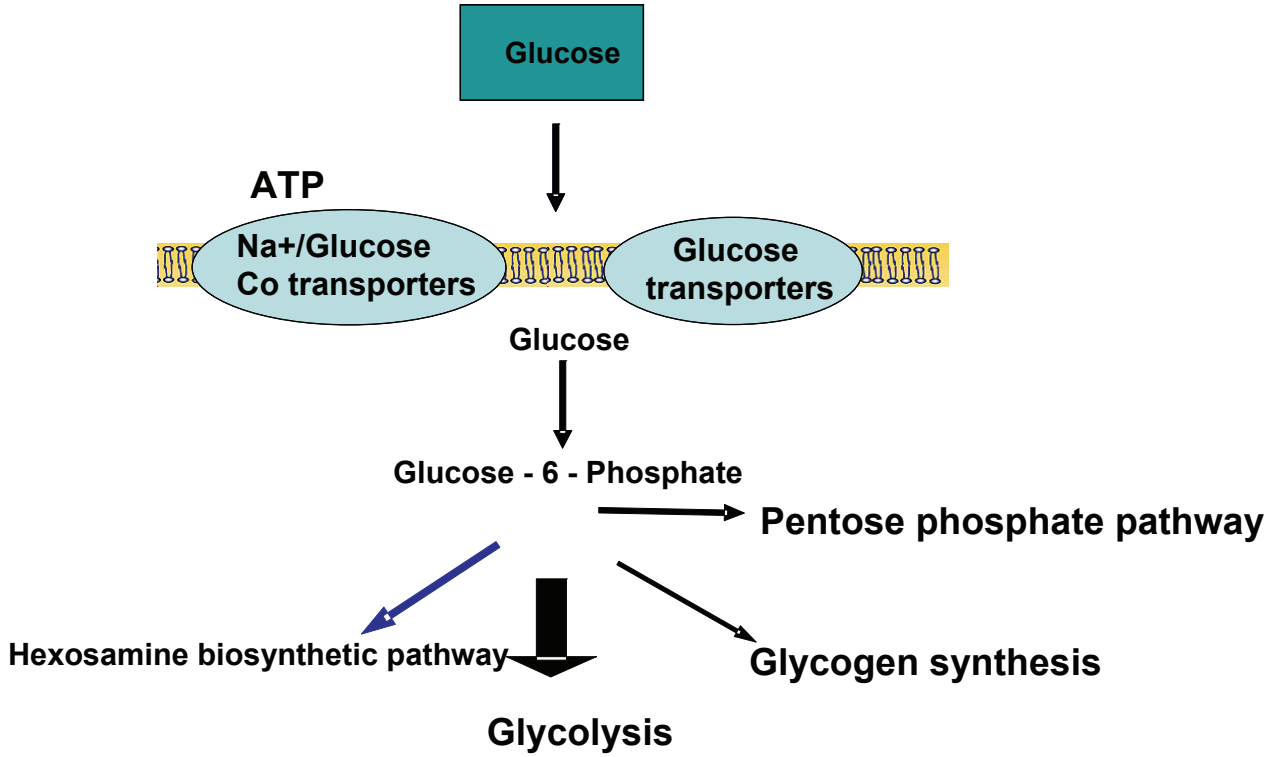

Figure 9. The multiple pathways responsible for glucose metabolism (Adapted from Bouche et al., 2004).

The HBP was first discovered by Marshall *et al.* (1991) demonstrating that glutamine participates in glucose-induced insulin resistance (Fig. 10). After completing a series of experiments, they found a link between HBP and insulin resistance (Marshall *et al.,* 1991). About 1-3% of glucose taken up enters the HBP. Here the rate limiting

enzyme glutamine: fructose-6-phosphate amidotransferase (GFAT) catalyzes the conversion of fructose-6-phosphate, in the presence of L-glutamine, to glucosamine-1-phosphate (Marshall *et al.,* 1991; Rossetti *et al.,* 1995; Nelson *et al.,* 2000). The latter is converted in a three-step process into the final products of the HBP, i.e. uridine diphosphate-N-acetylhexosamines (UDP-HexNAc). There are two UDP-HexNAc, namely UDP-N-acetylglucosamine (UDP-GlcNAc) and UDP-N-acetylgalactosamine (UDP-GalNAc) that is produced in a ~3:1 ratio (Marshall *et al.,* 1991; Fig. 10). Firstly, UDP-GalNAc is converted to N-linked β-N-acetylgalactosamine, a process that is catalyzed by the enzyme N-linked β-N-acetylgalactosamine transferase. This process takes place in the endoplasmic recticulum and the Gogi-apparatus and is essential for the synthesis of glucosamino glycans, glycolipids and glycoproteins. On the contrary, UDP-GlcNAc becomes the obligatory donor substrate of, O-linked-β-N-acetylglucosamine transferase (O-GlcNAc transferase or termed OGT) that converts UDP-GlcNAc into its final product, i.e. O-linked-β-N-acetylglucosamine (O-GlcNAc).

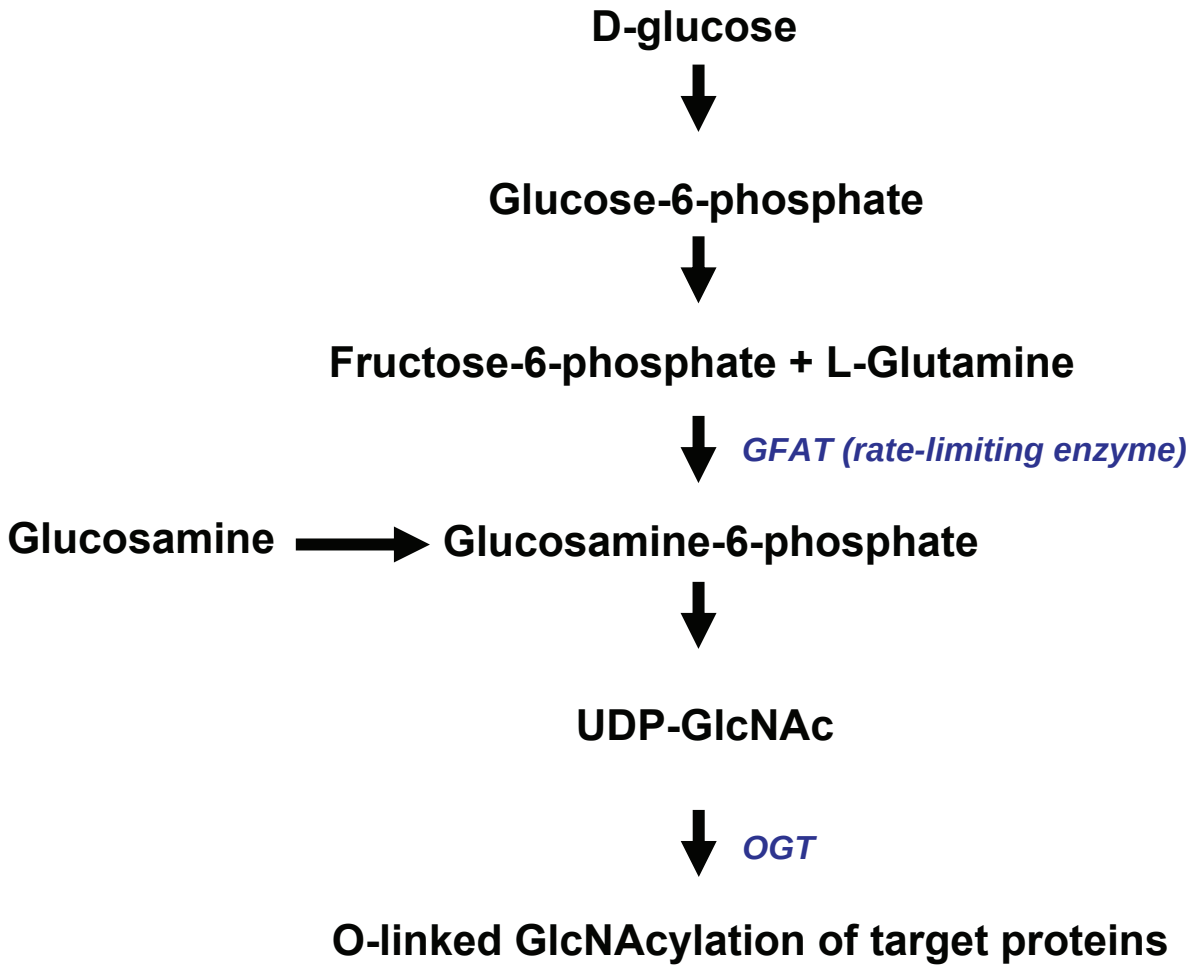

Figure 10. The hexosamine biosynthetic pathway (Adapted from Amy J. Davidhoff 2005).

4.2 HBP and insulin resistance

Post translation modification of proteins occurs through various processes, including acetylation, methylation, ubiquitination and phosphorylation (Kouzarides 2000; McBride and Silver 2001) Mimnaugh *et al.,* 1999). O-GlcNAcylation is another novel way in which proteins may be modified post translationally (Torres and Hart. 1984). O-GlcNAc is proposed to act in a way analogous to protein phosphorylation (Hart *et al.,* 1995; Vossler *et al.,* 2001; Wells *et al.,* 2001). Moreover, O-GlcNAcylation is thought to reciprocally counteract phosphorylation at similar/adjacent sites (Kamemura and Hart, 2003). While there are ~ 600 genetically distinct protein kinases and ~ 150 protein phosphatases that regulate phosphorylation (Forrest *et al.,* 2003; Manning *et al.,* 2002), O-GlcNAcylation is regulated by only two enzymes. Here, OGT is responsible for the addition of O-GlcNAc residues, and O-linked-β-N-acetylglucosaminidase (O-GlcNAcase) for its removal from target proteins (Dong and Hart 1994; Haltiwanger *et al.,* 1992; Haltiwanger *et al.,* 1990; Kreppel *et al.,* 1997; Lubas *et al.,* 1997; Goa *et al.,* 2001; Wells *et al.,* 2002; Fig. 11).

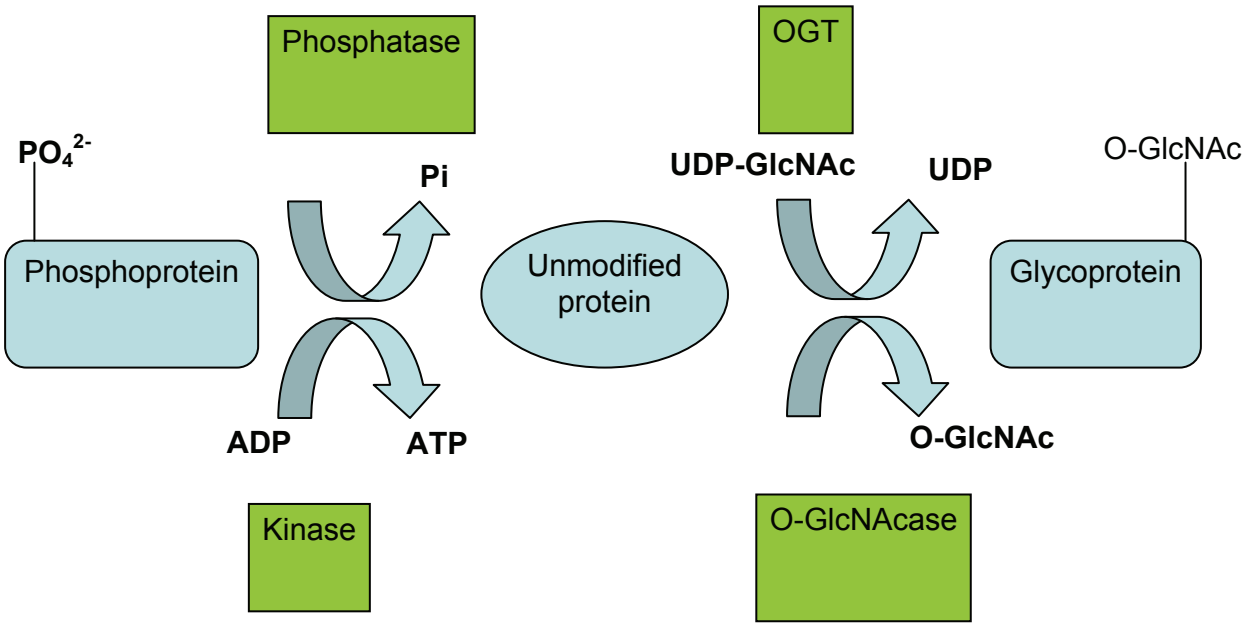

Figure 11. The reciprocal relation between O-GlcNAcylation and protein phosphorylation. Here O-GlcNAc and phosphorylation competes for the same hydroxyl units of the Ser/Thr residues and thus may regulate the levels of each other (Adapted from N. Zacharra and G.W. Hart 2006).

There are a variety of mechanisms which may lead to an increase in the biosynthesis of O-GlcNAc. Firstly, sustained or chronic hyperglycemia will lead to increased HBP flux and ultimately result in elevated biosynthesis and addition of O-GlcNAc moieties to target proteins (Maria G. Buse, 2000). Secondly, over-expression of the HBP rate-limiting enzyme, GFAT, will also lead to increased O-GlcNAc levels (Donald A. McClain, 2002; Hebert *et al.,* 1996; Crook *et al.,* 1993). Finally, glucosamine, like excess glucose, is metabolized via the HBP where it bypasses GFAT and is phosphorylated rapidly to produce glucosamine 6-phosphate. Glucosamine is ~ 40 times more potent than glucose in mediating glucose transport and is used at a concentration 10 x lower than that of glucose (Maria G. Buse, 2000; Marshal *et al.,* 1991; Fig. 12). Over-expression of OGT and the pharmacological inhibition of O-GlcNAcase with O-(2-acetamido-2-deoxy-D glucopyranosylidene) amino-N-phenyl-carbamate (PUGNAc) will also lead to increased O-GlcNAcylation (Fig. 12). Furthermore, Zacharra *et al.,.* (2004) demonstrated that O-GlcNAc levels may be increased using a variety of stressors including hyperthermia, UVB, ethanol and sodium arsenite.

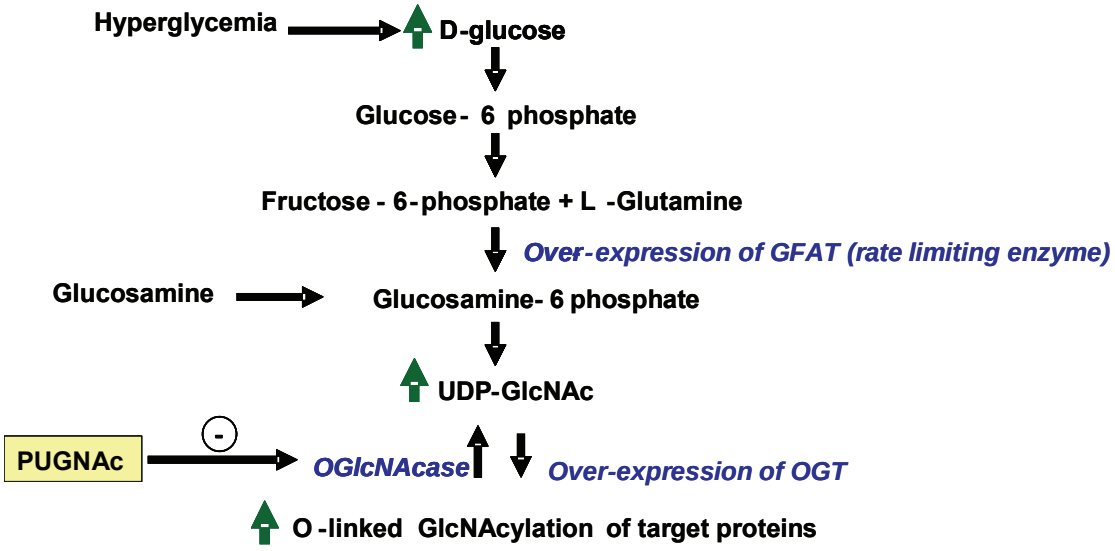

Figure 12 Hyperglycemia, glucosamine and over-expression of GFAT will lead to increased O-GlcNAcylation of target proteins.

O-GlcNAc modification imparts functional changes within target proteins and as a result can affect transcription, translation and intracellular signalling (56; 57). Hyperglycemia-induced increases in HBP flux (Marshall *et al.,* 1991; Rossetti *et al.,* 1990; Hazel *et al.,* 2004), over-expression of GFAT (Herbert *et al.,* 1996; Donald

McClain 2002) and glucosamine infusions (Buse *et al.,* 1993; Giaccari *et al.,* 1995; Rossetti *et al.,* 1995) all result in insulin resistance. Since all these mechanisms lead to insulin resistance, it was not surprising that over-expression of OGT (McClain *et al.,* 2002) and pharmacological inhibition of O-GlcNAcase with PUGNAc (Arias *et al.,* 2004) were also linked to insulin resistance.

In the light of these findings, several studies have been performed to lower O-GlcNAc levels and thereby attempt to attenuate HBP-mediated insulin resistance. For example, inhibition of the rate-limiting enzyme GFAT with a glutamine analogue 6-diazo-5-oxo-L-norleucine (DON; Marshall *et al.,* 1991) and over-expression of O-GlcNAcase (58) reversed HBP-mediated insulin resistance. Furthermore, they attempted to reverse insulin resistance by caloric restriction. Here, caloric intake of rats were restricted for 20 days, since it was shown that it leads to increased insulin-stimulated glucose transport (Cartee and Dean 1994; Dean and Cartee 1996; Dean *et al.,* 1998; Gazdag *et al.,* 1998,2000; Davidson *et al.,* 2002; McCurdy *et al.,* 2003). In parallel, caloric restriction reduced UDP-GlcNAc and UDP-GalNAc levels (Gazdag *et al.,* 2000). However, when muscle strips of calorie restriction rats were incubated with PUGNAc (O-GlcNAcase inhibition) it did not result in any significant findings. These data are in contrast with studies that show that glucose deprivation leads to increased O-GlcNAc modification (McClain *et al.,* 2008). For the caloric restriction study, decreased UDP-GlcNAc levels resulted in lowered O-GlcNAc levels since UDP-GlcNAc is the obligatory donor substrate of OGT. On the other hand, the glucose deprivation protocol activates several stress signaling pathways like AMPK and the MAPK pathway (McClain *et al.,* 2008). AMPK seems to increase the expression of OGT and interacts with p38 to increase the O-GlcNAc levels (McClain *et al.,* 2008).

4.3 HBP and insulin signaling pathway

The cellular mechanisms that link activation of HBP to insulin resistance are currently poorly understood. The insulin signalling pathway from insulin binding to its receptor until the docking/fusion of GLUT4 storage vesicle with the plasma membrane is regulated by phosphorylation (Fig. 13). Since O-GlcNAcylation reciprocally counteracts the effect of phosphorylation at similar/adjacent sites in a reciprocal

manner (Kamemura and Hart, 2003), it would be expected that increased O-GlcNAcylation should abrogate the effects of phosphorylation. In agreement, several studies (Vosseller *et al.,* 2002) demonstrated that O-GlcNAc modification of IRS1/IRS2 imparts a signalling defect leading to insulin resistance (Federici *et al.,* 2002; Patti *et al.,* 1999). Moreover, when both IRS1/IRS2 and PI-3 kinase were O-GlcNAcylated this interfered with normal insulin signaling (Rordorf-Nikolic *et al.,* 1995). Downstream regulators of the insulin signaling pathway were also investigated. For example, O-GlcNAcylation of AKT/PKB also interferes with insulin signalling (Vosseller *et al.,* 2002; Boehmelt *et al.,* 2000), while glycogen synthase (GS) was also shown to be O-GlcNAc modified (Parker *et al.,* 2003).

GLUT4 is the most important down stream target of AKT/PKB and is the focus of this thesis. For example, previous studies implicate that over-expression of GFAT caused a defect in GLUT4 translocation (Herbert *et al.,* 1996; Donald McClain 2002). Moreover, Buse *et al.,.* (2000) found that glucosamine treatment inhibited GLUT4 translocation, whereas high glucose exposure impaired the intrinsic activity of GLUT4 or membrane intercalation in adipocytes. Glucosamine exposure also results in O-GlcNAc modification of Munc 18c, leading to insulin resistance (Chen *et al.,* 2003; Nelson *et al.,* 2002).

4.4 HBP: evaluation in different tissues

Although O-GlcNAcylation was first discovered in lymphocytes (Torres and Hart. 1984), it was Marshall *et al.,.* (1991) that first discovered HBP using cultured adipocytes. The majority of HBP studies done have focused skeletal and adipose tissues (Garvey *et al.,* 1995; Buse *et al.,* 1997; Patti *et al.,* 1999; Rosetti *et al.,* 2000; McClain *et al.,* 2002; Hazel *et al.,* 2004). In addition, other tissues like retinal neuronal cells, T lymphocytes, mast cells, rat-1 fibroblasts, endothelial cells, chondrocytes, intestinal crypt cells, mesangial cells, pancreatic tissue and neonatal cardiomyocytes have also been examined (Torres and Hart 1984; Buse *et al.,* 1993; Schleicher *et al.,* 1998; James *et al.,* 2000; Weigert *et al.,* 2000). Several human HBP studies have also been done e.g. employing cultured human skeletal and adipose tissues (McClain *et al.,* 1995; Farooq *et al.,* 2007; Lehman *et al.,* 2005; Monauni *et al.,* 2000; Pouwels *et al.,* 2001; Pouwels *et al.,* 2002; Pouwels *et al.,*

2004; Yki-Jarvinen *et al.,* 1996). However, despite these advances HBP studies on the heart are fairly limited.

4.5 Insulin resistance and diabetic cardiomyopathy

The diabetic cardiomyopathy was first described 36 years ago as a complication of diabetes mellitus without its conventional symptoms such as changes in blood pressure and coronary artery disease (Rubler *et al.,* 1972). Several clinical and animal studies have linked insulin resistance with the diabetic cardiomyopathy (Rossetti *et al.,* 1990; Marshall *et al.,* 2005; Elbedour *et al.,* 1994; Smith *et al.,* 2007; Yue *et al.,* 2007; Fulop *et al.,* 2006; Taegtmeyer *et al.,* 2002). Skeletal muscle accounts for ~ 75% of whole body glucose uptake (DeFronzo *et al.,* 1981) and insulin resistance (Rossetti *et al.,* 1990). However, myocardial insulin resistance develops in both type 1 and type 2 diabetic animal models (Abel 2005). Although myocardial insulin resistance plays a minor role in the development of whole-body insulin resistance, morbidity and mortality due to cardiovascular complications have been linked with insulin resistant obese and type 2 diabetic patients (Mensah *et al.,* 2004; Fox *et al.,* 2004; Grundy 2004; Tang and Young 2001; Bertoni *et al.,* 2003). It is therefore crucial to understand the underlying mechanisms causing myocardial insulin resistance. In light of this, my thesis investigates a relatively understudied phenomenon, i.e. mechanistic aspects underlying the onset of myocardial insulin resistance.

5. Hypothesis

We hypothesize that increased flux through the HBP impairs myocardial GLUT4 translocation by greater O-linked glycosylation of the insulin signaling pathway, ultimately leading to myocardial insulin resistance*.*

6. Aims

1. To establish *in vitro* fluorescence microscopy- and flow cytometry-based models for visualization and assessment of myocardial GLUT4 translocation using H9c2 cardiac-derived myoblasts.

2. After successful establishment of our *in vitro*-based model for myocardial GLUT4 translocation, we set out to determine the role of the HBP in this process. Here, we employed HBP modulators to alter flux and subsequently evaluate its effect on myocardial GLUT4 translocation. To further strengthen our hypothesis, we also investigated the role of the HBP in hearts of an *in vivo* type 2 diabetes mouse model.

7. References

Abel ED. Myocardial insulin resistance and cardiac complications of diabetes. Curr. Drug. Targets Immune. *Endocr. Metabol. Disord*. 2005; 5:219-26.

Beck-Nielsen H., Vaag A., Damsbo P., Handberg A., Nielson OH., Henriksen EJ., Thye-Ronn P.: Insulin resistance in skeletal muscle in patience with NIDDM. *Diabetes Care* 15:418-429, 1992

Bertoni AG., Tsai A., Kasper EK., Brancati FL.: Diabetes and indiopathic cardiomyopathy: a nationwide case-control study. *Diabetes Care* 26: 2791-2795, 2003

Boehmelt G, Wakeham A., Elia A., Sasaki T., Plyte S., Potter J., Yang Y., Tsang E., Ruland J., Iscove NN., Dennis JW., Mak TW., Decreased UDP-GlcNAc levels abrogate proliferation control in EMeg 32-deficient cells, *EMBO J*. 19 (2000) 5092 – 5104.

Brownlee M. Biochemistry and molecular cell biology of diabetic complications. *Nature* 2001; 414:813-820. [Pubmed: 11742414]

Brownlee M. The pathobiology of diabetic complications: a unifying mechanism. *Diabetes 2005*; 54:1615-1625 [Pubmed: 15919781]

Burant CF., Lemmon SK., Treutlaar MK., Buse MG. (1984) Insulin resistance of denervated tate muscle: a model for impaired receptor-function coupling *Am J Physiol Endocrinol Metab*. 247, E657-E666

Butler PC., Kryshak EJ., Marsh M., Rizza RA. (1990) Effect of insulin on oxidation of intracellularly and extracellularly derived glucose in patients with NIDDM. Evidence for primary defect in glucose transport and/or phosphorylation but not oxidation. *Diabetes* 39:1373–1380

Cain CC., Trimble WS., and Lienhard GE. (1992) Members of the VAMP family of synaptic vesicle proteins are components of glucose transporter vesicles in 3T3-L1 adipocytes. *J. Boil. Chem*. 270:8233-8240.

Calakos N., and Scheller RH. (1996) Synaptic vesicle biogenesis, docking and fsion: a molecular description. *Physiol. Rev*. 76:1-29

Calakos N., Bennet MK., Peterson KE., and Scheller RH. (1994) Protein-protein interactions contributing to the specificity of intracellular vesicular trafficking. *Science* 263:1146-1149.

Cheatham B., Vlahos CJ., Cheatham L., Wang L., Blenis J. and Kahn CR. (1994) Phosphatidylinositol 3-kinase activation is required for insulin stimulation of pp70 S6 kinase, DNA synthesis, and glucose transporter translocation. *Mol. Cell. Biol*. 14, 4902–4911.

Chen G., Liu P. and Thurmond DC. Elemendorf JS. Glucosamine-ubuced insulin resistance is coupled to O-linked glycosylation of Munc 18c. *FEBS Lett* 2003;534:54 – 60 (PubMed: 12527361)

Chiang SH., Baumann CA., Kanzaki M., Thurmond DC., Watson RT., Neudauer CL., Macara IG., Pessin JE., Saltiel AR. Insulin –stimulated GLUT4 translocation requires the CAP-dependent activation of TC10. *Nature*, 2001, 410, 944-948.

Clark R., McDonough PM., Swanson E., Trost Su, Suzuki M., Fukuda M., Dillmann W. Diabetes and the accompanying hyperglycemia impairs cardiomyocyte calcium cycling through increased nuclear O-GlcNAcylation. *J Biol Chem* 2003; 278:44230-44237. [PubMed: 12941958]

Clark JF., Young PW., Yonezawa K., Kasuga M. and Holman GD. (1994) Inhibition of the translocation of GLUT1 and GLUT4 in 3T3-L1 cells by the phosphatidylinositol 3-kinase inhibitor, wortmannin. *Biochem. J.* 300, 631–635.

Crook ED., Daniels MC., Smith TM., McClain DA: Regulation of insulin-stimulated glycogen synthase activity by overexpression of glutamine:fructose-6- phosphate amidotranferase rat-1 fibroblasts. *Diabetes* 42:1289-1296,1993

Czech MP. and JM. Buxton. (1993). Insulin action on the internalization of the GLUT4 glucose transporter in isolated rat adipocytes. *J. Biol. Chem*. 268:9187-9190

DeFronzo RA., Jacot E., Jequier E., Maeder E., Wahren J. and Felber JP.: The effect of insulin on the disposal of intravenous glucose: results from indirect calorimetry and hepatic and femoral venous catheterization. *Diabetes* 30:1000-1007, 1981

Dong DL., Hart GW. Purification and Characterization of an O- GlcNAc selective N-acetyl-beta-D-glucosaminidase from rat spleen cytosol, *J. Biol.Chem*.269 (1994) 19321-19330

Elbedour K., Zucker N., Zalzstein E., Barki Y., Carmi R. Cardiac abnormalities in the Bardet-Biedl syndrome: echocardiographic studies of 22 patiens. *Am J Med Genet*. 1994;52:154-169.

Engelgau MM., Geiss LS., Saadine JB., Boyle JP., Benjamin SM., Gregg EW., Tierney EF., Rios-Burrows N., Mokdad AH., Ford ES., Imperator G., Narayan KM: The evolving diabetes burden in the United States. *Ann Intern Med* 140: 945-950, 2004

Federici M., Menghini RA., Mauriello ML., Hribal F., Ferrelli D., Lauro P., Sbraccia, LG., Spagnoli G., Sesti R., Lauro, Insulin-dependent activation of endothelial nitric oxide synthase is impaired by O-linked glycosylation modification of signaling proteins in human coronary endothelial cells, *Circulation* 106 (2002) 466-472.

Fink RI., Wallace P., Brechtel G., Olefsky JM. (1992) Evidence that glucose transport is rate-limiting for in vivo glucose uptake. *Metabolism* 41:897–902

Forrest AR., Ravasi T., Taylar D., Huber T., Hume DA and Gimond S. Phosphoregulators: protein kinases and protein phosphatases of mouse, *Genome Res*. 13 (2003) 1443-1454.

Fox CS., Coady S., Sorlie PD., Levy D., Meigs JB., D'Agostino RB. Sr., Wilson PW., Savage PJ.: Trends in cardiovascular complications of diabetes. *Jama* 292: 2495-2499, 204

Freymond D., Bogardus C., Okubo M., Stone K., Mott DM., Yomba BL., Zurlo F., Swinburn B.: Impaired insulin-stimulated muscle glycogen synthase activation in vivo in man is related to low fasting glycogen synthase phosphates activity. *J Clin Invest* 82:1503-1509, 1988

Fulop N., Manson MM., Dutta K., Wang P., Davidoff AJ., Marchase RB., Chatham JC. The impact of type-2 diabetes and aging on cardiomycocyte function and O-linked N-acetylglucosamine levels in the heart. *Am J Physiol Cell Physiol*. 2007 Apr;292(4):C1370-8

Gao YL., Wells FI., Comer GJ., Parker GW. Hart, DynamicO-glycosylation of a neutral, cytosolic beta-N-acetylglucosaminidase from human brain, *J. Biol. Chem*. 276 (2001) 9838-9845.

Garcia MJ., McNamara PM., Gordon T., Kannel WB., Morbidity and mortality in diabetics in the Framingham population: sixteen year follow-up study. *Diabetes*. 1974;23:105-111.

Garvey WT.: Gucose transport and NIDDM. *Diabetes Care* 15:396-417,1992

Grundy SM.. What is the contribution of obesity to the metabolic syndrome? *Endocrinol Metab Clin North Am* 33: 257-282, table of contents, 2004

Haltiwanger RS., Holt GD. and Hart GW. Enzymatic addition O-GlcNAc to nuclear and cytoplasmic proteins. Identification of a uridine diphospho-N-acetylglucosamine:peptide beta-N-acetylglucosaminyltransferase, *J. Biol. Chem*. 265 (1990) 2563-2568.

Haltiwanger RS., Blomberg MA. and Hart GW. Glycosylation of nuclear and cytoplasmic protein. Purification and characterization of a uridine diphospho-N-acetylglucosamine: polypeptide beta-N-acetylglucosaminyltransferase, *J. Boil. Chem*. 267 (1992) 9005-9013.

Hammes HP., Du X., Edelstein D., Taguchi T., Matsumura T., Ju Q., Lin J., Bierhaus A., Nawroth P., Hannak D., Neumaier M., Bergfeldt R., Giardino I., Brownlee M. Benfotiamine blocks three major pathways of hyperglycaemic damage and prevents experimental diabetic retinopathy. *Nat Med* 2003; 9: 294-299 [Pubmed 12592403]

Hara K., Yonezawa K., Sakaue H., Ando A., Kotani K., Kitamura T., Kitamura Y., Ueda H., Stephens L., Jackson TR., Hawkins PT., Dhand R., Clark AE., Holman G D., Waterfield MD. & Kasuga M. (1994) 1-Phosphatidylinositol 3-kinase activity is

required for insulin-stimulated glucose transport but not for RAS activation in CHO cells. *Proc. Natl. Acad. Sci*. USA 91, 7415–7419.

Hediger MA., Coady MJ., Ikeda TS., and Wright EM. (1987) Expression cloning and cDNA sequencing of the Na+/glucose co-transporter. *Nature* (London) 330, 387-381

Herbert LF. Jr, Daniel MC., Zhou J., Crook ED., Turner RK., Neidigh JL., Zhu JS., Baron AD., McClain DA.: Overexpression of glutamine:fructose-6- phosphate amidotranferase in transgenic leads to insulin resistance. *J Clin Invest* 98:930-936,1996

Heydrick SJ., Ruderman NB., Kurowski TG., Adams HB., Chen KS. (1991) Enhanced stimulation of diacylglycerol and lipid synthesis by insulin in denervated muscle. Altered protein kinase C activity and possible link to insulin resistance *Diabetes* 40,1707-1711

Heydrick SJ., Ruderman NB., Kurowski TG., Adams HB., Chen KS. (1991) Enhanced stimulation of diacylglycerol and lipid synthesis by insulin in denervated muscle. Altered protein kinase C activity and possible link to insulin resistance *Diabetes* 40, 1707-1711

Itani SI., Ruderman NB., Schmieder F., Boden G. (2002) Lipid-induced insulin resistance in human muscle is associated with changes in diacylglycerol, protein kinase C, and IkappaB-alpha *Diabetes* 51 ,2005-2011

Jhun BH., Rampal AL., Liu H., Lachaal M., and Jung CY. 1992. Effects of insulin on the steady state kinetics of GLUT4 subcellular distribution in rat adipocytes. *J. Biol. Chem*. 268:17710-17715.

Kayano T., Buse JB., Burant CF., Takeda J., Lin D., Fukumoto H. and Seino S. (1990) Molecular biology of mammalian glucose transporters. *Diabetes Care*13, 198-208

Ki-Jarvinen H., Vuorinen-Markkola H., Koranyi L., Bourey R., Tordjman K., Mueckler M., Permutt AM., Koivisto VA. 1992 Defect in insulin action on expression of the muscle/adipose tissue glucose transporter gene in skeletal muscle of type 1 diabetic patients. *J Clin Endocrinol Metab* 75:795–799

Ki-Jarvinen H., Young AA., Lamkin C., Foley JE. 1987 Kinetics of glucose disposal in whole body and across the forearm in man. *J Clin Invest* 79:1713–1719

King H., Aubert RE., Herman WH. Global burden of diabetes, 1955-2025: prevalence, numerical estimates, and projection. *Diabetes Care* . 1998:21:1414-1431.

Kolter T., Uphues I., Wichelhaus A., Reinauer H. and Eckel J. (1992). Contraction-induced translocation of the glucose transporter Glut4 in isolated ventricular cardiomyocytes. *Biochem. Biophys. Res. Commun*. 189. 1207-1214

Kouzarides T. Acetylation: a regulatory modification to rival phosphorylation? *EMBO J*. 2000; 19: 1176–1179.

Kreppel LK., Blomberg MA., and Hart GW. Dynamic glycosylation of nuclear and cytosolic protein. Cloning and characterization of a unique O-GlcNAc transferase with multiple tetratricopeptide repeats, *J. Biol. Chem*. 272 (1997) 9308-9315

Kurth-Kraczek EJ., Hirshman MF., Goodyear LJ. and Winder WW. (1999) 5' AMP-activated protein kinase activation causes GLUT4 translocation in skeletal muscle. *Diabetes* 48, 1667-1671

Lehman DM., Fu DJ., Freeman AB., Hunt KJ., Leach RJ., Johnson-Pais T., Hamlington J., Dyer TD., Arya R., Abbound H., Goring HH., Duggirala R., Blangero J., Konrad RJ., Stem MP. A single nucleotide polymorphism in MGEA5 encoding O-GlcNAc-selective N-acetyl-beta-D glucosaminidase is associated with type 2 diabetes in Mexican Americans*. Diabetes* 2005:54:1214-121. (PubMed: 15793264)

Lubas WA., Frank DW., Krause M., Hanover JA. O-Linked GlcNAc transferase is a conserved nucleocytoplasmic protein containing tetratricopeptide repeats, *J. Biol. Chem.* 272 (1997) 9316-9324.

Lund S., Holman GD., Schmitz O, and Pedersen O. (1995) Contraction stimulates translocation of glucose transporter GLUT4 in skeletal muscle through a mechanism distinct from that of insulin. *Proc. Natl. Acad. Sci*. USA. 92, 5817-5821

Manning G., Whyte DB., Martinez R., Hunter T., Sudarsanam S. The protein kinase complement of the human genome, *Science* 298 (2002) 1912-1934

Marshall JD., Bronson RT., Collin GB., Nordstrom AD., Maffei P., Paisey RB., Carey C., Macdermott S., Russel-Eggit I., Shea SE., Davis J., Beck S., Shatirishvili G., Mihai CM., Hoeltzenbein M., Pozzan GB., Hopkins I., Sicolo N., Naggert JK., Nishina PM. New Alstrom syndrome phenotypes based on the evaluation of 182 cases. *Arch Intern Med.* 2005;165:675-683.

Marshall S., Bacote V., Traxinger RR.: Discovery of a metabolic pathway mediating glucose-induced desensitization of the glcose transport system: role of hexosamine biosynthesis n the induction of insulin resistance. *J Biol Chem* 266: 4706-4712, 1991

McBride AE., Silver PA. State of the arg: protein methylation at arginine comes of age. *Cell*. 2001; 106: 5–8.

McClain DA. Hexosamines as mediators of nutrient sensing and regulation in diabetes. *J Diabetes Complications* 2202; 16: 72-80 [Pubmed: 11872372]

McGarry JD. (2002) Banting lecture 2001: dysregulation of fatty acid metabolism in the etiology of type 2 diabetes. *Diabetes* 51,7-18

Mensaah GA., Mokdad AH., Ford E., Narayan KM., Giles WH., Vinicor F., Deedwania PC.: Obesity, metabolic syndrome, and type 2 diabetes: emerging epidemics and their cardiovascular implications. *Cardiol Clin* 22: 485-504, 2004

Mimnaugh EG., Bonvini P., Neckers L. The measurement of ubiquitin and ubiquitinated proteins. *Electrophoresis*. 1999; 20: 418–428.

Monauni T., Zenti MG., Cretti A., Daniels MC., Targher G., Caruso B., Caputo M., McClain D., Del Prato S., Giaccari A., Muggeo M., Bonora E., Bonadonna RC. Effects of glucosamine infusion on insulin secretion and insulin action in humans. *Diabetes* 2000:49:926-935. (PubMed: 10866044)

Myers MG., Sun X., J. and White MF. (1994). The IRS-1 signaling system. *Trends Biochem. Sci.* 19, 289–294.

Nelson BA., Robinson KA., Buse MG. Insulin acutely regulates Munc 18-c subcellular trafficking: altered response in insulin-resistant 3T3-LI adipocytes. *J Boil Chem* 2002: 277:3809-3812 (PubMed: 1171846)

Nelson BA., Robinson KA., Buse MG. (2000) High glucose and glucosamine induce insulin resistance via different mechanisms in 3T-L1 adipoctyes. *Diabetes* 49: 981-991

Okada T., Kawano Y., Sakakibara T., Hazeki O. and Ui M. (1994) Essential role of phosphatidylinositol 3-kinase in insulin-induced glucose transport and antilipolysis in rat adipocytes. Studies with a selective inhibitor wortmannin. *J. Biol. Chem*. 269, 3568–3573.

Passa P.: Diabetes trends in Europe. *Diabetes Metab Res Rev* 18(Suppl 3):S3-S8, 2002

Patti ME., Virkamaka A., landaker EJ., Kahn CR., Yki-Jarvinen H. Activation of the hexosamine pathway by glosamine in vivo induces insulin resistance of early postrecptor insulin signalling events inskeletal muscle, *Diabetes* 48 (1999) 1562 – 1571.

Pevsner J., Hsu SC., Braun JEA., Calakos N., Ting AE., Bennett MK. and Scheller RH. (1994) Specificity and regulation of a synaptic vesicle docking complex. *Neuron* 13:353-361.

Pouwels MJ., Jacobs JR., Span PN., Lutterman JA., Smits P., Tack CJ. Short-term glucosamine infusion does not affect insulin sensitivity in humans. *J Clin Endocrinol Metab* 2001:86:2099-2103. (PubMed: 11344213)

Pouwels MJ., Span PN., Tack CJ., Olthaar AJ., Sweep CG., van Engelen BG., de Jongh JG., Lutterman JA., Hermus AR. Muscle uridine dishosphate-hexosamines do not decrease despite correction of hyperglycemia-induced insulin resistance in type 2 diabetes. *J Clin Endocrinol Metab* 2002;87:5179-5184. (PubMed: 12414889)

Pouwels MJ., Tack CJ., Span PN., Olthaar AJ., Sweep CG., Huvers FC., Lutterman JA., Hermus AR. Role of hexosamines in insulin resistance and nutrient sensing in

human adipose and muscle tissue. *J Clin Endocrinol Metab* 2004:89:5132-5137. (PubMed: 15472217)

Ribon V., Printen JA., Hoffman NG., Kay BK., Saltiel AR. A novel, multifunctional c-Cbl binding protein in insulin receptor signalling in 3T3-L1 adipocytes. *Mol Cell Boil.* 1998.18.872-879.

Riste L., Khan F., Cruickshank K.: High prevalence of type 2 diabetes in all ethnic groups, including Europeans, in a British inner city: relative poverty, history, inactivity, or 21 st century Europe? *Diabetes Care* 24: 1377-1383, 2001

Rordorf-Nikolic T., Van Horn DJ., Chen D., White MF., Backer JM. Regulation of phosphatidylinositol 3'-kinase by tyrosyl phosphoproteins: full activation requires occupancy of both SH2 domains in the 85-kDa regulatory subunit. *J Biol Chem*. 1995; 270: 3662–3666

Rossetti L., Giaccari A., DeFronzo RA. Glucose toxicity. *Diabetes Care* 1990:13:610-630. (PubMed: 2192847)

Rossetti L., Hawkins M., Chen W., Gindi J., Barzilia N. (1995) in vivo glucosamine infusion induces insulin resistance normoglycemic but not in hyperglycaemic conscious rats. *J Clin Invest* 96;932-140

Rossetti L. Perspective: Hexosamines and nutrient sensing. *Endocrinology* 2000; 141: 1922-1925

Rubler S., Dlugash J., Yuceoglu YZ., Kumral T., Branwood AW., Grishman. New type of cardiomyopathy associated with diabetic glumerulosclerosis. *Am J Cardiol*. 1972:30:595-602.

Ruderman NB., Saha AK., Vavvas D., Witters LA. (1999) Malonyl-CoA, fuel sensing, and insulin resistance. *Am J Physiol*. 276,E1-E18

Ruderman NB. (2006) The metabolic syndrome DeGroot, LJ Jameson, JL eds. *Endocrinology*, 5th edition ,1149-1166 Elsevier Philadelphia, PA

Saha AK., Kurowski TG., Ruderman NB. (1995) A malonyl-CoA fuel-sensing mechanism in muscle: effects of insulin, glucose, and denervation. *Am J Physiol*. 269,E283-E289

Satoh S., Nishimura H., Clark AE., Kozka IJ., Vannucci SJ., Simpson IA., Quon MJ., Cushman SW. and Holman GD. 1993. Use of bismannose photolabel to elucidate insulin-regulated GLUT4 subcellular trafficking kinetics in rat adipose cells. Evidence that exocytosis is a critical site hormone action. *J. Biol. Chem*. 268:17820-17829

Seidell JC.: Prevalence and time trends of obesity in Europe. *J Endocrinol Invest* 25: 816-822, 2002

Shulman GI. (2000) Cellular mechanisms of insulin resistance. *J Clin Invest*. 106,171-176

Slot JW., Geuze HJ., Gigengack S., James DE., and Lienhard GE. (1991) Translocation of the glucose transporter GLUT4 in cardiac myocytes of the rat. *Proc. Natl. Acad. Sci.* USA. 88, 7815-7819

Smith JC., McDonnell B., Retallick C., McEniery C., Carey C., Davies JS., Barrett T., Cockcroft JR., Paisey R. Is arterial stiffening in Alstrom syndrome linked to the development of cardiomyopathy? *Eur J Clin Invest*. 2007; 37:99-105.

Sollner T. 1995 SNAREs and targeted membrane fusion. *FEBS Letters* 369:80-83

Stephens JM. and Pilch PF. The metabolic regulation and vesicular transport of GLUT-4, the major insulin-responsive glucose transporter. *Endocr Rev* 16: 529-546, 1995

Strumpf E.: The obesity epidemic in the United States: causes and axtent, risks and solutions. Issue Brief (*Commonw Fund*) 1-6, 2004

Sun X., Crimmins J., Myers DL., Miralpeix MG. and White MF. (1993) Pleiotropic insulin signals are engaged by multisite phosphorylation of IRS-1. *Mol. Cell. Biol.* 13, 7418–7428.

Sun XJ., Rothenberg P., Kahn CR., Backer JM., Araki E., Wilden PA., Cahill A., Goldstein BJ. & White MF. (1991) Structure of the insulin receptor substrate IRS-1 defines a unique signal transduction protein. *Nature* (London) 352, 73–77.

Taegtmeyer H., McNulty P., Young ME. Adaption and maladaptation of the heart in diabetes: Part 1. General concepts. *Circulation* 105: 1727-1733, 2002.

Tang WH., Young JB.: Cardiomyopathy and heart failure in diabetes. *Endocrinol Metab Clin North Am* 30: 1031-1046, 2001

Volchuk A., Sargeant R., Sumitani S., Liu Z., L. He L. and Klip A. (1995) Cellubrevin is a resident protein of insulin sensitive GLUT4 glucose transporter vesicles in 3T3-L1 adipocytes. *J. Biol. Chem*. 270:8233-8240.

Wang LM., Myers MG. Jr., Sun X., Aaronson SA., White MF. and Pierce JH. (1993) IRS-1: essential for insulin- and IL-4-stimulated mitogenesis in hematopoietic cells. *Science* 261, 1591–1594.

Wells L., Vosseller K., Hart GW. A role for N-acetylglucosamine as a nutrient sensor and mediator of insulin resistance. *Cell Mol Life Sci*. 2003; 60:222-228

Wells L., Gao Y., Mahoney JA., Vosseller K., Chem C., Rosen A., Hart GW., Dynamic O-glycosylation of nuclear and cytsosolic proteins: further characterization of the nucleocytoplasmic beta-N-acetylglucosaminidase O-GlcNAcase, *J. Biol. Chem*. 277 (2002) 1755-1761.

Whelan SA., Hart GW. Proteomic approaches to analyze the dynamic relationships between nucleocytoplasmic protein glycosylation and phosphorylation. *Circ Res*. 2003; 93: 1047-1058.

White MF., Maron R. and Kahn CR. (1985). Insulin rapidly stimulates tyrosine phosphorylation of a Mr-185,000 protein in intact cells. *Nature* (London) 318, 183–186.

Wild S., Roglic G., Green A., Sicree R., King H.: Global prevalence's of diabetes: estimates for the year 2000 and projections for 2030. *Diabetes Care* 27:1047-1053, 2004

Winder WW., and Hardie DG. (1999) AMP-activated protein kinase, a metabolic master switch: possible roles in type 2 diabetes. *Am. J. Physiol*. 277, E1-E10

Yang J., and Holman GD. 1993. Comparison of GLUT4 and GLUT1 subcellular trafficking in basal and insulin-stimulated 3T3-L1 cells. *J. Biol. Chem*. 268:4600-4603

Yki-Jarvinen H., Daniels MC., Virkamaki A., Makimattila S., DeFronzo RA., McClain D. Increased glutamine: fructose-6-phosphate amidotransferase activity in skeletal muscle of patients with NIDDM. *Diabetes* 1996:45:302-307. (PubMed: 8593934)

Yki-Jarvinen H., Helve E., Koivisto VA., Hyperglycemia decreases glucose uptake in type I diabetes. *Diabetes*1987:36:892-896. (PubMed: 3297883)

Yue P., Arai T., Terashima M., Sheikh AY., Cao F., Charo DN., Hoyt G., Robbins RC., Ashley EA., Wu J., Yang PC-M., Tsao PS. Magnetic resonance imaging of progressive cardiomyopathic changes in the db/db mouse. *Am J Physiol Heart Circ Physiol*. 2007;292:H2106-H2118..

Chapter 2

Materials and Methods

2.1. Antibodies and reagents

Cell culture media and supplements were purchased from Highveld Biological (Cape Town, South Africa) and Invitrogen (Carlsbad, CA). Intracellular-bound GLUT4 antibody was purchased from Santa Cruz Biotechnologies (Santa Cruz, CA) and membrane-bound GLUT4 antibody from Chemicon International (Temecula, CA). The following products were purchased from Sigma-Aldrich (St Louis, MO): human insulin, anti c-myc monoclonal antibody (clone 9E10), Hoechst 33342 (DAPI) stain, wortmannin, 5 aminoimidazole 4 – carboxamide riboside (AICAR) and 6-diazo-5-oxo-L-norleucine (DON).

We also purchased the following products from Jackson Immunoresearch (West Grove, PA): donkey serum, rabbit IgG Texas Red, mouse IgG Texas Red, R-phycoerythrin-conjugated donkey F(ab)2 anti-mouse IgG secondary antibody, rabbit IgG phalloidin- fluorescein isothiocyanate (FITC), mouse IgG Fluorescein isothiocyanate (FITC). The anti-O-GlcNAc (CTD110.6) antibody was purchased from Pierce Biotechnology (Rockford, IL), O-(2-acetamido-2-deoxy-D-glucopyranosylidene) amino-N-phenyl-carbamate (PUGNAc) from CarboGen Labs (Aarau, Switzerland) and β-dystroglycan (4F7) from Santa Cruz Biotechnologies (Santa Cruz, CA). The Lab-Tek chambered coverglass was bought from Nunc Lab-Tek (South Africa), FuGENE 6 transfection reagent from Roche (Penzberg, Germany) and myc-GLUT4-EGFP generously donated by Dr. Michael P. Czech (Massachusetts Medical School, USA).

2.2 Cell culture

H9c2 cells (ECACC No. 88092904), a cardiomyoblast cell line derived from embryonic rat cardiac tissue (Kimes and Brandt, 1976; Levy *et al.,*.,1996) were cultured in T75 culture flasks with Dulbecco's Modified Eagle's Medium (DMEM; Highveld Biological Cape Town, South Africa) supplemented with 10% foetal calf serum (Invitrogen, Carlsbad, CA) and 4 mM L-glutamine (Invitrogen, Carlsbad, CA). The cells were then incubated at 37ºC under an atmosphere of 95% air and 5% CO_2 until it reached 70% - 80% confluency.

2.3 Experimental protocol for the assessment of GLUT4 translocation

H9c2 cells were subcultured and incubated for 24 hours. After subculturing the cells were resuspended in a 50 ml Falcon tube (Greiner Bio-One, Germany). The cell count was then adjusted to ~ 1 million cells/ ml (Fig. 1). Cells were then subcultured onto a Lab-Tek chambered coverglass for 24 hours to allow it to be anchored on the surface of the chambered slides (Fig. 2). About 15,000 cells (15 µl) per chamber were subcultured with 500 µl preparation media that consisted of DMEM, 10% foetal calf serum and 4 mM L-glutamine. This amounts to a total of 515 µl of medium (500 µl preparation media + 15 µl H9c2 cells) per Nunc chamber. Gentle pipetting of cells (up and down) with a 1 ml pipette is crucial to prevent clumping-clustering of cells before its plating anchorage to the surface of the chambered slides. Cells were then incubated for 24 hours at 37ºC under an atmosphere of 95% air and 5% CO_2, where after we performed insulin treatments.

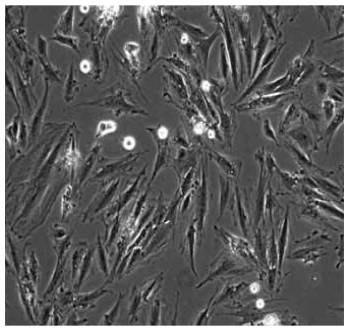

Figure 1. Photograph of H9c2 cardiac-derived myoblasts, 70-80% confluent before subculturing onto Lab-Tek chambered coverslides

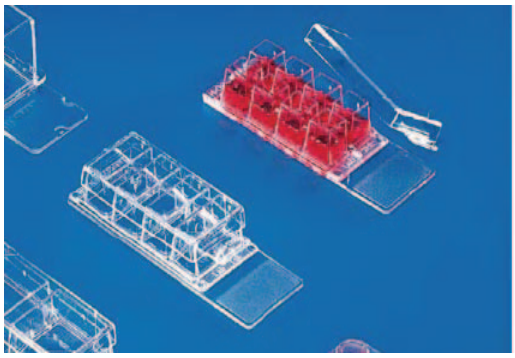

Figure 2. Lab-Tek chambered coverslides employed for subculturing of H9c2 cells

2.3.1 Treatment of H9c2 cells with insulin

On the day of the insulin treatments, the insulin stock solution was prepared as follows:

(i) Pipette 290 µl of human insulin from original container and transfer into a 1 ml microcentrifuge tube (Greiner Bio-One, Germany)

(ii) Make up 710 µl PBS (phosphate buffer saline) in a 1 ml microcentrifuge tube

(iii) Combine these aliquots to a final volume of 1 ml = 710 µl PBS + 290 µl of human insulin.

Various insulin concentrations were tested in this study (Table 1). However, cells were serum starved for at least 3 hours before insulin treatments.

Chamber #	**Insulin concentration (nM)**	**Volume of insulin pipetted (µl)**
1	0	0
2	10	18
3	50	90
4	100	180

Table 1. Insulin treatments performed and various volumes pipetted.

We also assessed the temporal nature of insulin-mediated stimulation of GLUT4 translocation (Table 2).

Chamber #	**Insulin concentration (nM)**	**Volume of insulin pipetted (µl)**	**Duration of treatments (minutes)**
1	100	180	0
2	100	180	2
3	100	180	5
4	100	180	30

Table 2. The experimental protocol to evaluate temporal nature of insulin-mediated GLUT4 translocation.

2.3.2 Immunofluorescence microscopy

H9c2 cells were grown in Lab-Tek chambered cover slides and incubated for 24 hours in preparation media consisting of DMEM, 10% foetal calf serum and 4 mM L-glutamine. Cells were cultured in high glucose (25 mM) and low glucose (5 mM) media for 24 hours. Subsequently, cells were serum starved for 3 hours and thereafter stimulated with 100 nM insulin for 5, 15 and 30 minutes. However, we also

employed 100 nM wortmannin or AMPK activators for at least 60 minutes prior to insulin stimulation. The insulin treated cells were now ready for immunolabeling or staining procedures. Cells were washed with cold 0.1 M PBS immediately after insulin treatment to block further insulin effects. The cells were then fixed with 1:1 methanol and acetone solution to permeabilize for the cell membrane, to allow access for the primary antibodies into the cell. Cells were also fixed with formal saline to allow the membrane-bound antibodies to react to the cell membrane. The cells were hereafter incubated at 4ºC for 10 minutes. The fixative was then removed and cells were air dried for 20 minutes. Cells were thereafter rinsed with PBS and then blocked with 5% donkey serum in PBS for 20 minutes. At least 50 µl of donkey serum was used per chamber. Subsequently, the serum was drained and a cocktail of primary antibodies prepared:

(i) membrane-bound GLUT4 antibody (1:200 dilution in PBS)

(ii) intracellular-bound GLUT4 antibody (1:50 dilution in PBS)

(iii) membrane marker β-dystroglycan antibody (1:50 dilution in PBS).

The formal saline fixative step was done first and the cells were then stained with a membrane-bound GLUT4 antibody (1:200 dilution in PBS) and incubated for at least 2 hours at 4ºC. The cells were then washed with PBS and then fixed again with methanol and acetone solution, and subsequently stained with an intracellular-bound GLUT4 antibody (1:50 dilution in PBS). Cells were incubated overnight at 4ºC, where after primary antibodies were washed off using PBS. We then prepared the secondary antibodies:

(i) The intracellular-bound GLUT4 antibody was targeted by the FITC anti-rabbit IgG antibody (1:200 dilution in PBS)

(ii) The membrane bound-GLUT4 antibody and β-dystroglycan antibody were targeted by Texas Red donkey anti-rabbit IgG antibody (1:100 dilution in PBS).

It is important to centrifuge antibodies after the mixing process to remove any crystal formation that distorts visual images obtained by immunofluorescence microscopy. Cells were incubated with the secondary antibodies for 30 minutes at room temperature. Furthermore, it was incubated for 10 minutes with 100 µl Hoechst (DAPI; 1:200 dilution in PBS). The cells were then rinsed with PBS (at least 5 times) and then viewed by immunofluorescence microscopy (Olympus IX 81 microscope equipped with the Cellˆ® software; Loos, 2006). The fluorescence intensity and z-stack analysis was performed as described (Loos, 2006).

2.3.3 Co-localization analysis

Co-localization refers to the presence of two or more types of molecules at the same physical location. Therefore it involves comparison of the spatial localization of two proteins. Within the context of digital imaging it means the colours emitted by fluorophores, i.e. FITC (green) and Texas Red share the same pixel in the image. For example, overlapping of FITC (green) and Texas Red produces a yellow colour. A technique called FRET (fluorescence resonance energy transfer) may be used to obtain higher resolution, and for measuring the interaction between two proteins. Here two different fluorophores (donor and acceptor) are used to label the proteins of interest. FRET is observed by exciting the sample at the donor excitation wavelength and measuring fluorescence intensities emitted at the wavelengths corresponding to the emission peaks of the donor compared to those of the acceptor (Fig. 3).

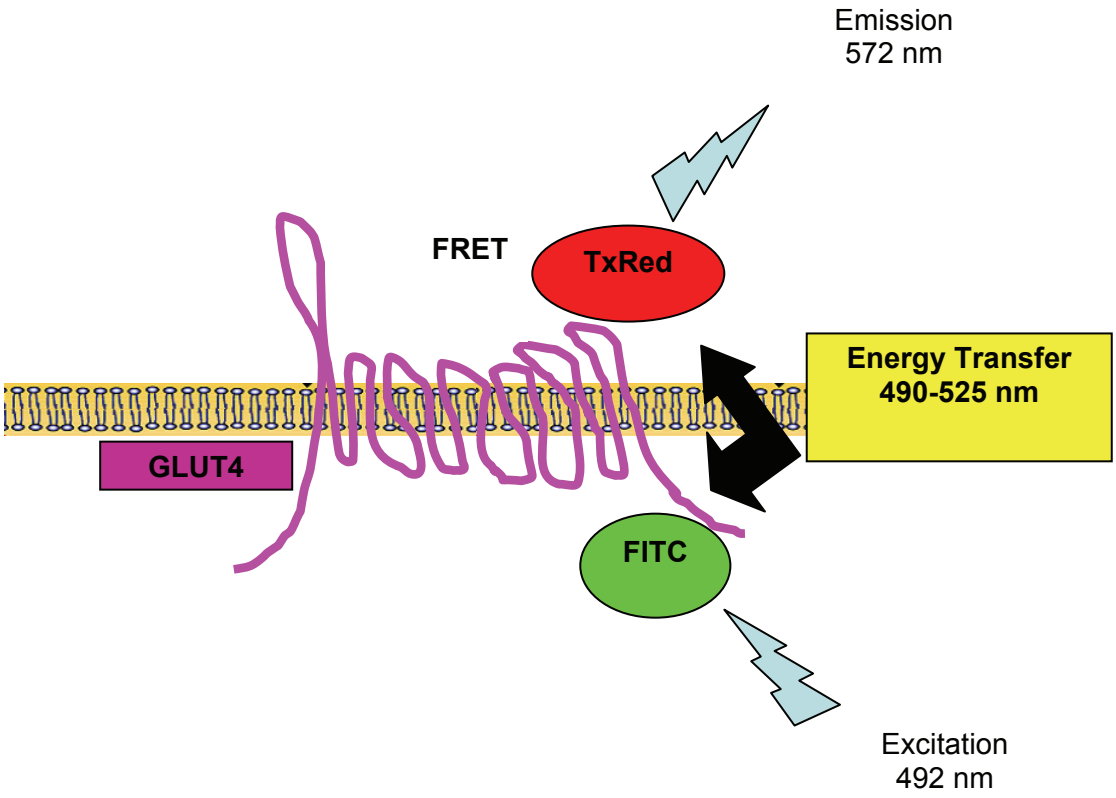

Figure 3. An overview of FRET (fluorescence resonance energy transfer), that measures protein-protein interactions. The blue Argon-ion laser excites the FITC fluorophore at 488 nm, close to FITC's absorbance peak of 492 nm. FITC emits fluorescence (475-700 nm) that falls within the green spectrum. In parallel, the Argon-ion laser excites Texas Red at 572 nm, emitting fluorescence (550-700 nm) that falls within the red spectrum. An energy transfer takes place between 490-525 nm. Here the green and red colours appear in the same spectral plane and therefore produces a yellow colour.

When the donor and the acceptor are in close proximity (1-10 nm) due to the interaction of the two candidate proteins, the acceptor emission is predominantly observed because of the intermolecular FRET from the donor to the acceptor (Gordon G. *et al.,*1998; Sohn H-W. *et al.,* 2006; Treanor B. *et al.,* 2006; Hunger, K. *et al.,* 2006; Herrick-Davis, K. *et al.,* 2006; and Kramer, J. *et al.,* 2006).

2.4 Assaying GLUT4 trafficking to the plasma membrane

2.4.1 Transfection with GLUT4

Construction of a GLUT4 reporter. The Myc-GLUT4-EGFP construct was generously donated by Dr. Michael P. Czech (Massachusetts Medical School, USA). The generation of this construct was described previously (Jiang *et al.,* 2002). Here site – directed mutagenesis was performed within the GLUT4 cDNA by inserting the DNA sequence encoding myc epitope (AEEQKLISEEDLLK) between the 66th and 67th amino acid of GLUT4. A PCR fragment of EGFP was inserted at the end of GLUT4 and the final myc-GLUT4-EGFP clone was excised by EcoRI and XbaI restriction enzymes and then inserted into a modified pGreen Lantern Vector.

Transfection method. H9c2 cells were subcultured in Lab-Tek chambered coverslides and incubated in preparation media consisting of DMEM, 10% foetal calf serum and 4 mM L-glutamine. Four microcentrifuge tubes were each filled with 100 µl DMEM and 1 µg myc-GLUT4-EGF added per tube. The contents were briefly mixed for 5 seconds, where after 10 µl of FuGENE 6 was added. Again the tube contents were gently mixed, but not vortexed. Samples containing the DNA and the FuGENE 6 were then incubated for 15 minutes at room temperature. Meanwhile, media in the Lab-Tek chambered coverslides with the H9c2 cells was removed and replaced with fresh media. After the 15 minute incubation period, 100 µl of the DNA and FuGENE 6 mixture was added to each Lab-Tek well. Cells were then incubated for 48 hours at 37ºC under an atmosphere of 95% air and 5% CO_2. This is an important step since sufficient time is allowed for cells to make the myc-GLUT4-EGFP protein. However, it is important to replace the media the following day to blunt the toxic effects of FuGENE 6 on cells incubated for a 48-hour period.

2.4.2 Immunofluorescence microscopy

To observe myc-GLUT4-EGFP translocation in the H9c2 cells, the cells were washed, fixed, and immunostained as described above under the immunofluorescence microscopy section. The cell surface myc-GLUT4-EGFP was detected with an anti-myc monoclonal antibody (clone 9E10). The secondary antibody employed was Texas Red donkey anti-rabbit IgG antibody (1:100 dilution in PBS). Cells were then viewed by immunofluorescence microscopy (Olympus IX 81 microscope equipped with the Cellˆ® software; Loos, 2006). The fluorescence intensity analysis, z-stack analysis and co-localization analysis was done as described in (Loos B, MSc 2006).

2.4.3 Flow cytometry

Flow cytometry is a procedure that simultaneously measures the physical characteristics of single particles, usually cells, when flowing in a fluid stream through a beam of light (Watson, 2004). The properties that are measured include a particle's relative size FSC (forward scatter channel), relative granularity or internal complexity SSC (side scatter channel), and the relative fluorescence intensity FL (fluorescence channels). These characteristics are determined using an optical-to-electronic coupling system that records how the cell or particle scatters incident laser light and emits fluorescence. A flow cytometer consist of 3 main systems (Fig. 4):

(i) The fluidics system transports particles in a stream to the laser beam for evaluation

(ii) The optics system consists of lasers to illuminate particles in the sample stream, and optical filters that direct the resulting light signals to the appropriate detectors

(iii) The electronics system converts the detected light signals into electronic signals that can be process by the computer.

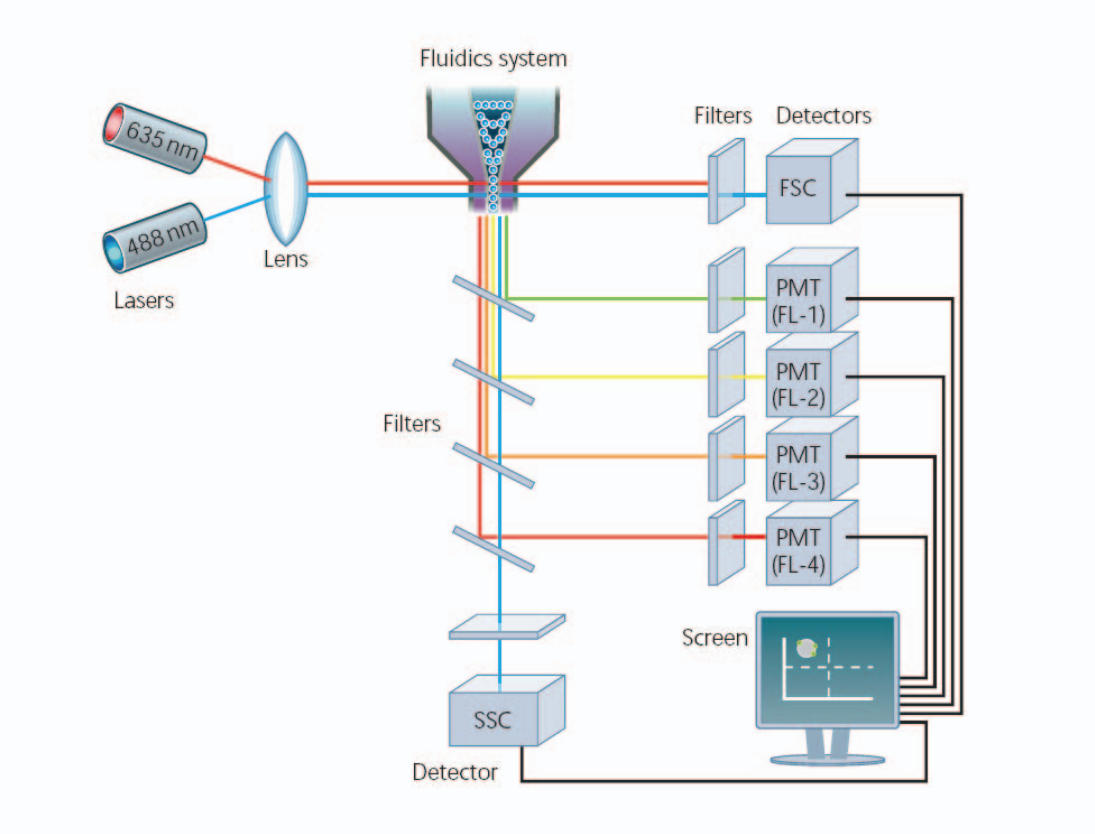

Figure 4. A schematic overview of a typical flow cytometry setup

Inside the flow cytometer particles are transported in a fluid stream to the laser intercept. Any suspended particle cell ~ 0.2-150 micrometers in size is suitable for analysis. When the particles pass through the laser intercept, it scatters laser light and any fluorescent molecules present on the particle will fluoresce. The scatter and fluorescent light is collected by appropriately positioned lenses. A combination of beam splitters and filters steer the scattered and fluorescent light to the appropriate detectors. The detectors produce electronic signals proportional to the optical signals striking them. The electronic signals are then processed by a computer that allows further evaluation of the data.

2.4.4 Measurement of plasma membrane GLUT4 trafficking by flow cytometry

H9c2 cells were sub-cultured in 6-well plates and then transfected as described above under the transfection method section, i.e. with the myc-GLUT4-EGFP construct. About 600, 000 cells/well were incubated with 1 ml/well of special media made of DMEM, 10% foetal calf serum and 4 mM L-glutamine for 48 hours at 37ºC under an atmosphere of 95% air and 5% CO_2. Prior to the insulin stimulation (100

nM), the cells were serum starved for 3 hours. The H9c2 cells in the 6-well plate were cultured and transfected according to the following system (Fig. 5):

Well 1 – Transfected cells + unstained cells

Well 2 – Transfected cells + phycoerythrin (PE)-stained control (no insulin)

Well 3 – Transfected cells + PE-stained

Well 4 – Transfected cells + PE-stained

Well 5 – Untransfected cells + unstained cells

Well 6 – Untransfected cells + PE-stained only

Note that the primary antibody used for untransfected cells was the membrane-bound GLUT4, since these cells were not transfected with the myc-GLUT4-EGFP.

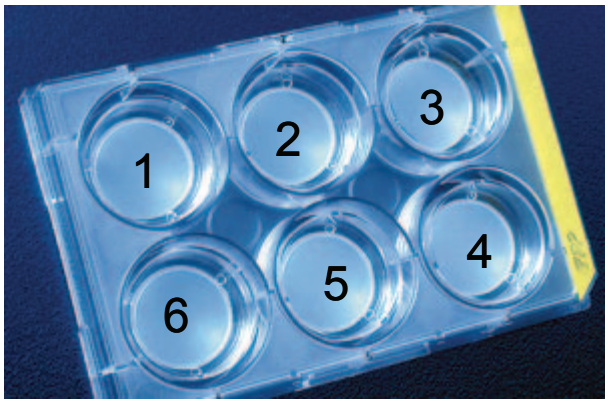

Figure 5.The 6-well plate with the numbers that correspond to the experimental protocol described above

After the transfection and insulin stimulation, all the cells except for well # 6, were stained with the primary antibody (anti-myc, monoclonal antibody 9E10) at 4ºC for 2 hours. Cells in well # 6 were stained with the membrane-bound GLUT4 primary antibody (1:200 dilution in PBS). After the 2 hour incubation period, cells were washed 3 times with PBS and incubated with PE secondary antibody (1:200 dilution in PBS) for 45 minutes. Note that it is also important to prepare the primary and secondary antibodies in 5% donkey serum and PBS. The cells were incubated for 45 minutes with the secondary antibody (1:200 dilution in PBS). After incubation, cells were trypsinized with 10 mM EDTA, 1 ml PBS and 10% FCS and then transferred to a flow cytometry tube for flow cytometric analysis using a BD FACS Aria cell sorter (BD Biosciences, San Jose, CA). The settings for flow cytometry for this protocol and the optimization of the instrument are as described (Bogan, 2001).

2.5 Increased HBP flux in vitro

2.5.1 High glucose and glutamine concentrations

H9c2 cells were subcultured in Lab-Tek coverslides for 24 hours and were there after incubated for 24 hours in high glucose media (25 mM) and 500 µl preparation media consisting of DMEM, 10% foetal calf serum and 4 mM L-glutamine. As before, cells were serum starved for 3 hours before stimulated with 100 nM insulin treatment. Before insulin stimulation the cells were then treated with HBP activators/inhibitors: 40 µM 6-diazo-5oxo-L-norleucine (DON; HBP inhibitor) and 50 µM O-(2-acetamido-2-deoxy-D-glucopyranosylidene) amino-N-phenyl-carbamate (PUGNAc; HBP activator). HBP modulators were added for at least an hour before insulin stimulation took place. Afterwards, cells were immediately washed with cold PBS to stop any further insulin stimulation and stained with primary and secondary antibodies as previously described in this thesis. GLUT4 translocation was there after assessed by immunofluorescence microscopy or flow cytometry.

2.5.2 Low glucose and glucosamine stimulation

H9c2 cells were subcultured in Lab-Tek coverslides for 24 hours and were there after incubated for 24 hours in low glucose media (5 mM) and 500 µl preparation media consisting of DMEM, 10% foetal calf serum and 4 mM L-glutamine. These cells were simultaneously cultured with 2.5 mM, 5 mM or 10 mM glucosamine concentrations for 24 hours. Cells were then serum starved for 3 hours, stimulated with 100 nM insulin for 5, 10 or 30 minutes, where after cells were immediately washed with cold PBS to stop any further insulin stimulation. Cells were then stained with primary and secondary antibodies as already described for the assessment of GLUT4 translocation by immunofluorescence microscopy or flow cytometry.

2.5.3 Over expression of the HBP rate limiting enzyme

2.5.3.1 Transfection methods

Transfection refers to the process of introducing foreign DNA into target cells by non-viral methods (Graham FL, van der Eb AJ, 1973). This process is distinct from infection, i.e. a viral method of introducing foreign DNA into cells. There are several transfection methods for the physical and chemical introduction of foreign DNA into target cells. The physical methods include e.g. microinjection, electroporation, nucleofection, heat shock and magnetofection (Promega methods). Chemical methods consist of transfection reagents that assist the transfer of exogenous DNA into target cells (Fig. 6). There are numerous chemical reagents employed for this purpose, e.g. DEAE-dextran, calcium phosphate and artificial liposomes (Promega methods).

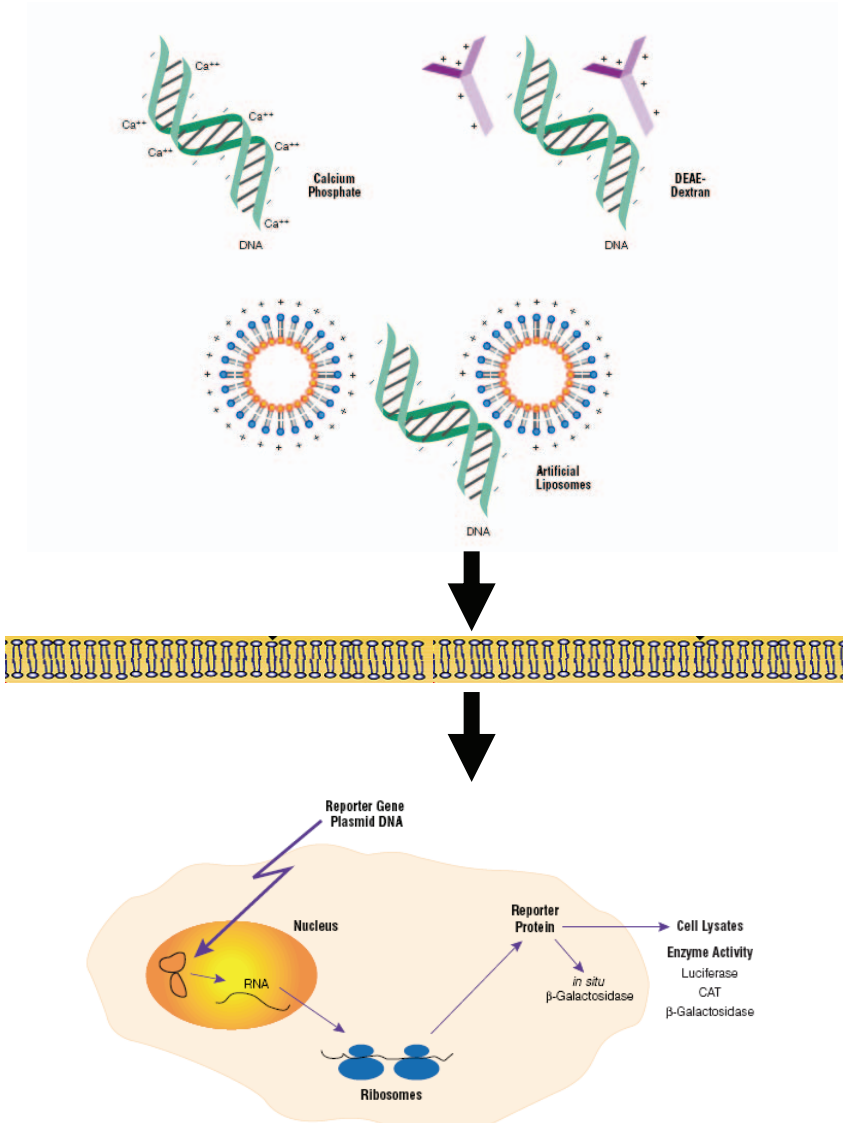

Figure 6. Schematic representation of transfection methods used

2.5.3.2 Experimental protocol

We used the exact transfection protocol established by Imbriolo (2008) in our laboratory. H9c2 cells were transfected with a GFAT expression construct kindly donated by Dr. Cora Weigert of the University of Tübingen (Germany) and 10 ng of pRL CMV-Renilla to correct for transfection efficiency. FuGENE 6 transfection reagent was diluted and then added to GFAT plasmid DNA. The FuGENE 6: DNA complex was incubated for 15 minutes at room temperature, where after it was added to the cells and incubated for 48 hours at 37ºC under an atmosphere of 95% air and 5% CO_2. The insulin stimulation and protocol for immunofluorescence microscopy are the same as described above under the insulin stimulation immunofluorescence microscopy section. The cells were then assessed for GLUT4 translocation by immunofluorescence microscopy.

2.5.4 Assessment of the degree of O-GlcNAcylation using immuno-fluorescence microscopy

H9c2 cells were subcultured in Lab-Tek coverslides for 24 hours and were then incubated for 24 hours in either low glucose (5 mM) or high glucose media (25 mM). We also cultured cells in the presence of 500 µl preparation media consisting of DMEM, 10% foetal calf serum and 4 mM L-glutamine. Cells were co-transfected with GFAT plasmid DNA and a dominant negative construct pcDNA3-GFAT667 as previously described by our laboratory (Imbriolo, 2008). Cells were probed with a primary O-GlcNAc antibody coupled to FITC green. The degree of GlcNAcylation was assessed using immunofluorescence microscopy.

2.6 Western Blotting analysis

2.6.1 Protein purification

Protein extracts were generated from heart muscle tissue of 18-20 week old transgenic db/db mice. This is a well described model of obesity induced type 2 diabetes, and its phenotype results due to a defective leptin receptor (101-103).

Heart tissue was homogenized 3 times for 5 seconds each time, using a Polytron homogenizer for 5 seconds. The total protein was extracted with ice-cold lysis buffer (modified radioimmunoprecipitation [RIPA] (buffer), pH 7.4, containing: 2.5 mM Tris/HCL, 1 mM ethylenediaminetetra-acetic acid (EDTA), 50 mM NaF, 50 mM NaPPi, 0.1 mM dithiothreitol-1 (DTT), 2 mM Phenylmethylsulfonyl fluoride (PMSF), 0.1 mM benzamidine, 1,4 µg/ml soybean trypsin inhibitor (SBTT), 10 µg/ml leupeptin, 1% NP40, 0.1% SDS and 0.5% Na deoxycholate. The homogenates were transferred to micocentrifuge tubes and then centrifuged for 10 minutes at full speed in a microfuge and thereafter incubated for 1 hour at 4°C. The supernatant was collected and transferred to fresh microcentrifuge tubes and centrifuged for 10 minutes at 4°C. The supernatant was collected again and stored at -80°C.

2.6.2 Bradford protein quantification

The Bradford protein assay is an accurate, rapid and sensitive spectroscopic analytical procedure used to measure protein concentration (Bradford *et al.,* 1976). The assay relies on the binding of the dye Coomassie Briliant Blue G-250 to protein and the intensity of colour measured at 595 nm is proportional to the protein concentration in the sample. The absorption at 595 nm is measured using a spectrophotometer (Cary/Varian Inc., North Carolina).

2.6.2.1 Experimental protocol for Bradford quantification of proteins

Before a standard curve was designed, the following reagents were first prepared.

Bradford reagent

- 100 mg Coomassie Brilliant Blue G-25 in 50 ml 95% ethanol
- Add 100 ml 85% (w/v) phosphoric acid before mixing it thoroughly
- Dilute to 1 liter with distilled water and filter through Whatman # 1 paper
- To rid the reagent of the blue colour, a continuous filtration is necessary until the reagent turns to a light brown colour
- The reagent is now ready to use

Bradford method

- Thaw 1 mg/ml bovine serum albumin (BSA) stock solution
- Thaw protein samples if frozen and keep on ice at all times

- Make up a working stock solution of 100 µl BSA: 400 µl distilled water, and vortex thereafter
- Mark 7 microcentrifuge tubes for standards and also 7 tubes for the unknown protein samples
- Transfer BSA and distilled water to the marked centrifuge tubes as stipulated in Table 3

BSA working stock (µl)	Protein (µg)	Distilled water (µl)	Bradford reagent (µl)
100	20	0	900
80	16	20	900
60	12	40	900
40	8	60	900
20	4	80	900
10	2	90	900
0	0	100	900 (blank)

Table 3. Working solutions for the establishment of the Bradford standard curve.

The dilutions indicated (Table 3) were incubated for 5 minutes at room temperature. At least 95 µl distilled water and 900 µl of Bradford reagent were added to the sample tubes. The solutions were incubated for 5 minutes at room temperature. In the meanwhile, the spectrophotometer was switched on and the absorbance was measured (semi-micro cuvettes) at 595 nm wavelength against a reagent blank (Table 3). However, if sample absorbance fell outside the range of the highest standard, then a dilution was made using RIPA buffer. The weight of protein in µg/ml was plotted using Excel software and the amount of sample to be added to aliquots was accordingly calculated.

2.6.3 Sodium-dodecyl-sulfate-polyacrylamide gel electrohoresis (SDS-PAGE)

A sample buffer was prepared containing 0.5 M TRIS, pH 6.8, 0.2 ml 0.5% bromophenol blue, 2.5 ml glycerol, 10% SDS and distilled water. At least 850 µl of sample buffer was added to 150 µl of mercaptoethanol. A number of aliquots were prepared by the addition of the required amount of sample buffer (obtained from Excel plot). The aliquots were boiled for 5 minutes, centrifuged for 15 seconds in a microfuge and then stored at -80°C. Equal amounts of samples (15-40 µg) were

subjected to SDS-polacrylamide gel electophoresis (PAGE; 4% stacking gel and 10% separation gel).

2.6.4 Immunoblotting

After SDS-PAGE, proteins were transferred to a polyvinylidene difluoride (PVDF) membrane (Millipore, Bedford, MA) using a semi dry transfer system (Bio-Rad, Hercules, CA). The system was allowed to run for 2 hours (0.5 A and 15 V). The membrane was thereafter blocked in 5% non-fat dry milk in Tris-buffered saline-0.1% Tween 20 (polyoxyethylenesorbitan monolaurate, Tween 20; TBS-Tween) buffer for 2 hours at room temperature. The membrane was washed 5 times for 5 minutes, and then incubated overnight at 4°C with a primary antibody that is directed at the C-terminus of GFAT. The latter was kindly donated by Dr. Cora Weigert of the University of Tubingen (Germany). We employed a dilution of 1:3000 of GFAT antiserum for Western blotting analysis. Given that GFAT1 and GFAT2 are identical at the same location (C-terminus), the antibody employed will recognize both isozymes (Schleicher *et al.,* 2000). After the overnight incubation, the membrane was then washed for 30 minutes with TBS-T buffer (changed every 5 minutes) before a one hour incubation with a 1:10,000 diluted horseradish peroxidase-labelled secondary anti-rabbit antibody (Amersham Life Sciences, Arlington Heights, IL) at room temperature. Blots were washed of excess antibody and then developed by a light-emitting nonradioactive method, i.e. using ECL reagent (Amersham Life Sciences, Arlington Heights, IL). Immunoreactive proteins were quantified by densitometry as is routinely done in our laboratory (UN-SCAN-IT, Silkscience, Utah).

2.7 Statistical analysis

Statistical analysis was performed with the INSTAT statistical package (Graphpad Software, San Diego, CA). Significance was defined as $P < 0.05$.

2.8. References

Bogan JS., McKee AE., Lodish HF. Insulin-responsive compartments containing GLUT4 in 3T30L1 and CHO cells: Regulation by amino acid concentrations, Molecular and Cellular Biology 2001;4785-4806

Bradford MM. (1976) A Rapid and Sensitive Method for the Quantitation of Microgram Quantities of Protein Utilizing the Principle of Protein-Dye Binding. Anal. Biochem. 72:248-254.

Coleman DL., Hummel KP.: Hyperinsulinemia in pre-weaning diabetes(db) mice. Diabetologia 10 (Suppl.):607-610,1974

Coleman DL.: Diabetes-obesity syndrome in mice. Diabetes 31 (Suppl. 1): 1-6,1982

Ducluzeau PH., Fletcher LM., Vidal H., Laville M., Tavare JM. Molecular mechanisms of insulin-stimulated glucose uptake in adiposities, Diabetes Metabolism 2002;28,85-92

Given AL. (2002) Flow Cytometry: First principles, Second Edition. John Wiley and Sons, Inc. New York

Schleicher ED. and Weigert C. (2000) Role of the hexosamine biosynthetic pathway in diabetic nepropathy, Kidney International supplement 2000:77():S13-8

Watson JV. (2004). Introduction to flow cytometry, First paperback Edition, Cambridge University Press

Wyse BM., Dulin WE.: The influence of age and dietary conditions diabetes in the db mouse. Diabetologia 6:268-273, 1970

http://www.promega.com/guides/transfxn_guide/transfxn.pdf

www.amaxa.com

www.corning.com/life sciences

www.Midwest scientific.com

Chapter 3

Results

3. Increased HBP flux in vivo

3.1 Over-expression of GFAT in a db/db mouse

A transgenic db/db mouse strain was used to assess GFAT expression. The db/db mouse strain possesses a defective leptin receptor, leading to hyperphagia. This results in obesity and ultimately leads to the onset of type 2 diabetes. The db/db mouse therefore represents an ideal model to confirm our hypothesis in an *in vivo* context. Since the HBP represents a biochemical sensing mechanism for hyperglycemia and hyperlipidemia, we predicted that the db/db mouse would display increased GFAT expression. In agreement, our preliminary results show increased GFAT expression versus heterozygous db/+ controls (Fig. 1).

Figure 1. Immunoblot of GFAT for db/db male mice versus matched controls. Heart homogenates were subjected to 10% SDS-PAGE. Protein blots were probed with anti-GFAT and visualized following enhanced chemiluminescence.

3.2. Increased HBP flux in vitro

Since our *in vivo* data exhibited over-expression of GFAT, we set up an *in vitro* model trying to better elucidate the molecular mechanisms underlying HBP-mediated induction of insulin resistance.

3.2.1 Establishing optimized experimental protocol to detect GLUT4 translocation

3.2.1.1 Determination of optimal insulin concentration and peak response time

We began by stimulating H9c2 cells with different insulin concentrations (18, 50 and 100 nM) at various lengths of time (2 and 14 hours, respectively). The overnight stimulation was equivalent to the 14 hour time period (Fig. 2).

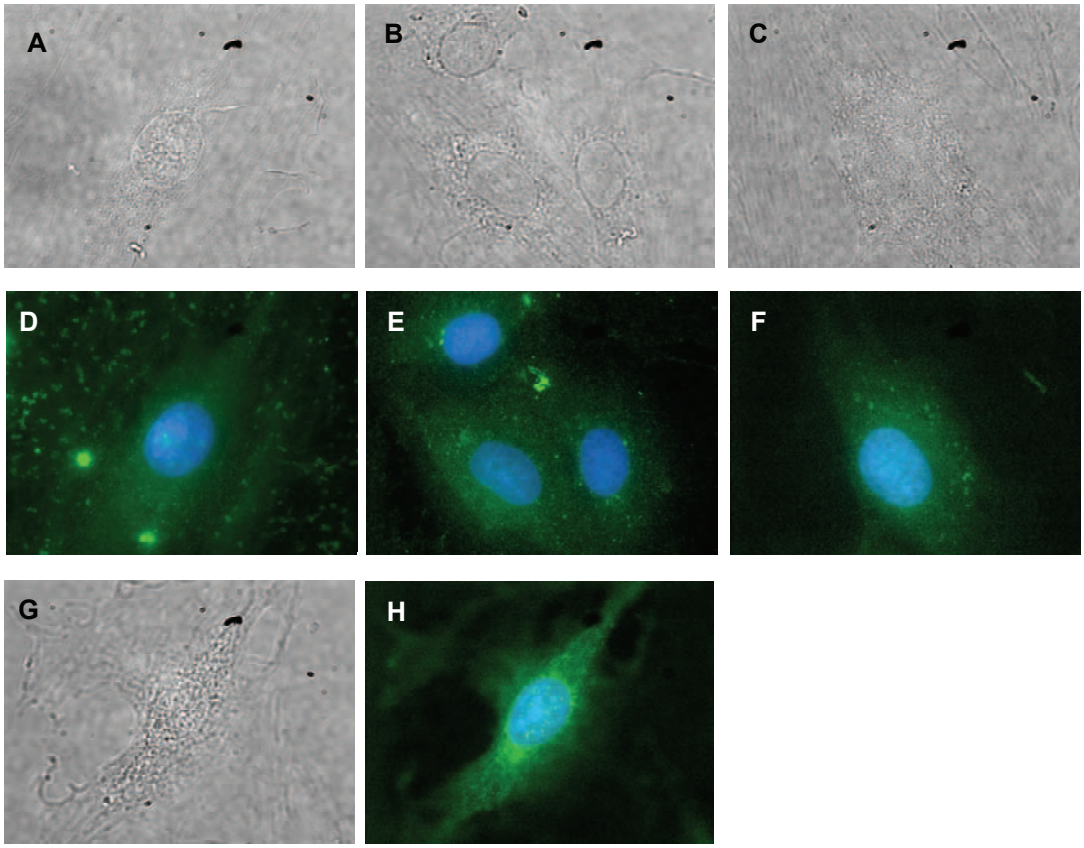

Figure 2. Evaluating GLUT4 translocation in response to varying insulin concentrations. A, B, C and G represents phase contrast images with 0, 18, 50 and 100 nM insulin, respectively, while D, E, F and H represents immunofluorescence microscopic images with various insulin concentrations (0, 18, 50 and 100 nM respectively). Pictures depicted are DAPI (blue), which stained the nuclei of the H9c2 cells, FITC (green)-labeled GLUT4 (D, E, F and H;60x oil immersion objective). Note the cells were stimulated with insulin for a 2-hour time period.

These data show that increasing insulin concentrations caused a progressive shift of green stain from the perinuclear region to further located regions within the cell. The key finding of these experiments was the optimal concentration of 100 nM insulin (Fig. 2H). This is consistent with the literature showing that 100 nM is the optimal *in vitro* insulin concentration for detecting GLUT4 translocation (Holman *et al.,* 1994; Pak *et al.,* 2005). However, we did not gain any information regarding the spatial-temporal aspects of GLUT4 vesicular translocation. We therefore repeated the same experiment, except that the cells were stimulated for 14 hours and treated with varying insulin concentrations (Fig. 3).

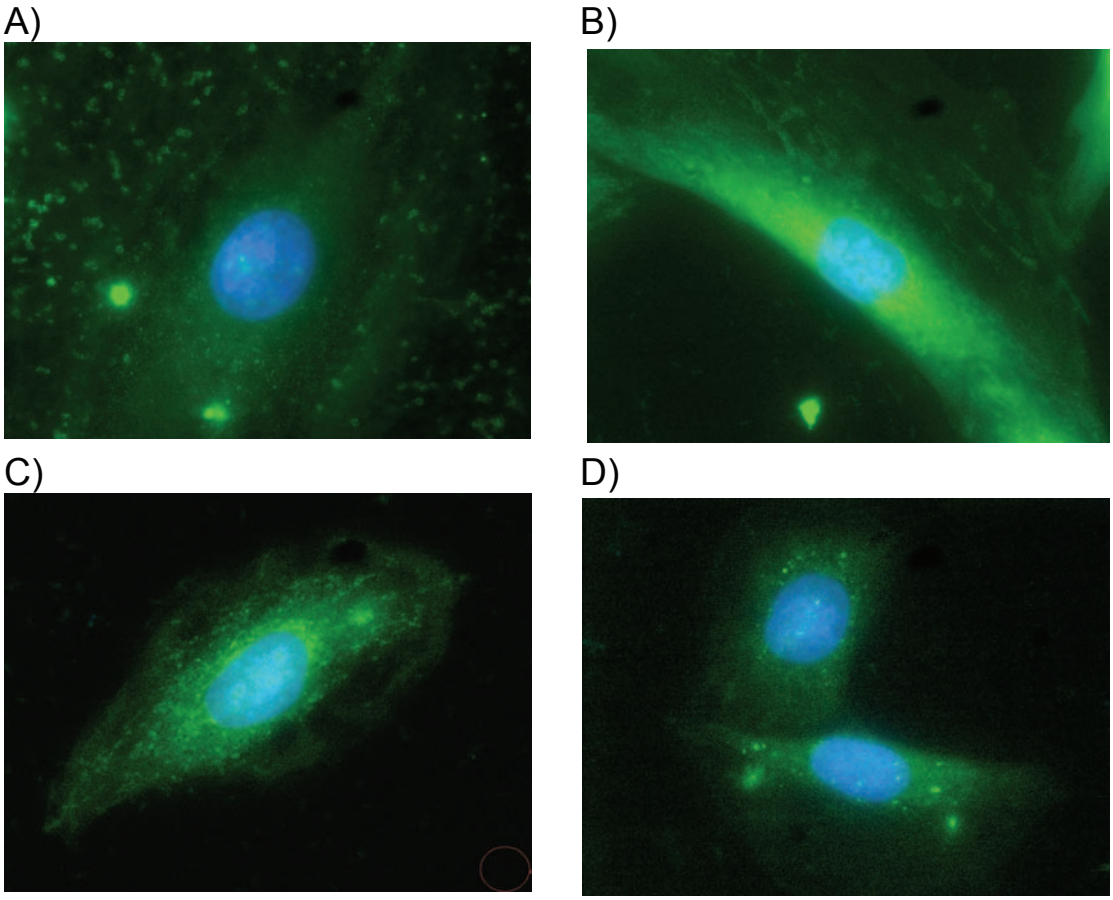

Figure 3. Evaluating GLUT4 translocation in response to varying insulin concentrations. A) – No insulin ; B) – 18 nM insulin ; C) – 50 nM insulin and D) – 100 nM insulin. Pictures depicted are DAPI (blue), which stained the nuclei of the H9c2 cells, FITC (green)-labeled GLUT4 (A, B, C and D;60x oil immersion objective). Note these cells were stimulated with insulin for a 14-hour time period.

Here, we again observed that GLUT4 vesicles centered around the nucleus, i.e. perinuclear arrangement before insulin stimulation (Fig. 3A). Upon insulin stimulation (18 nM) we found a diffuse pattern of GLUT4 vesicles that became more punctate with higher insulin concentrations, i.e. 50 and 100 nM insulin. Again, these data show the optimal insulin concentration, i.e. 100 nM. However, the peak response, i.e. the time point when the GLUT4 vesicles are actually at the sarcolemma, could still not be determined.

Since these images did not clearly define the precise moment(s) of GLUT4 translocation to the sarcolemma, we next amended our protocol by a) serum starving cells for 24 hours to improve the reaction to insulin stimulation and b) investigating shorter insulin stimulation times (5, 15 and 30 minutes, respectively; Fig. 4). We also performed z-stack analysis of these images (Fig. 5) to obtain additional insight into GLUT4 translocation to the sarcolemma.

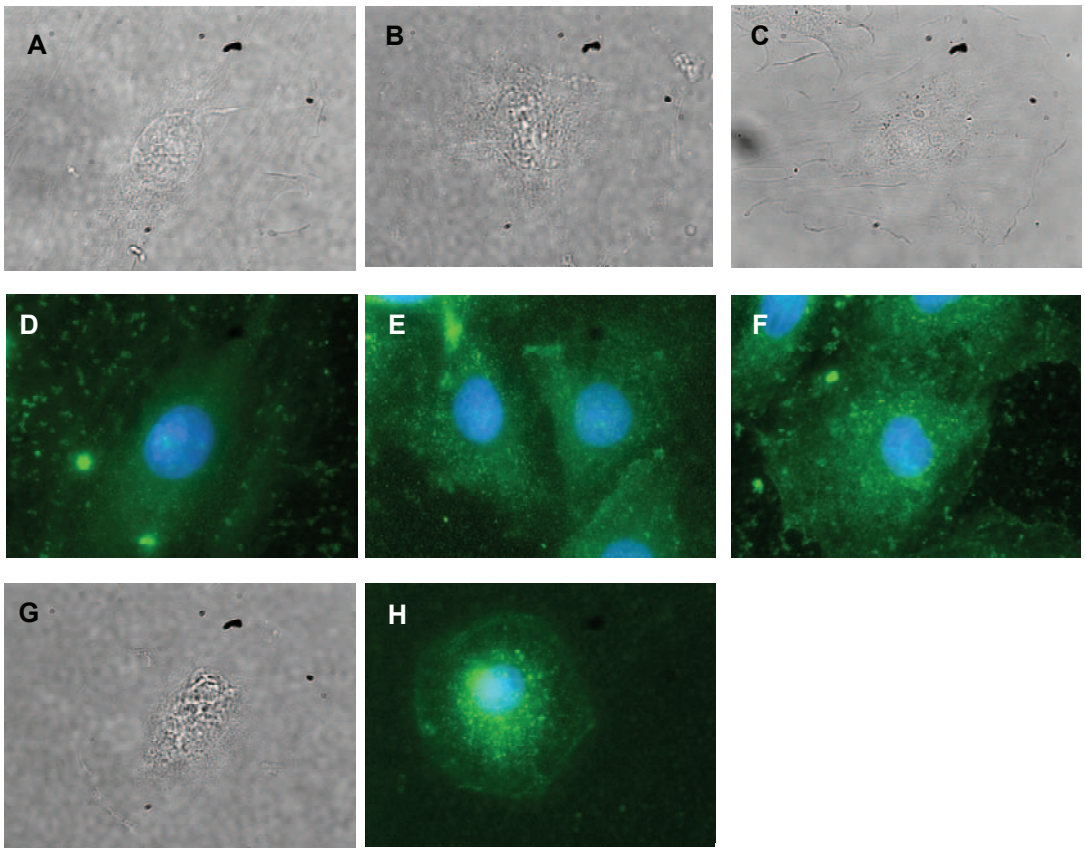

Figure 4. Evaluating GLUT4 translocation in response to shorter insulin stimulation times. H9c2 cells were exposed to 100 nM insulin for 5, 15 and 30 minutes, respectively. A, B, C and G represents phase contrast images with 100 nM insulin stimulation, while D, E, F and H represents immunofluorescence microscopic images with 100 nM insulin stimulation. Pictures depicted are DAPI (blue), which stained the nuclei of the H9c2 cells, FITC (green) labeled GLUT4 (D, E, F and H;60x oil immersion objective). A) and D) – 0 minutes; B) and E) – 5 minutes; C) and F) – 15 minutes and G) and H) – 30 minutes.

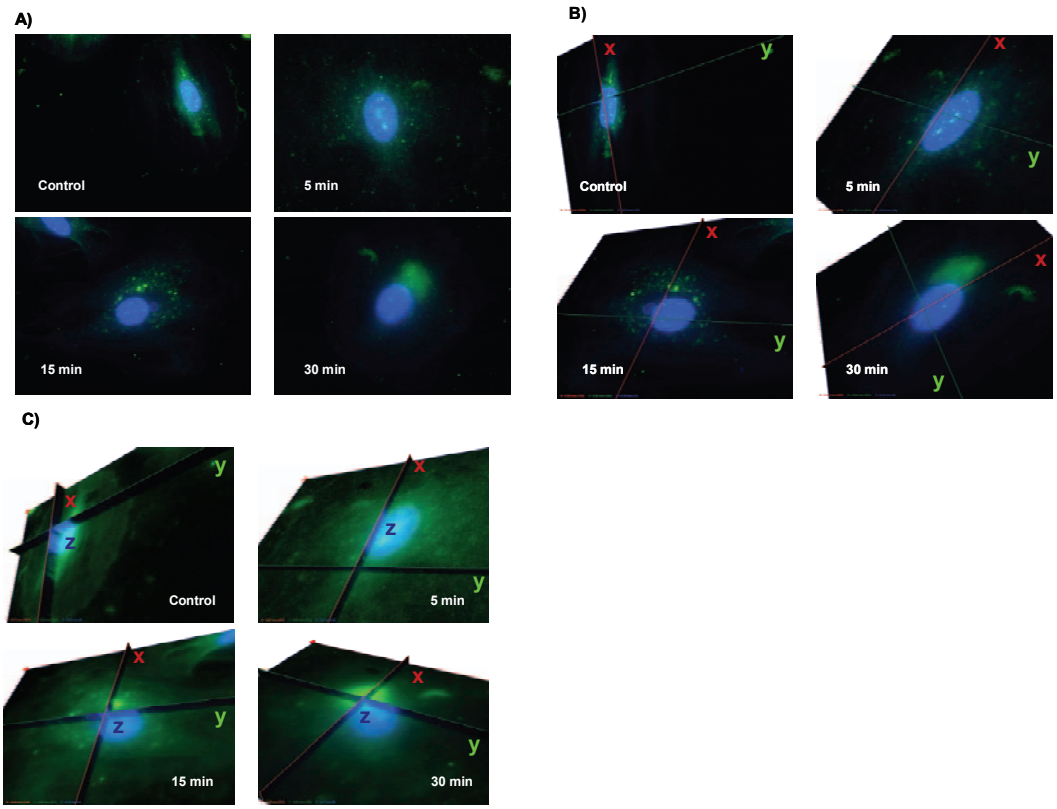

Figure 5. Immunofluorescence microscopy images showing z-stack analysis done on H9c2 cells stimulated with 100 nM insulin for the various time points indicated. A) – normal view; B – slice view with x, y and z spatial dimensions; and C) – slice view with x, y and z spatial dimensions together with the lower wall (60x oil immersion objective).

Together these data show that although translocation of GLUT4 vesicles can clearly be observed upon insulin stimulation, the peak response could still not be established.

3.2.2. Confirmation of GLUT4 translocation to sarcolemma

To confirm whether GLUT4 vesicles were indeed localized at the sarcolemma, we next co-stained cells with α-tubulin coupled to a Texas Red secondary antibody. GLUT4 translocation was then assessed using co-localization analysis (Fig. 6) as described in the Materials and Methods section of this thesis. The rationale for assessing the role of α-tubulin is that previous studies found that insulin-stimulated glucose uptake and redistribution of GLUT4 vesicles to the sarcolemma requires an intact microtubule cytoskeleton (Emoto *et al.,* 2001; Olson *et al.,* 2001; Patki *et al.,* 2001).

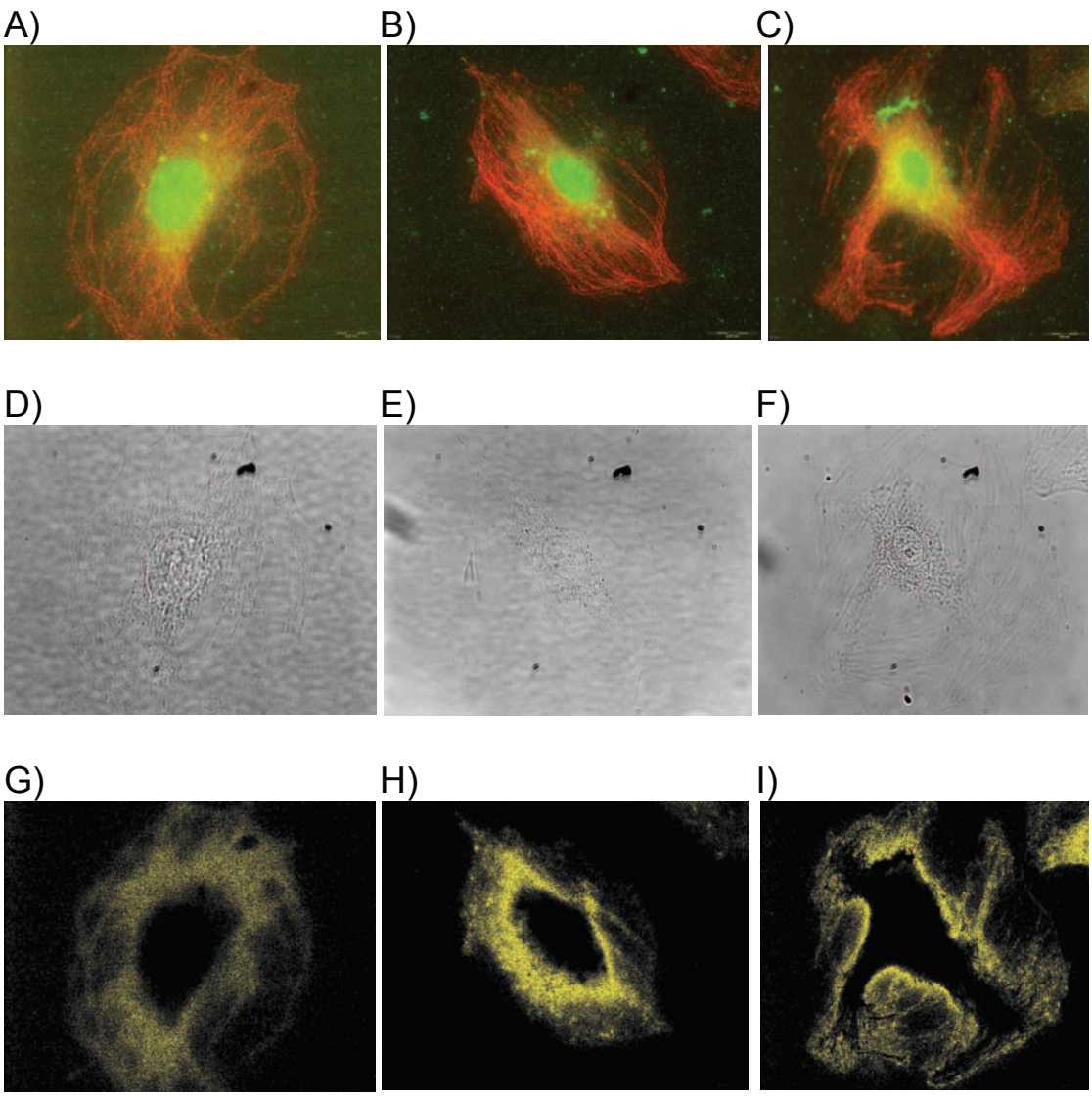

Figure 6. GLUT4 translocation assessed by α-tubulin staining of H9c2 cells. Immunofluorescence microscopy images (A – C) compared with phase contrast images (D – F) and co-localization images (G – I). H9c2 cells were serum starved for 3 hours and thereafter stimulated with 100 nM insulin for stipulated times (above). Green images represent the intracellular GLUT4 vesicles coupled to FITC, while red images represent α-tubulin coupled to Texas Red. Yellow images represent the co-localization analysis (overlap of green and red stains).

The α-tubulin experiments (co-localization) show GLUT4 vesicles are largely arranged around the nucleus and its immediate environment (endoplasmic reticulum and the *trans*-Golgi apparatus). These images did not, however, show clear translocation of GLUT4 to the sarcolemma. As a result, we next stained cells with β-dystroglycan, a membrane marker. Here cells were prepared with a fixation method

(using methyl-acetone) to permeabilize the sarcolema to allow primary antibodies to enter the cell (Fig. 7).

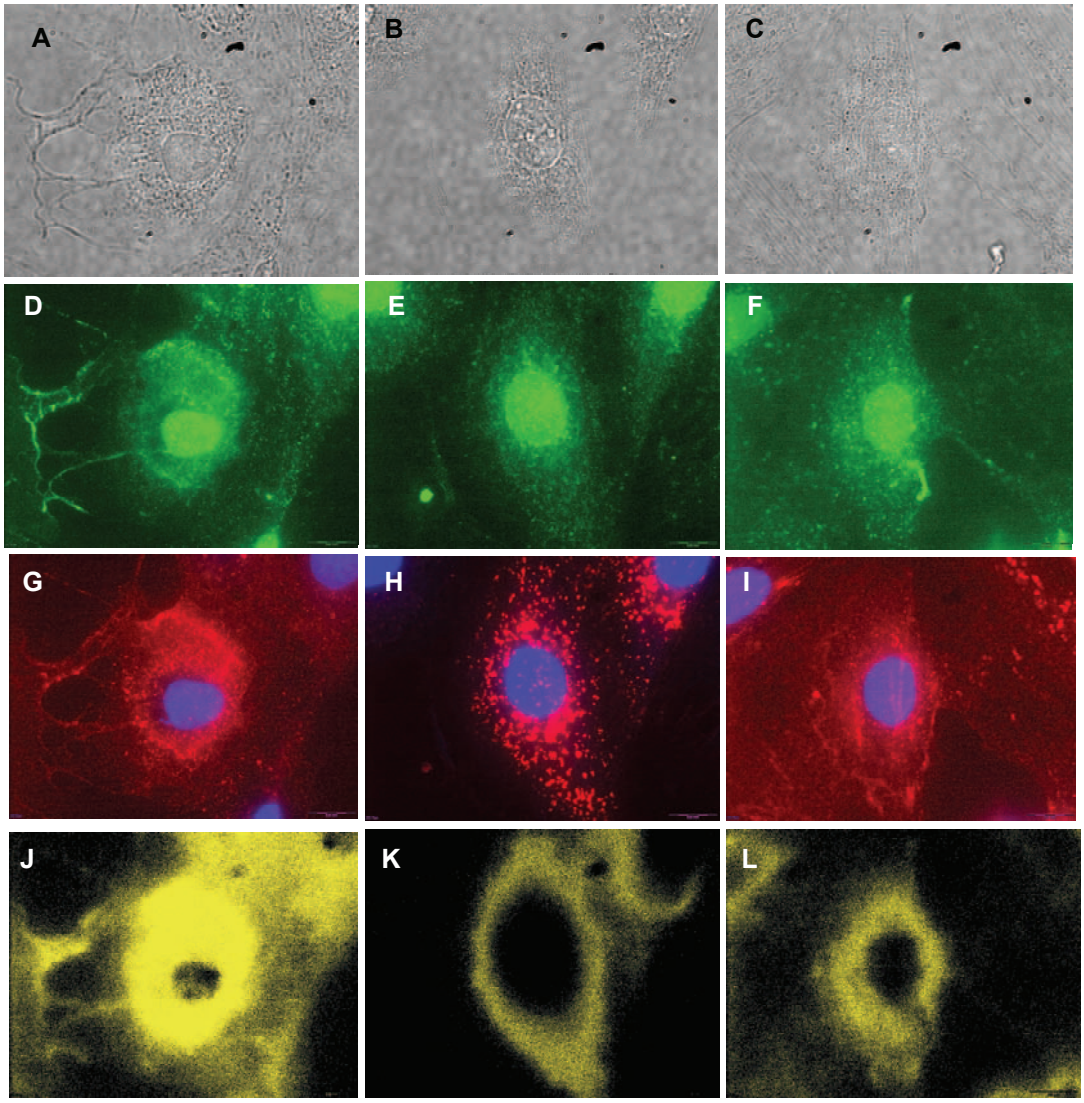

Figure 7. Evaluation of GLUT4 translocation using membrane marker (β-dystroglycan). A) – C) – phase contrast images ; D) – F) – intracellular GLUT4 vesicles coupled to FITC ; G) – I) – β-dystroglycan coupled to Texas Red ; J) – L) – Co-localization of green and red stains (60x oil immersion objective).

The β-dystroglycan studies show the peak response time, i.e. 5 minutes (Fig. 7K) after insulin stimulation the GLUT4 vesicles were actually at the sarcolemma.

3.2.3 Determination of cell line of choice

The next experiment was designed to compare the effects of insulin on H9c2 myoblasts with differentiated H9c2 myotubes, since one would expect that myotubes are more functional and would therefore respond better with insulin treatment.

However, no difference was observed in terms of GLUT4 translocation (Fig. 8). In the light of this, we employed H9c2 myoblasts for the rest of the study since it was easier to maintain and ensured a quicker turnover of results.

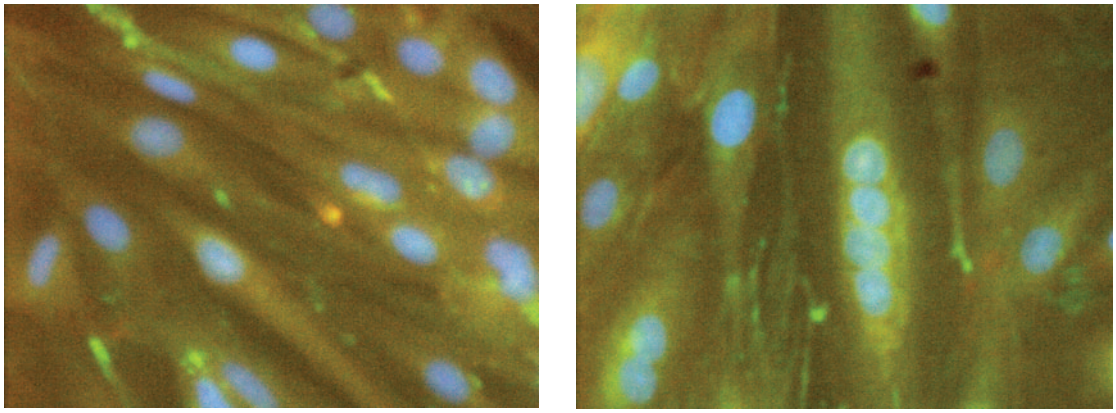

H9c2 myoblasts **Differentiated H9c2 myotubes**

Figure 8. H9c2 myoblasts and differentiated myotubes were serum starved for 3 hours and stimulated for 5 minutes with 100 nM insulin. Cells were stained with FITC and Texas Red to detect intracellular and sarcolemmal GLUT4 (60x oil immersion objective).

We also tested our protocol on different cell lines, including C2C12 myoblasts, L6 myoblasts, differentiated L6 myotubes and CV1 fibroblasts. Cells were stimulated with 100 nM insulin for 5 or 10 minutes, respectively, and GLUT4 translocation determined. However, these different cell types showed a relatively poor response in terms of GLUT4 translocation upon insulin stimulation (data not shown). These data further supported our cell line of choice for this study, i.e. H9c2 myoblasts.

3.2.4 Establishing the optimal protocol for GLUT4 translocation (immunofluorescence microscopy)

We next attempted to further refine our GLUT4 experimental assay. Here we employed intracellular and membrane-bound GLUT4 antibodies. Since we coupled the intracellular GLUT4 antibody to FITC (green) and the membrane-bound GLUT4 to Texas Red, we could do co-localization analysis to measure the differences in GLUT4 translocation. Moreover, we were able to quantify co-localization fluorescence intensities (Figs. 9 and 10). Here the characteristic perinuclear distribution is observed for the control with a spreading out after 5 minutes (peak response). After 30 minutes, there is a return to the perinuclear distribution (Fig. 9). These patterns are reflected in quantification of the yellow stain (Fig. 10).

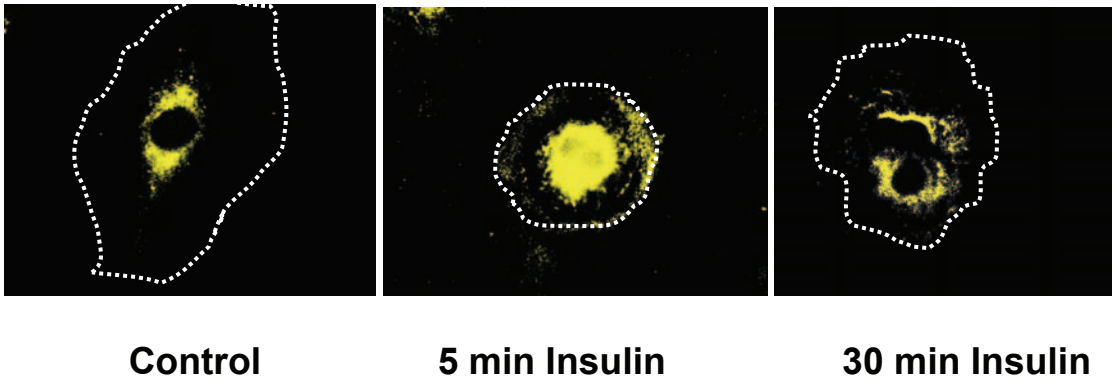

Figure 9. Co-localization analysis performed for H9c2 myoblasts. The dotted lines represent the outline of the sarcolemma. Cells were serum starved for 3 hours and then stimulated with 100 nM insulin for 5 or 30 minutes, respectively.

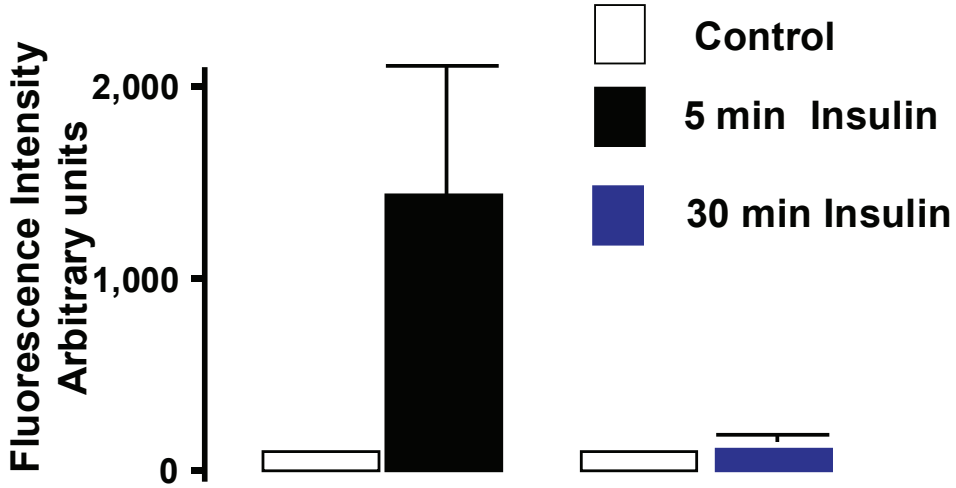

Figure 10. Quantification of co-localization (yellow) of intracellular GLUT4 (green) and membrane-bound GLUT4 (red) in response to insulin stimulation.

The key finding of this experiment was the establishment of the peak response time, i.e. 5 minutes time point when GLUT4 vesicles are located at the sarcolemma in response to insulin stimulation. GLUT4 vesicles subsequently return to the perinuclear region after 30 minutes. In light of these findings, we employed this experimental protocol throughout this thesis to investigate our hypothesis.

3.2.5 Transfection-based studies with fluorescent green-labeled GLUT4

3.2.5.1 Immunofluorescence microscopy-based studies

Since we successfully established an *in vitro* model for measuring wild-type GLUT4 translocation, we wanted to strengthen our results by assessing GLUT4 translocation using a novel reporter molecule under real time conditions. However, we transfected H9c2 cells with a GLUT4 construct which contains 7 c-Myc epitope tags in the first exofacial loop and enhanced green fluorescent protein (EGFP) fused in-frame at the carboxy terminus (Fig. 11). The cell surface Myc-GLUT4-EGFP was detected using an anti-myc monoclonal antibody (clone 9E10) labeled to Texas-Red and co-localization analysis was employed to assess GLUT4 translocation (Fig. 11).

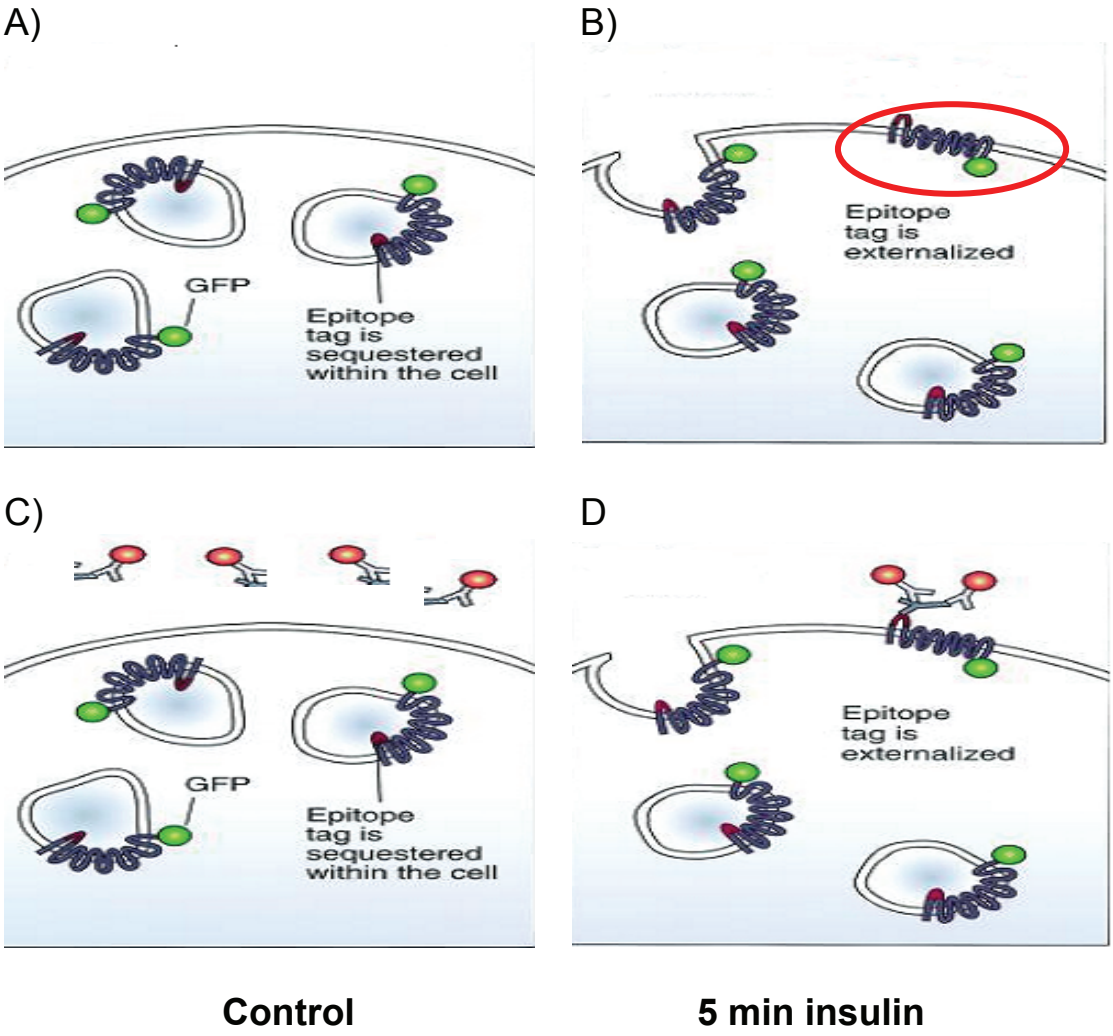

Figure 11. A schematic representation showing the effect of insulin stimulation on cells transfected with GLUT4-EGFP. After insulin stimulation, GLUT4 vesicles are detected on the sarcolemma by using a primary antibody specifically directed to the myc-GLUT4-EGFP construct. The cell surface Myc-GLUT4-EGFP anti-myc monoclonal antibody (clone 9E10) was then coupled to a secondary Texas Red antibody and visualized by immunofluorescence microscopy.

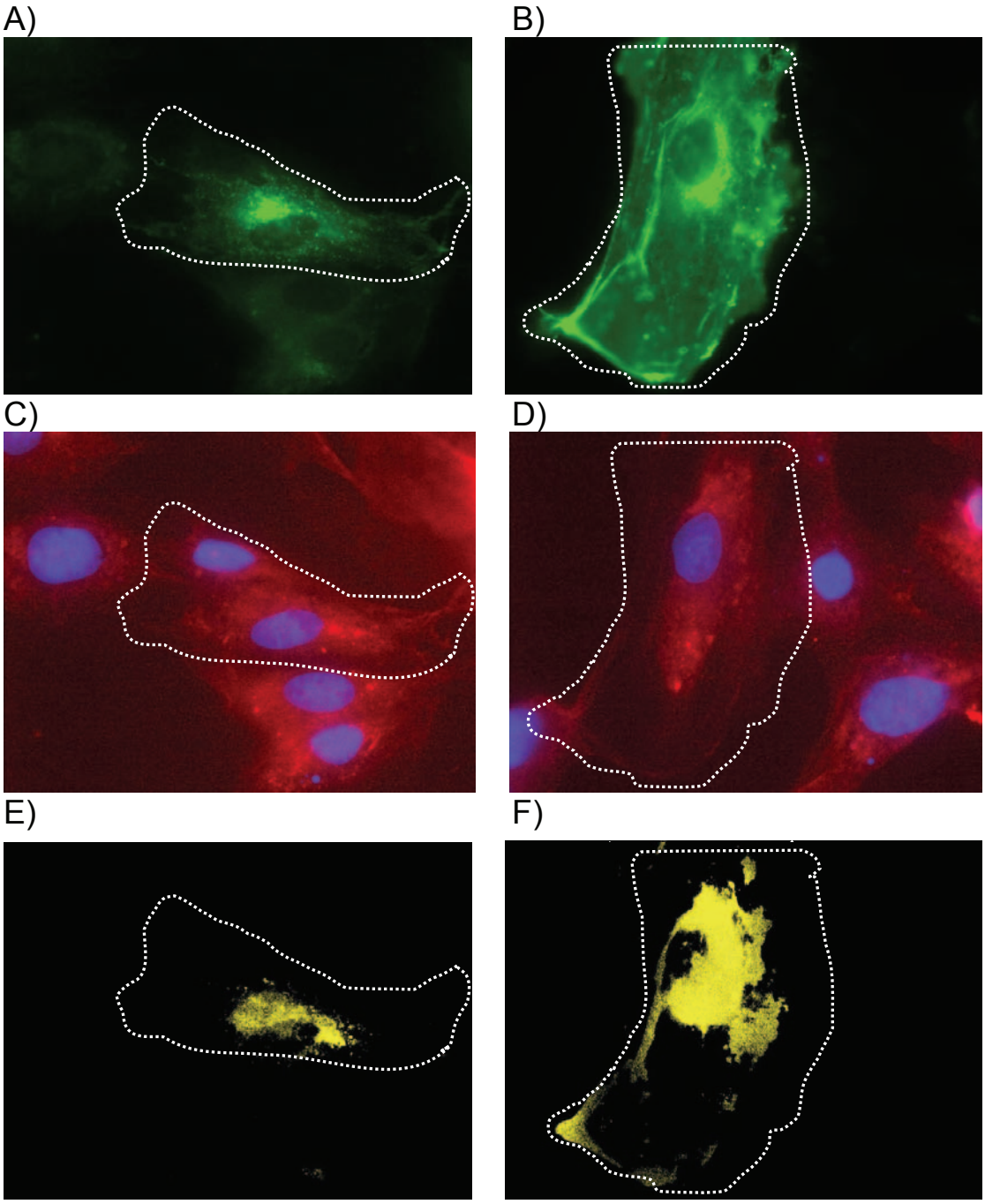

Figure 12. Immunofluorescence microscopy images demonstrating GLUT4 translocation in response to 5 minutes insulin stimulation. A) and B) fluorescent green-labeled GLUT4 ; C) and D) cell surface Myc-GLUT4-EGFP anti-myc monoclonal antibody coupled to a secondary Texas Red antibody. DAPI (blue) stains the nucleus; E) and F) Co-localization of green and red stains to assess GLUT4 translocation to the sarcolemma. The dotted lines represent the outlines of the sarcolemma.

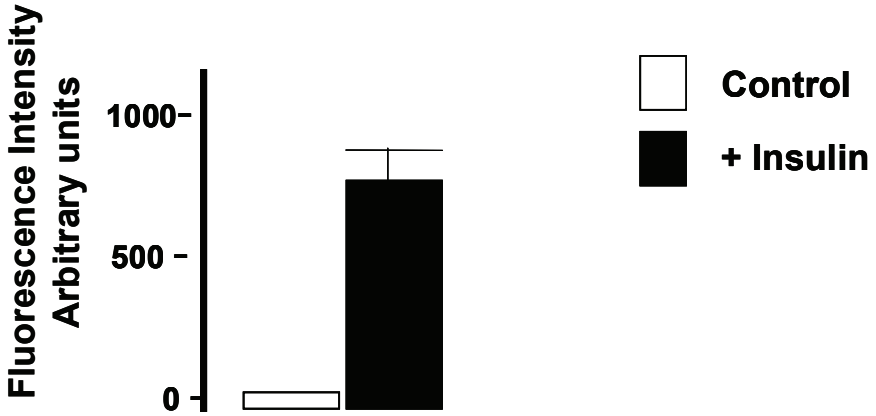

Figure 13. Quantification of co-localization (red and green stains overlapping) to assess GLUT4 translocation.

These data show that our transfection-based method was indeed successful, i.e. we could clearly detect GLUT4 translocation after 5 minutes of insulin stimulation (Figs. 12 and 13). We also observed that trafficking and location of the novel c-Myc-GLUT4-EGFP is similar to wild-type GLUT4.

3.5.2 Flow cytometry-based studies

We also quantified GLUT4 translocation by flow cytometry. H9c2 cells were stimulated with 100 nM insulin for 5 minutes and GLUT4 translocation was assessed by flow cytometry. Here, again we evaluated GLUT4 translocation using c-Myc-GLUT4-EGFP (Fig. 14). The cell surface Myc-GLUT4-EGFP was detected using an anti-myc monoclonal antibody (clone 9E10) labeled to phycoerythrin (PE; Fig. 15) and flow cytometric analysis was employed to assess GLUT4 translocation.

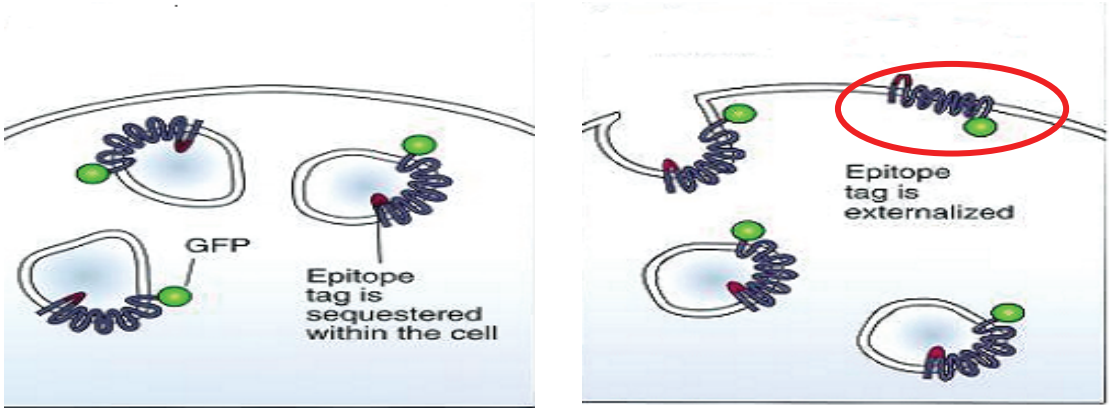

Control **5 min Insulin**

Figure 14. Schematic representation showing the effect of insulin stimulation on H9c2 cells transfected with the myc-GLUT4-EGFP. Note the GLUT4 vesicles translocated to the sarcolemma can be detected using flow cytometry.

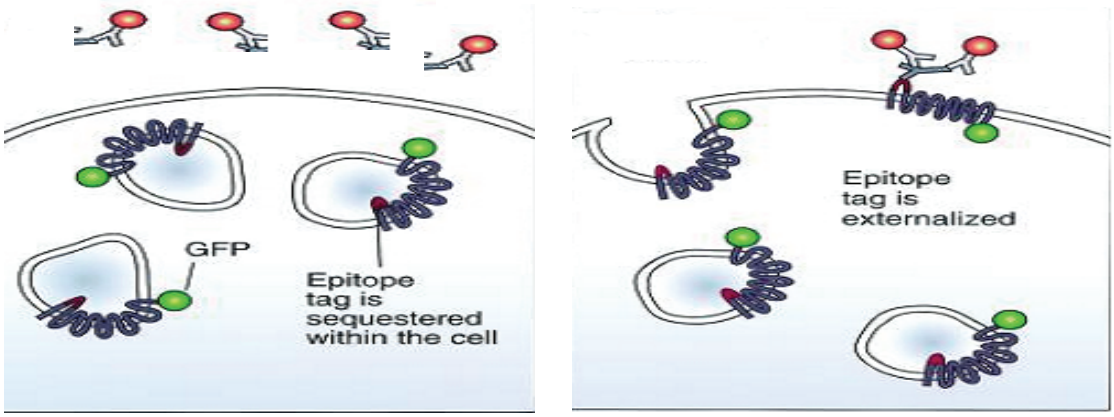

Control **5 min Insulin**

Figure 15. GLUT4 vesicles can be detected on the sarcolemma using a primary antibody that is specifically directed to the myc-GLUT4-EGFP construct. The cell surface myc-GLUT4-EGFP anti-myc monoclonal antibody was then coupled to a secondary antibody phycoerythrin (PE) and then detected using flow cytometry.

The forward scatter channel (FSC) measures the size of stream of cells as they passed through the nozzle in a flow cytometer, while the side scatter channel (SSC) measures the internal complexities or granular content of cells (Fig 17).

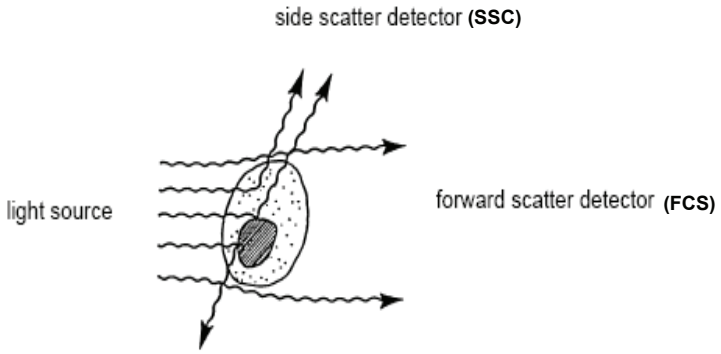

Figure 16. Light scattering properties of a cell as it passes through the nozzle of a flow cytometer (Alice L. Givan 2002).

For the transfection studies, we found increased GLUT4 translocation by flow cytometric analysis (Fig. 17). Here we observed an increase in number of cells displaying GLUT4 translocation, since we can detect 20 000-100 000 cells/second using flow cytometric analysis.

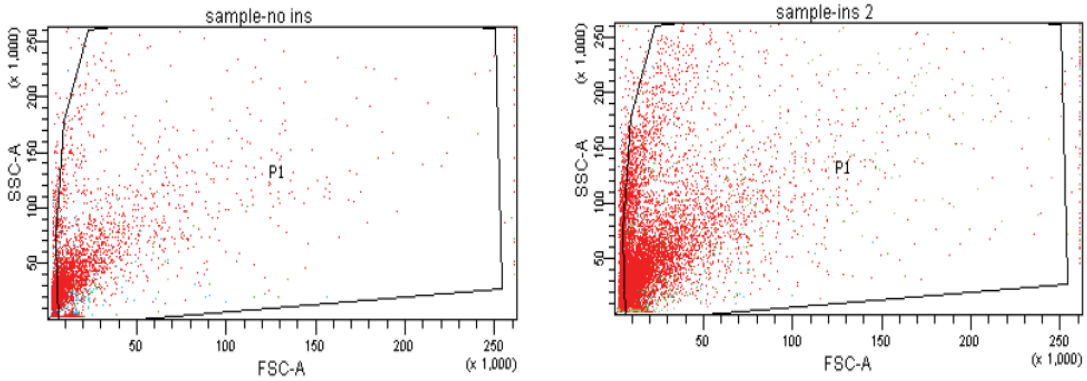

Control **5 min insulin**

Figure 17. Flow cytometric analysis to assess GLUT4 translocation in H9c2 cells (transfection studies). The forward scatter channel (FSC) roughly equates the particle size and can differentiate between living cells and cellular debris. The side scatter channel (SSC) provides information about the granular content within a cell. Note the red dots in the images display only the number of both wild-type GLUT4 and c-Myc-GLUT4-EGFP before the activation of the fluorophores with a light source.

Fig. 17 displays the number of both wild-type GLUT4 and c-Myc-GLUT4-EGFP before the activation of the fluorophores with a light source. Upon the activation of fluorophores with the light source, the c-Myc-GLUT4-EGFP signal can clearly be detected in the Alexa Fluor 488 range (green; Fig. 18A and B). Note the Alexa Fluor 488 (green) signal is present in both insulin treated and untreated cells, but it becomes more intensified upon insulin stimulation (Fig. 18A and B; green). The presence of Alexa Fluor 488 (green) signal in both insulin treated and untreated cells

differentiate c-Myc-GLUT4-EGFP from wild-type GLUT4. the PE signal (blue) can only be detected upon insulin stimulation (Fig. 18C and D; blue).

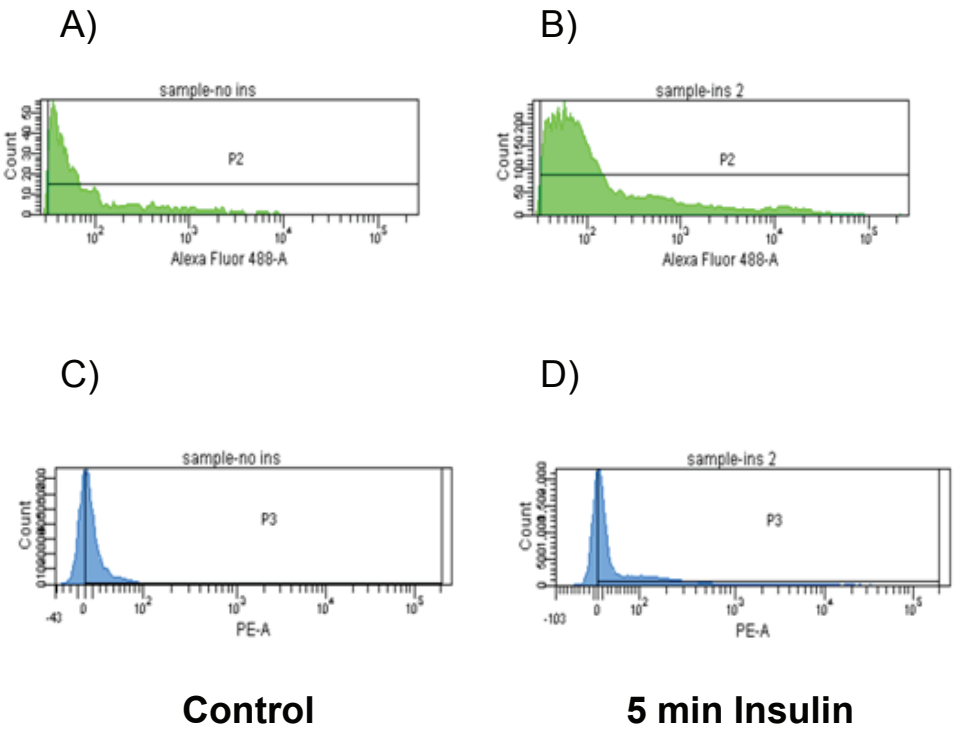

Figure 18. Flow cytometric analysis to assess GLUT4 translocation. A- control; B-insulin stimulation; C-D)- Alexa Fluor 488 signal (green) and PE signal (blue).

For the control, no fluorescence was detected (Fig. 18A and C). However, upon insulin stimulation an increase in both the GLUT4-EGFP (Alexa Fluor 488; green) and the phycoerythrin (PE; blue) signals can be detected (Fig. 18B and D). With phycoerythrin, we found an increase in the signal only upon insulin stimulation, as expected (Fig. 18D). With additional flow cytometric studies we found increased GLUT4 translocation to the sarcolemma when phycoerythrin was employed (Fig. 19). We subsequently quantified the fluorescent intensities of both GLUT4-EGFP and phycoerythrin by measuring the area under the fluorescence intensity curves (Fig. 20). These data show GLUT4 translocation after 5 minutes of insulin stimulation.

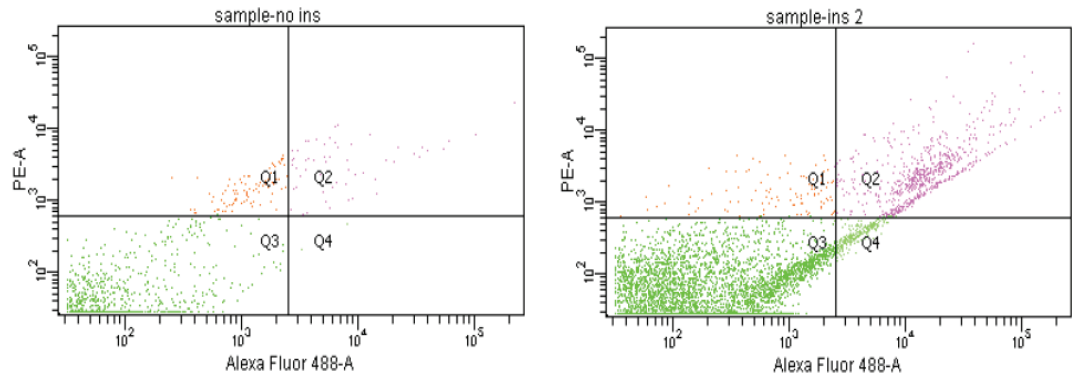

Figure 19. Transfection studies (myc-GLUT4-EGFP) of H9c2 cells to assess GLUT4 translocation. The cell surface myc-GLUT4-EGFP anti-myc monoclonal antibody was coupled to a secondary antibody phycoerythrin (PE) and GLUT4 translocation detected using flow cytometry. The quadrant Q2 represents GLUT4-EGFP located at the sarcolemma.

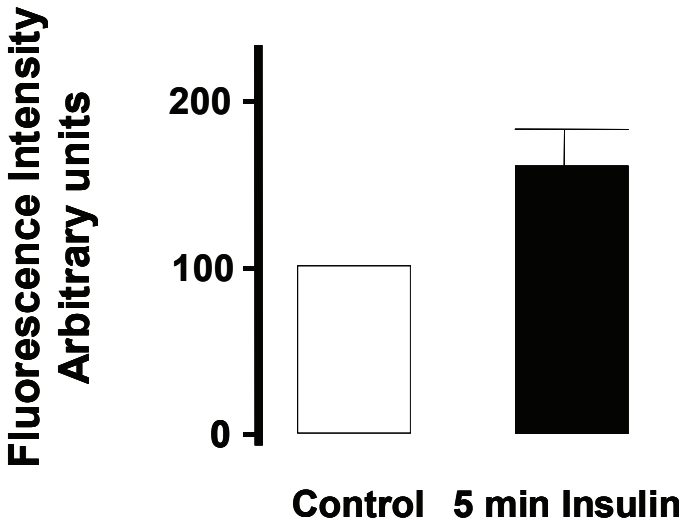

Figure 20. Quantification of GLUT4 translocation translocation by flow cytometric analysis.

3. Increased HBP flux in vitro

Since we successfully established and optimized a model for measuring GLUT4 translocation, we next pursued our hypothesis. Here we increased HBP flux by exposing H9c2 cells to:

(i) High glucose and glutamine concentrations ± HBP modulators

(ii) Low glucose and glucosamine levels

(iii) Overexpression of the HBP rate limiting enzyme GFAT ± HBP modulators

There after we confirmed increased HBP flux by measuring the degree of O-GlcNAcylation.

3.1 Exposure to high glucose and glutamine concentrations ± HBP modulators

We first cultured H9c2 cells in media containing 25 mM glucose, 4 mM L-glutamine and 100 nM wortmannin. We wanted to test our experimental system by inhibiting PI3-kinase signaling and therefore GLUT4 translocation. Our data show the typical perinuclear arrangement of GLUT4 vesicles under control conditions (Fig. 21A, D and G). However, upon insulin stimulation there is a pronounced migration to the sarcolemma (Fig. 21 B, E and H) which was blunted in the presence of a PI3–kinase inhibitor (wortmannin; Fig. 21C, F and I).

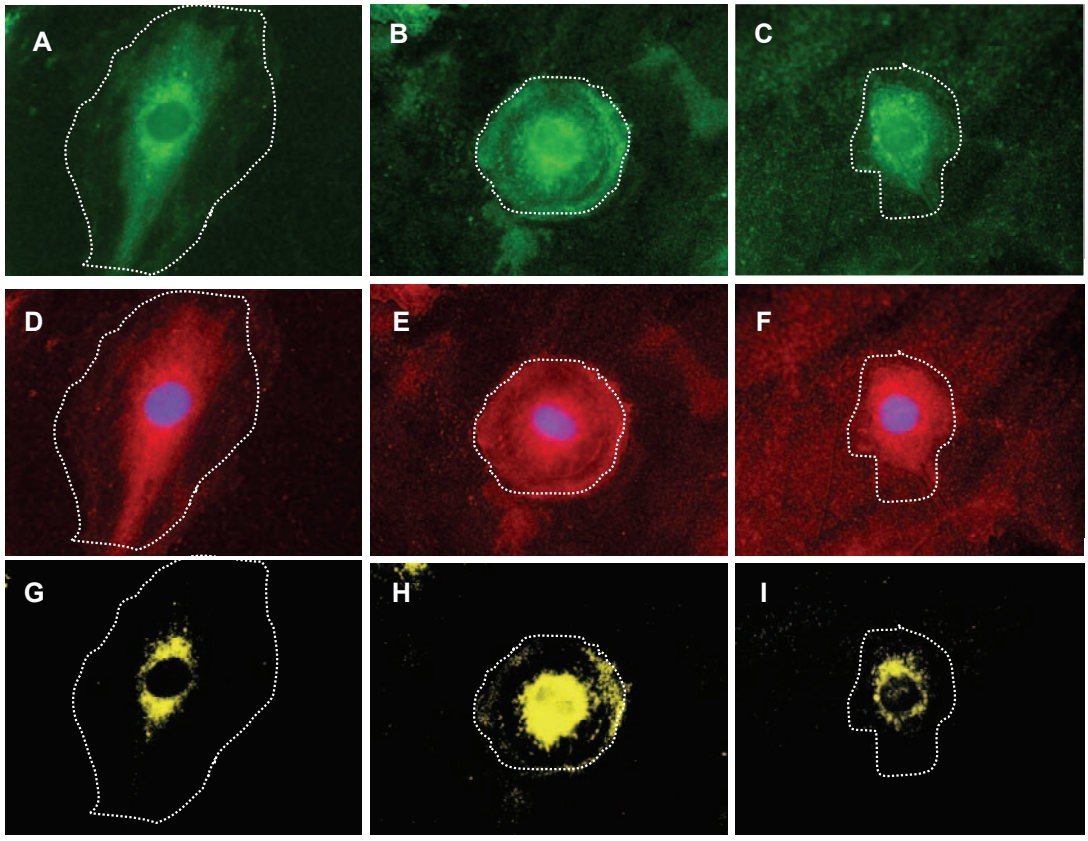

Control **Insulin** **Insulin + Wortmannin**

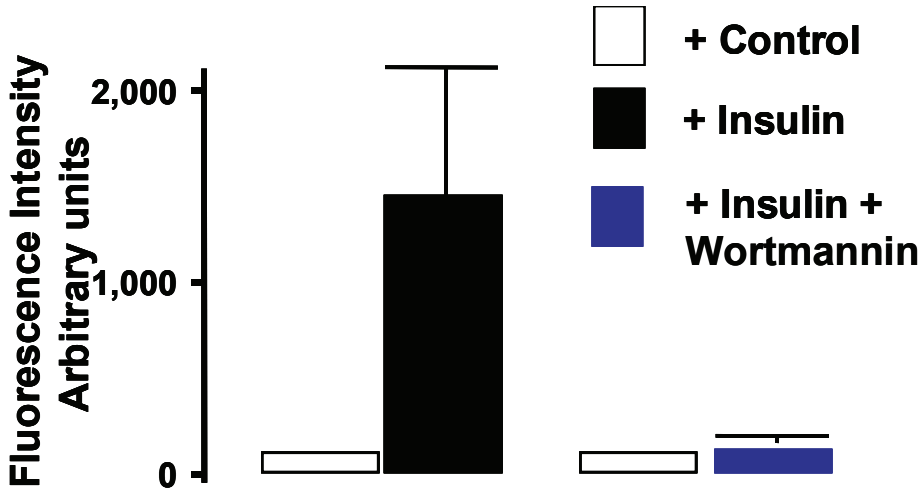

Figure 21. Inhibition of PI3–kinase blunts GLUT4 translocation (immunofluorescence microscopy). A) – C) – FITC-labeled GLUT4 ± 100 nM insulin ± 100 nM wortmannin. D) – F) – Texas Red labeled GLUT4 ± 100 nM insulin ± 100 nM wortmannin. G) – I) – Co-localization of FITC green and Texas Red stains.

We next tested our hypothesis under high glucose conditions. Here we increased HBP flux by pharmacologically inhibiting O-GlcNAcase with O-(2-acetamido-2-deoxy-D-glucopyranosylidene)amino-N-phenyl-carbamate (PUGNAc; Fig. 22).

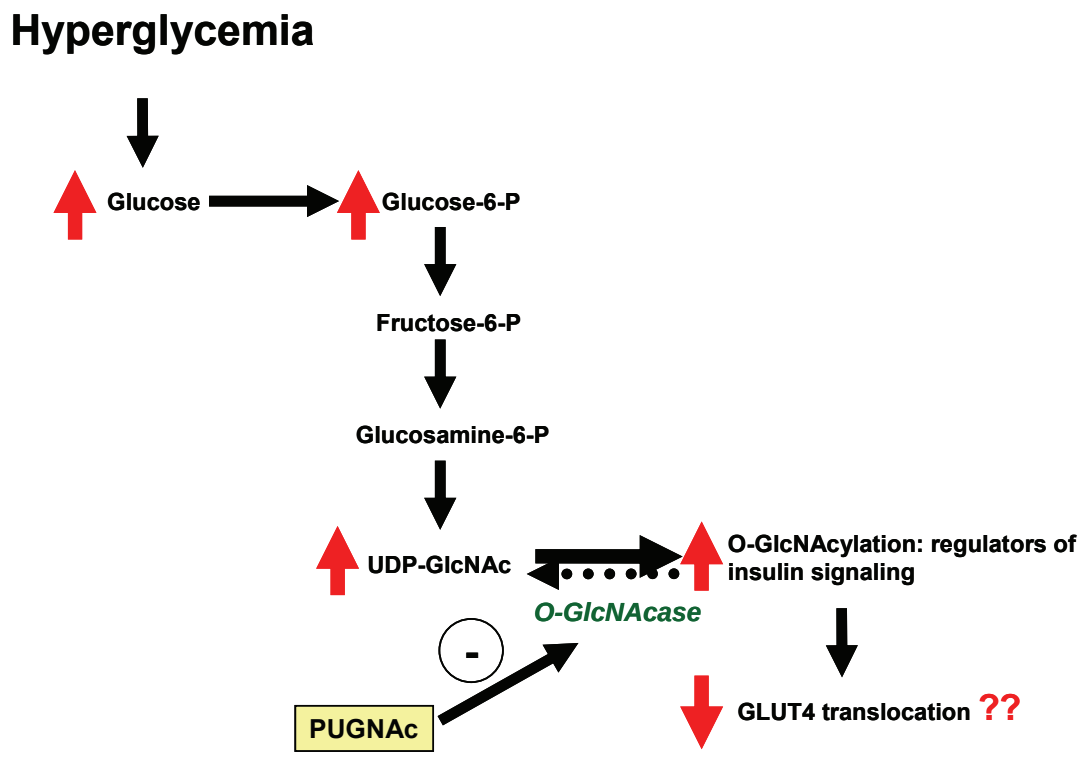

Figure 22. Increased HBP flux enhance O-GlcNAc levels predicted to inhibit GLUT4 translocation. HBP activation was achieved by pharmacologically inhibiting O-GlcNAcase with PUGNAc.

We found that PUGNAc treatment resulted in a marked reduction of insulin-mediated GLUT4 translocation to the sarcolemma (Fig. 23).

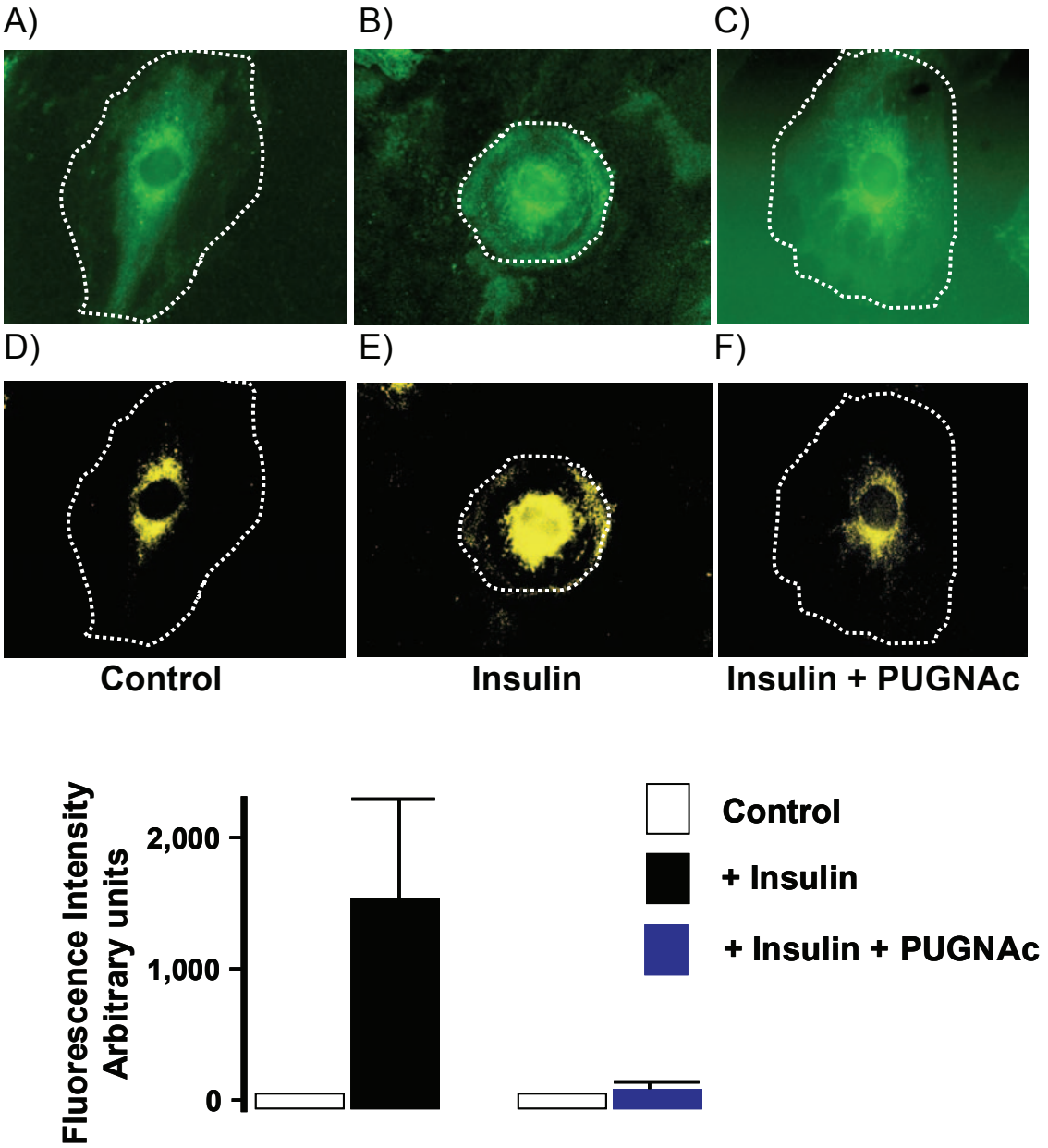

Figure 23. HBP activation attenuates GLUT4 translocation. A) – C) – FITC-labeled GLUT4 ± 100 nM insulin ± 50 μM PUGNAc. D) – F) – Co-localization of FITC green and Texas Red stains.

This interesting finding prompted us to ascertain whether the converse is true, i.e. whether pharmacological inhibition of the rate-limiting HBP enzyme GFAT, with 6-Diazo-5oxo-L-norleucine (DON) will restore GLUT4 translocation (Fig. 24).

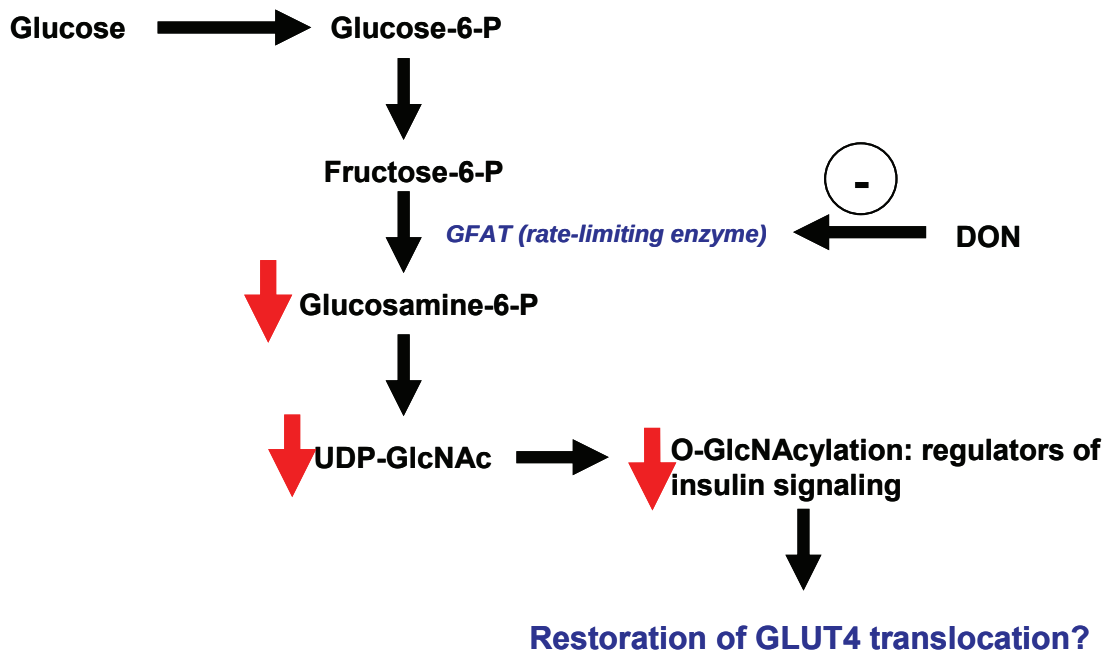

Figure 24. Does HBP inhibition with 6-Diazo-5oxo-L-norleucine (DON) restore GLUT4 translocation?

We found that DON does indeed inhibit the rate limiting enzyme GFAT and thus restore GLUT4 translocation (Fig. 25).

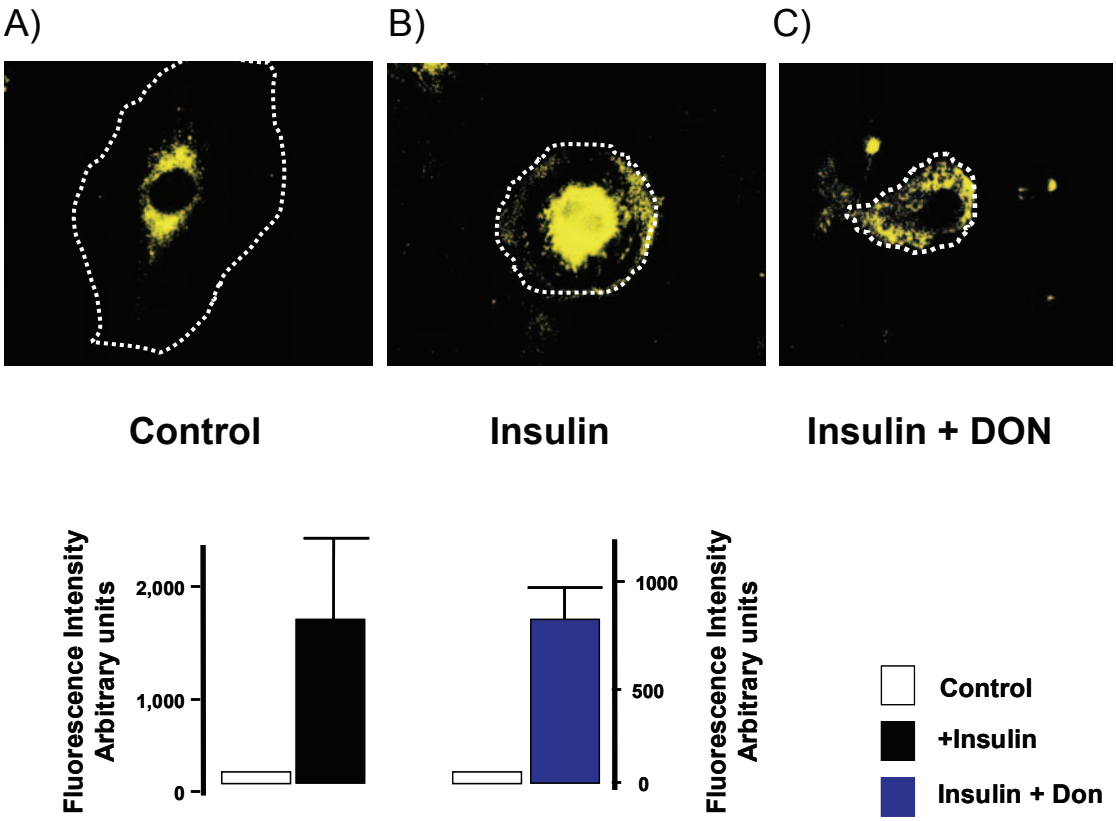

Figure 25. Normal GLUT4 translocation in the presence of HBP inhibition. A) – C) – Co-localization of FITC green and Texas Red stains.

3.2 Low glucose and glucosamine stimulation

H9c2 cells were cultured in low glucose (5 mM) and ± varying glucosamine concentrations, i.e. 2.5 mM, 5 mM and 10 mM, respectively. Here we predicted that increased glucosamine concentrations should inhibit GLUT4 translocation (Fig. 26). As expected, we found that glucosamine administration impaired GLUT4 translocation at all the concentrations employed (Fig. 27).

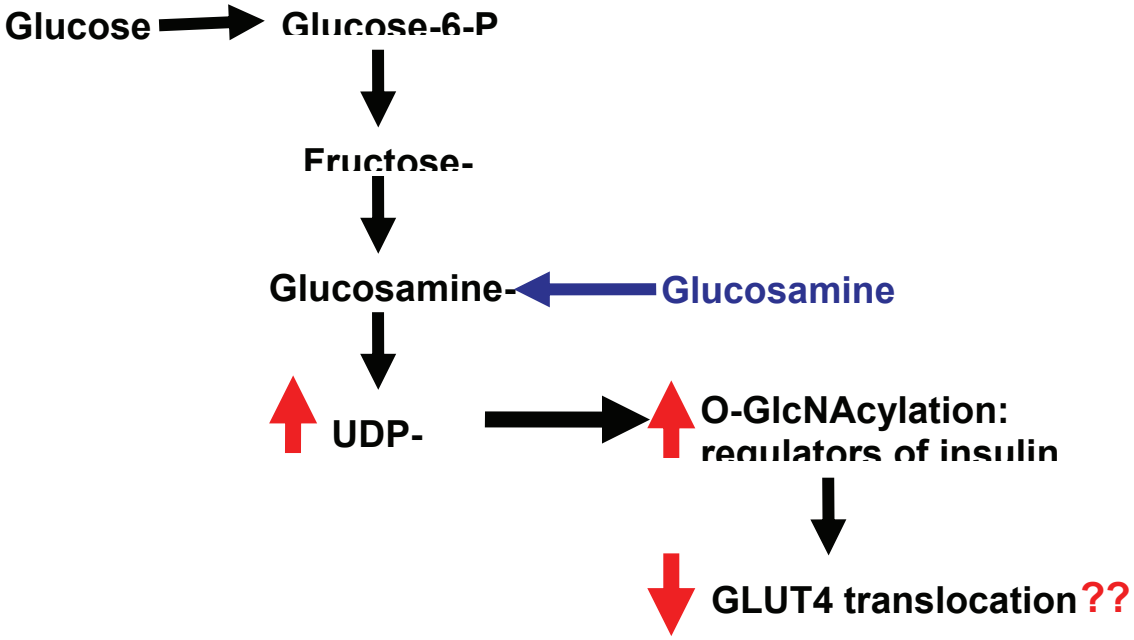

Figure 26. HBP activation by glucosamine is predicted to inhibit GLUT4 translocation.

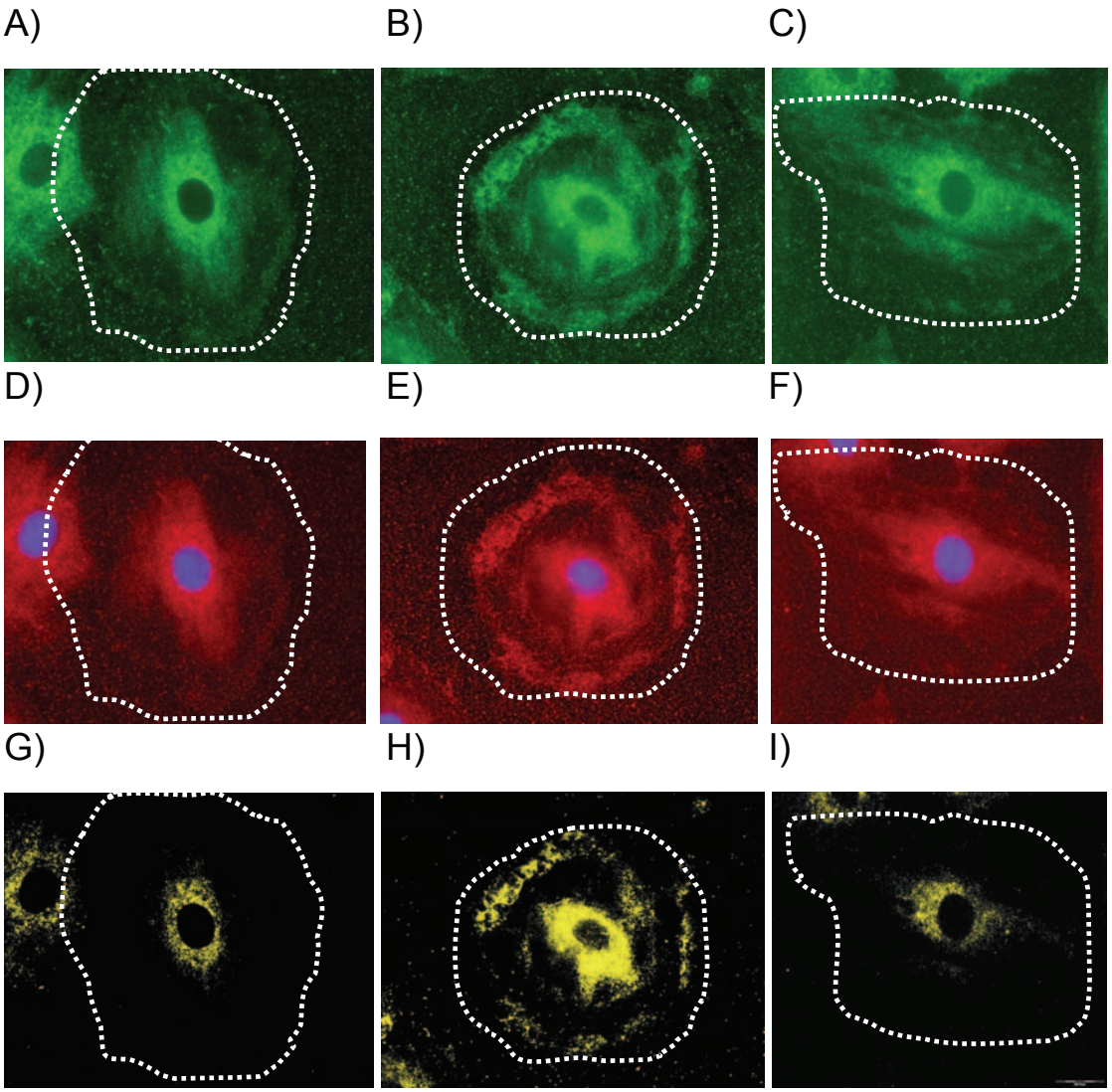
A)
B)
C)
D)
E)
F)
G)
H)
I)
Control
Insulin
Insulin + 2.5 mM Glucosamine

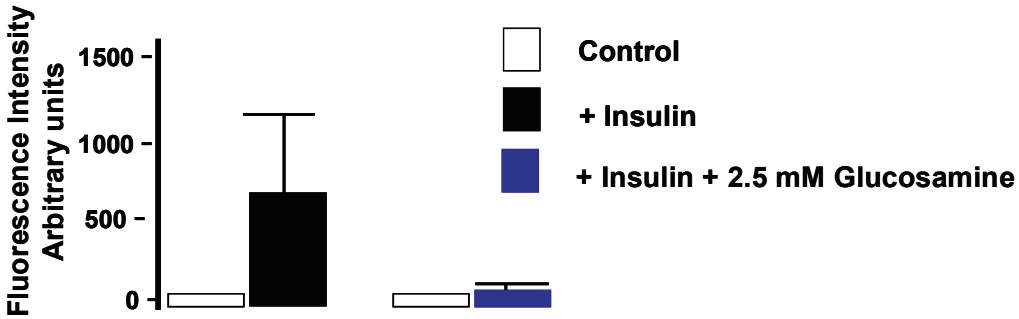
Fluorescence Intensity
Arbitrary units
1500
1000
500
0
Control
+ Insulin
+ Insulin + 2.5 mM Glucosamine

J) K) L)

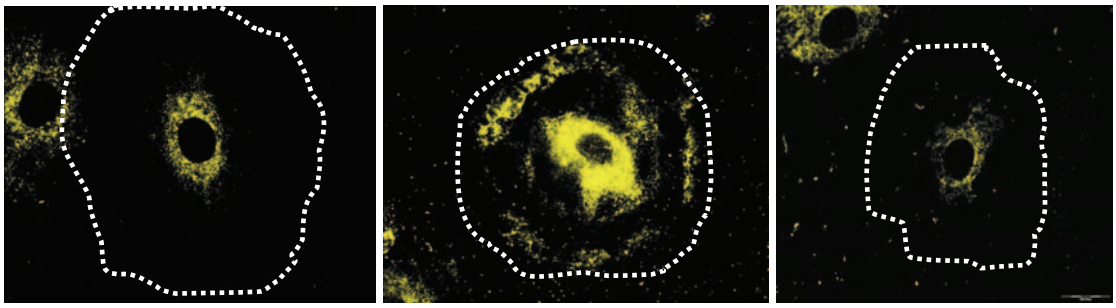

Control + Insulin + Insulin + 5 mM Glucosamine

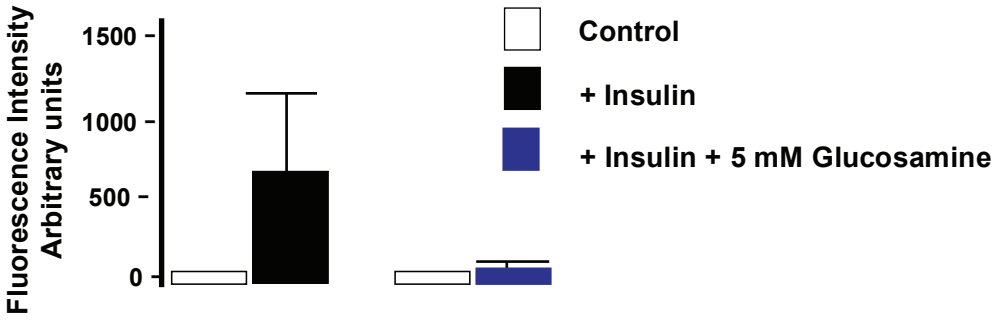

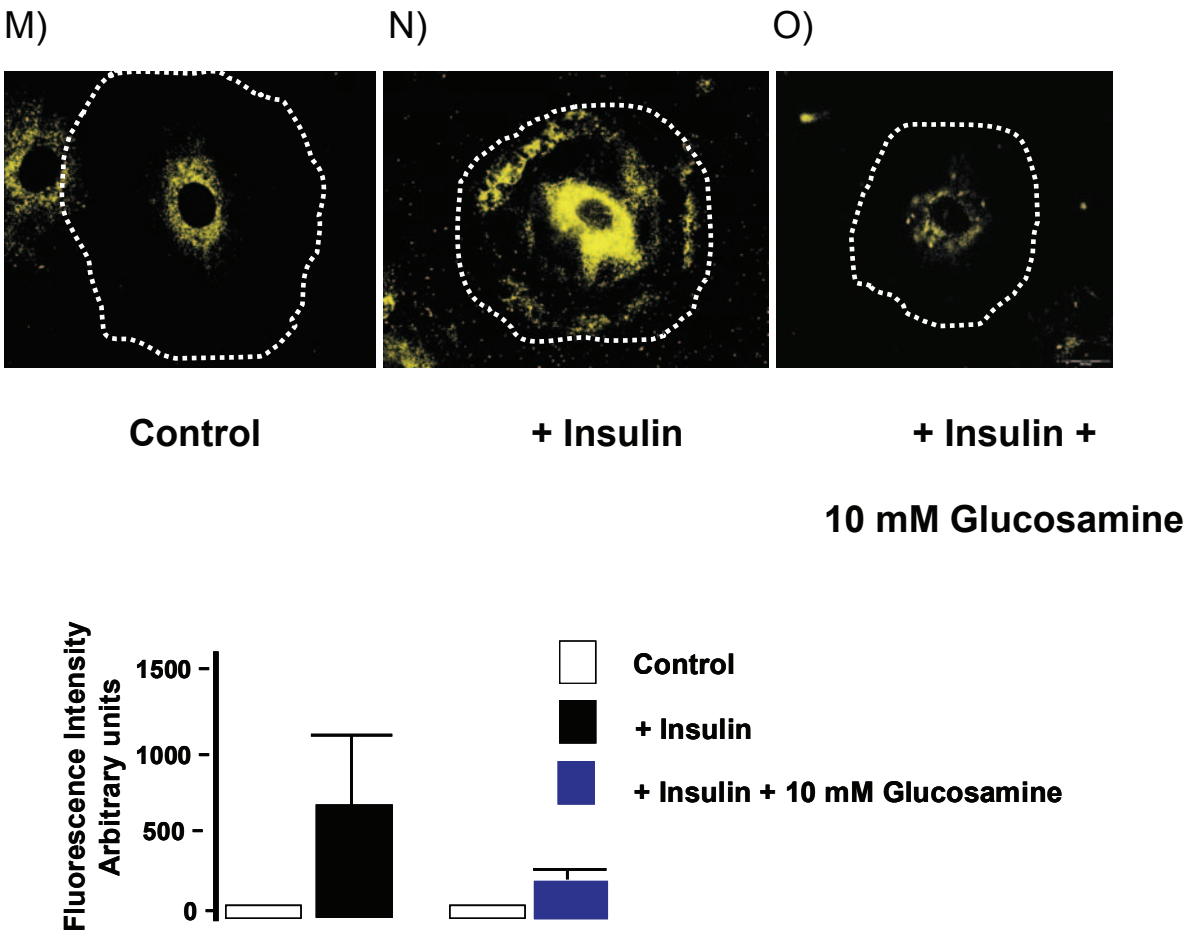

Figure 27. Gradual increased administration of glucosamine inhibits GLUT4 translocation. A) – C) – FITC-labeled GLUT4 ± 100 nM insulin ± 2.5 mM glucosamine. D) – F) – Texas Red labeled GLUT4 ± 100 nM insulin ± 2.5 mM glucosamine. G) – I) – Co-localization of FITC green and Texas Red stains. J) – L) – Co-localization of FITC green and Texas Red stains with ± 5 mM glucosamine. M) – O) – Co-localization of FITC green and Texas Red stains with ± 10 mM glucosamine.

3.3 Over expression of the HBP rate-limiting enzyme

In line with our hypothesis, we predicted that over-expression of the HBP rate-limiting enzyme i.e. (GFAT) should increase O-GlcNAc levels, thereby inhibiting GLUT4 translocation (Fig. 28).

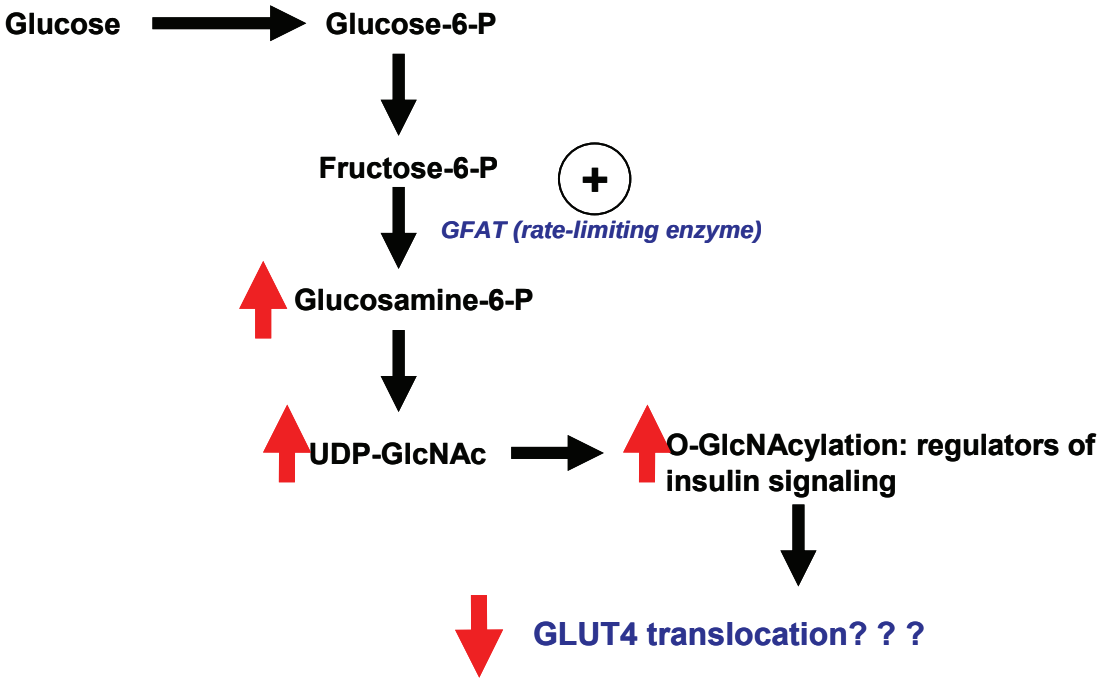

Figure 28. HBP activation by over expressing the rate-limiting enzyme GFAT should increase O-GlcNAc levels, thereby inhibiting GLUT4 translocation.

After transfection with a GFAT construct, we found that GFAT over expression markedly attenuated GLUT4 translocation to the sarcolemma (Figs. 29 and 30).

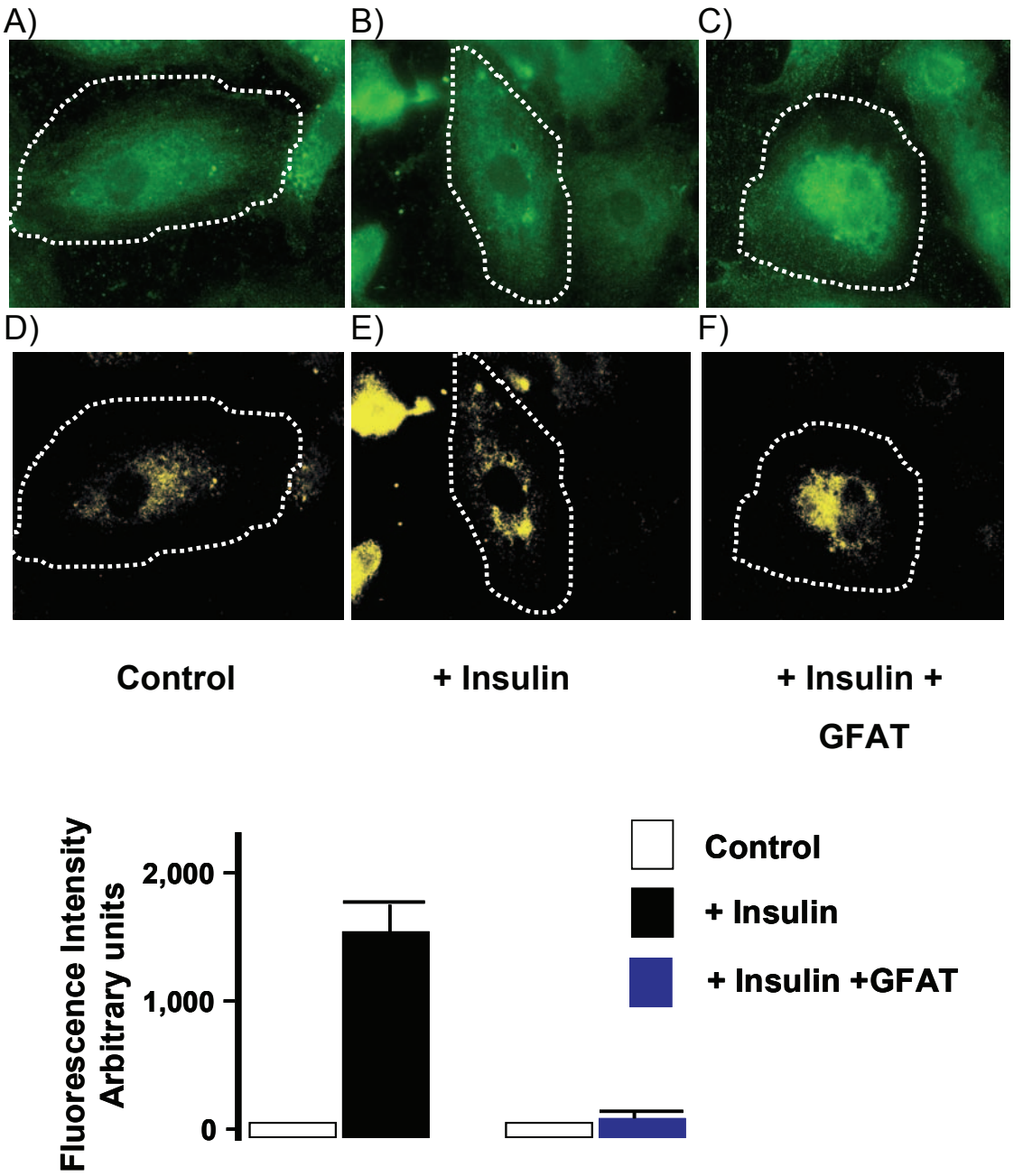

Figure 29. Over expression of GFAT inhibits GLUT4 translocation.
A) – C) – FITC-labeled GLUT4 ± 100 nM insulin + GFAT. D) – F) – Co-localization of FITC green and Texas Red stains + GFAT.

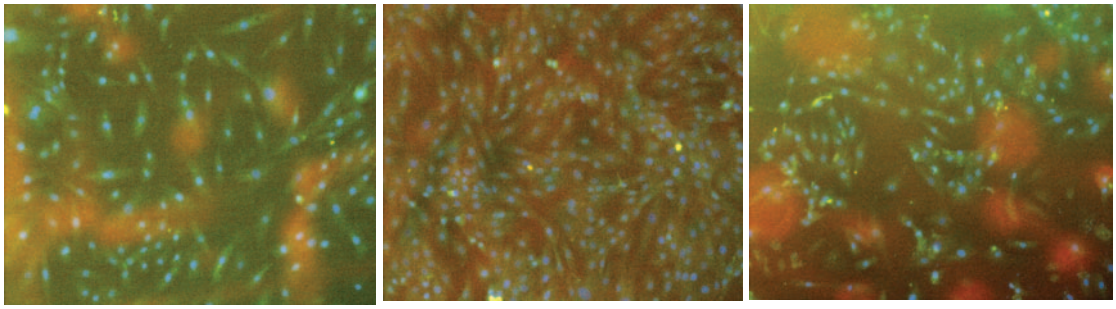

Control **+ Insulin + Vector** **+ Insulin + GFAT**

Figure 30. GFAT over-expression effects GLUT4 translocation (lower 20x magnification). Note the decrease in red fluorescence intensity signifying reduced GLUT4 translocation.

Encouraged by these findings, we performed an additional experiment to further confirm our data. We synergistically activated the HBP (GFAT over-expression) ± 50 μM PUGNAc treatments (Fig. 31). However, we found that PUGNAc treatment with GFAT overexpression did not further decrease GLUT4 translocation (Figs. 32 and 33). This suggests that GFAT over-expression experiments caused a maximal effect.

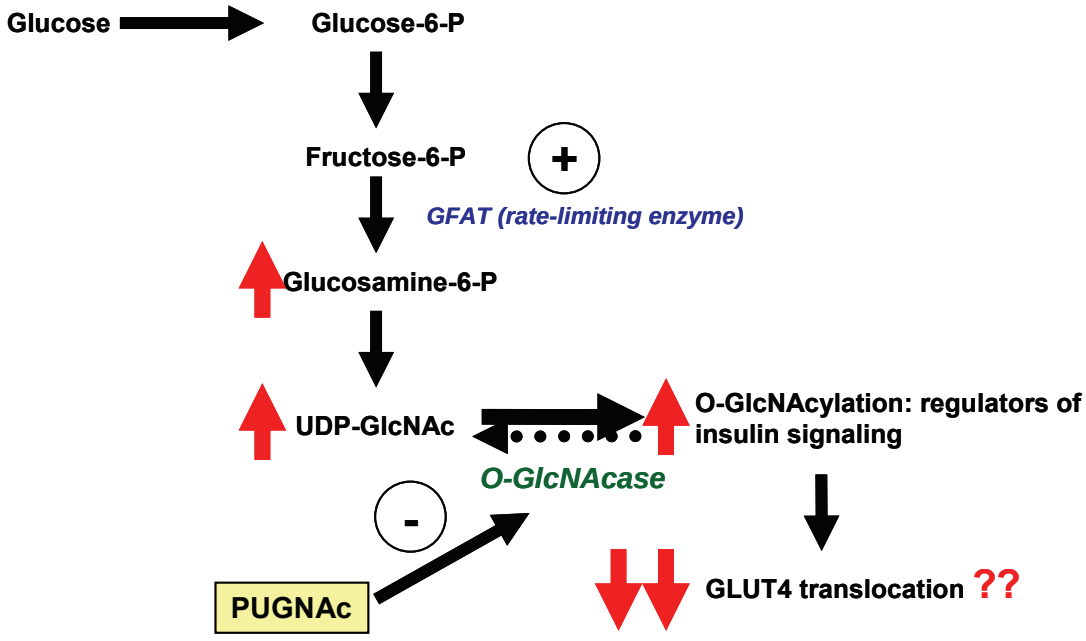

Figure 31. Does PUGNAc administration together with GFAT over-expression further decrease GLUT4 translocation?

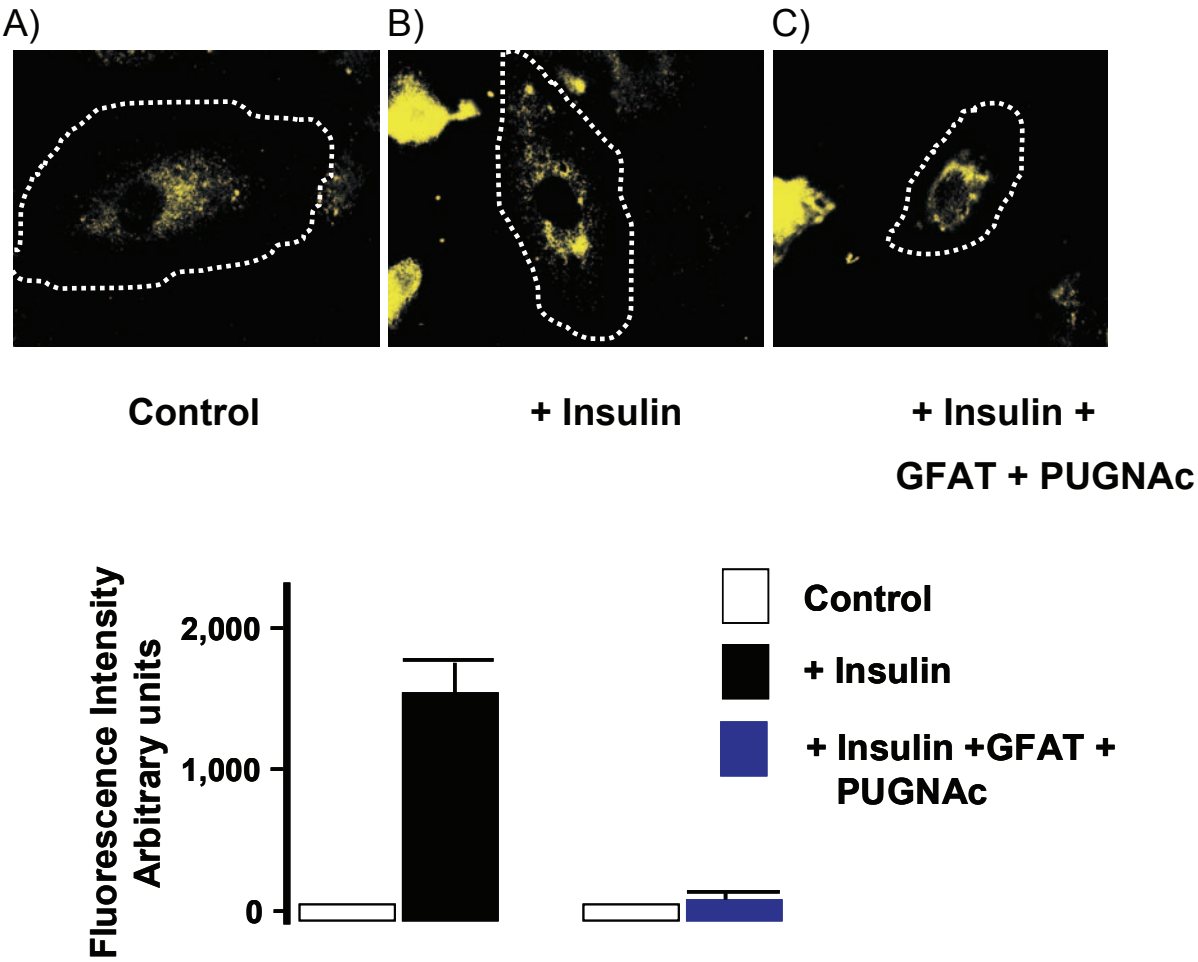

Figure 32. GFAT over-expression and PUGNAc treatments are not additive in attenuating GLUT4 translocation. A) – C) – Co-localization of FITC green and Texas Red stains with GFAT overexpression and ± 50 μM PUGNAc.

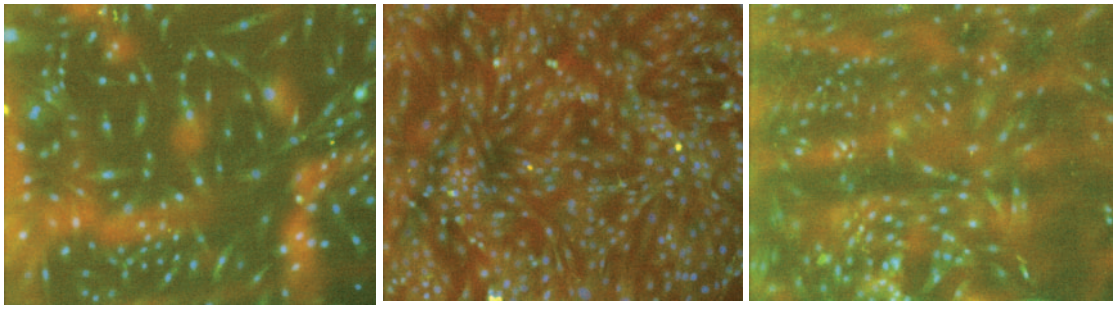

Control **+ Insulin** **+ Insulin + GFAT + PUGNAc**

Figure 33. Effects of GFAT overexpression and PUGNAc treatments are not additive in attenuating GLUT4 translocation (lower magnification-20x). Note also the decrease in red fluorescence intensity signifying reduced GLUT4 translocation.

We next employed a dominant negative GFAT construct (dnGFAT) in our transfection studies to confirm our earlier findings (Fig. 34). Here GLUT4 translocation was restored when GFAT over-expression experiments were performed in the presence of either DON or a dnGFAT construct (Figs. 35 – 37).

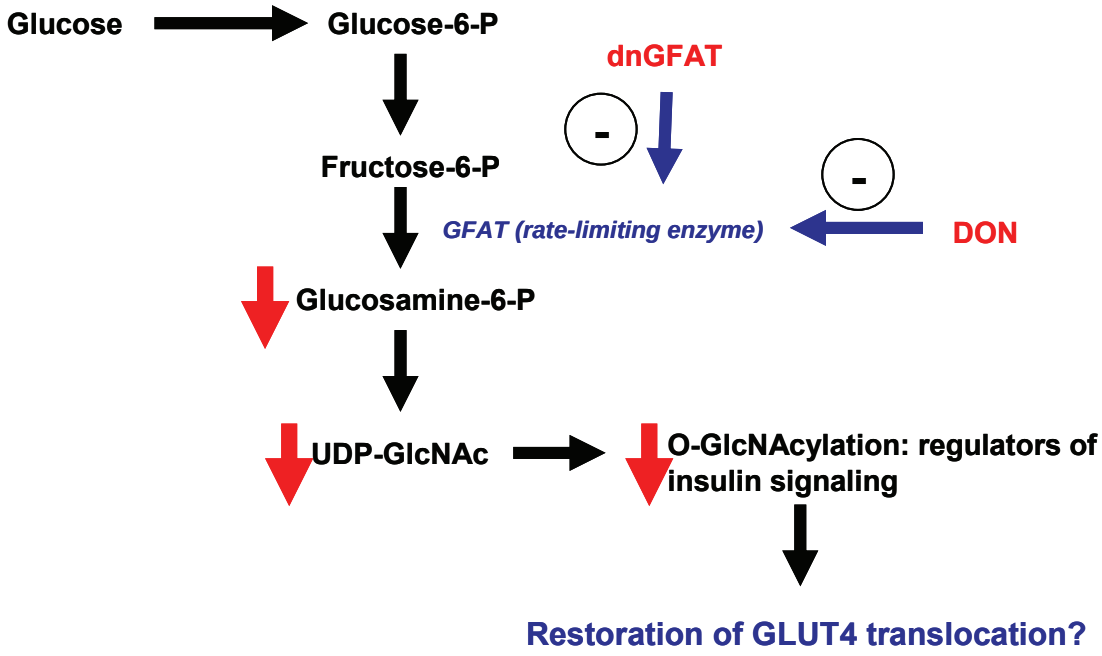

Figure 34. Does HBP inhibition with a dominant negative GFAT construct (dnGFAT) lead to GLUT4 translocation?

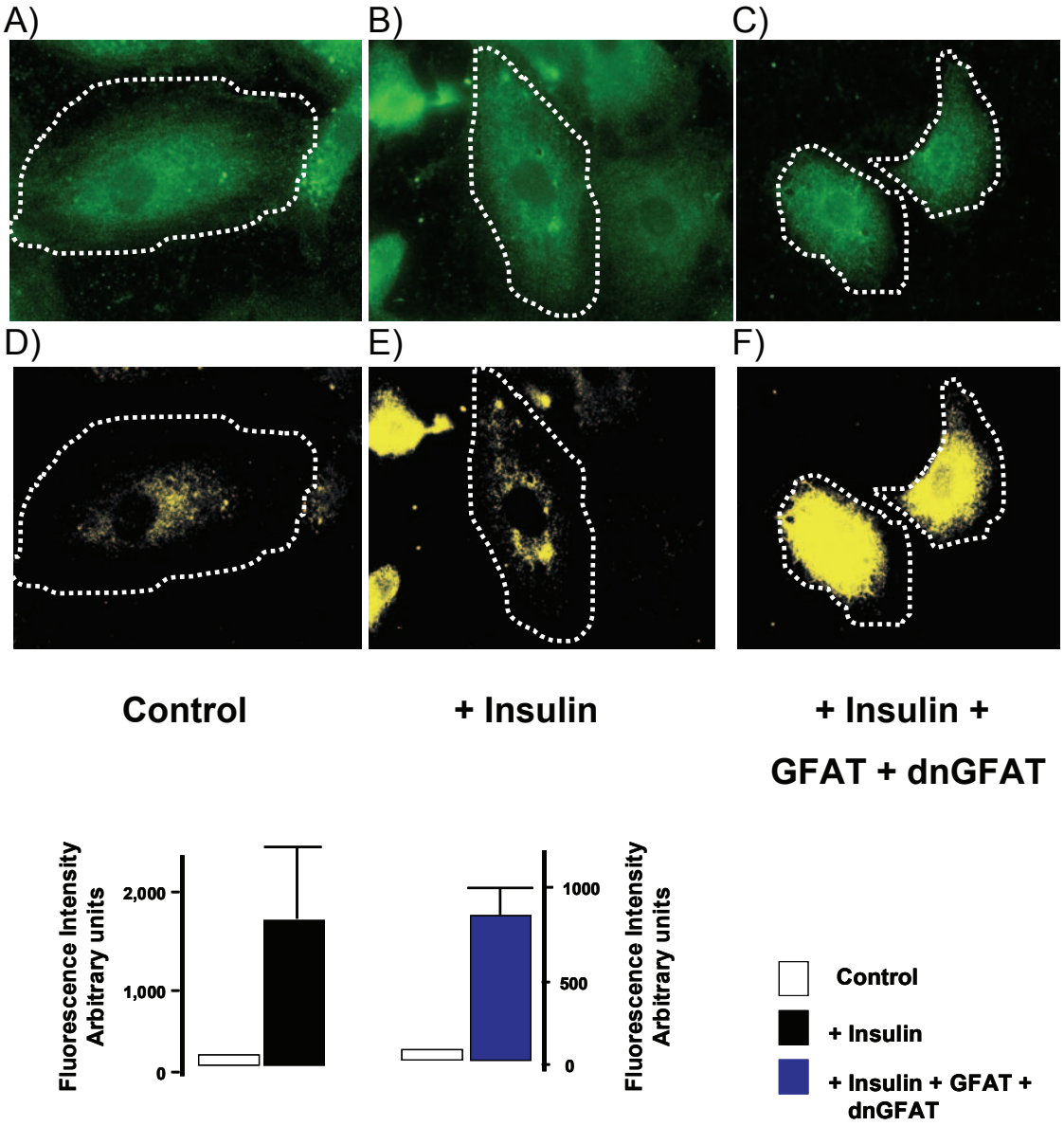

Figure 35a. GFAT overexpression in the presence of a dominant negative GFAT vector (dnGFAT) or DON, restoring GLUT4 translocation. A) – C) – FITC-labeled GLUT4 ± 100 nM insulin + GFAT + dnGFAT. D) – F) – Co-localization of FITC green and Texas Red stains with GFAT over-expression + dnGFAT.

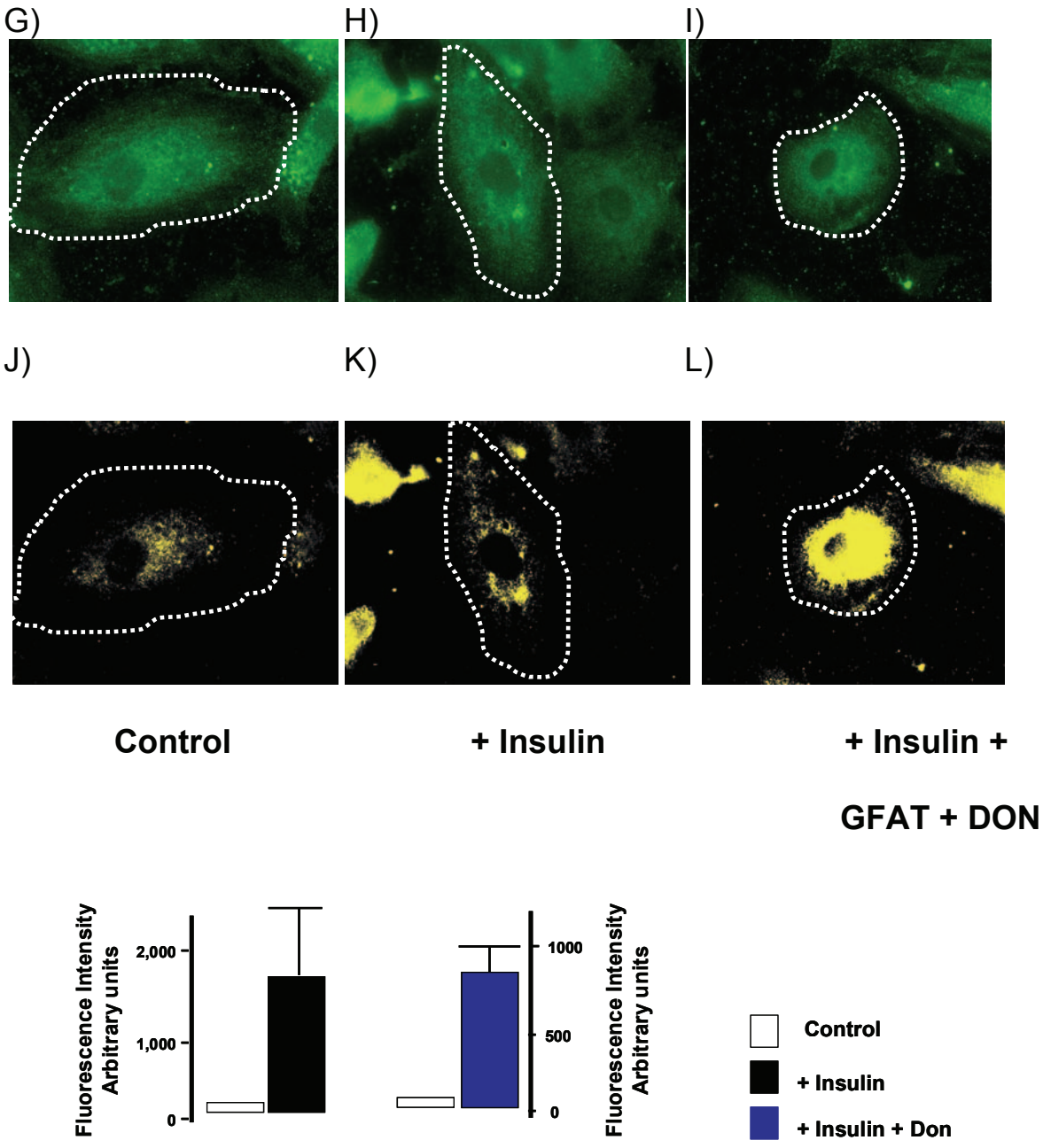

Figure 35b G) – I) – FITC-labeled GLUT4 ± 100 nM insulin + GFAT ± 40 μM DON. J) – L) – Co-localization of FITC green and Texas Red stains with GFAT over-expression ± 40 μM DON.

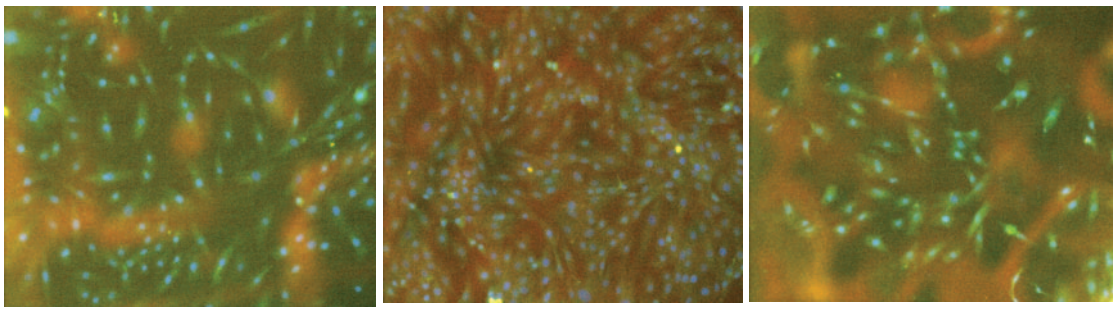

Control **+ Insulin** **+ Insulin + GFAT + dnGFAT**

Figure 36. GFAT overexpression in the presence of a dominant negative GFAT vector (dnGFAT; lower magnification-20x). Note the increase in green fluorescence intensity, which signifying increased GLUT4 translocation.

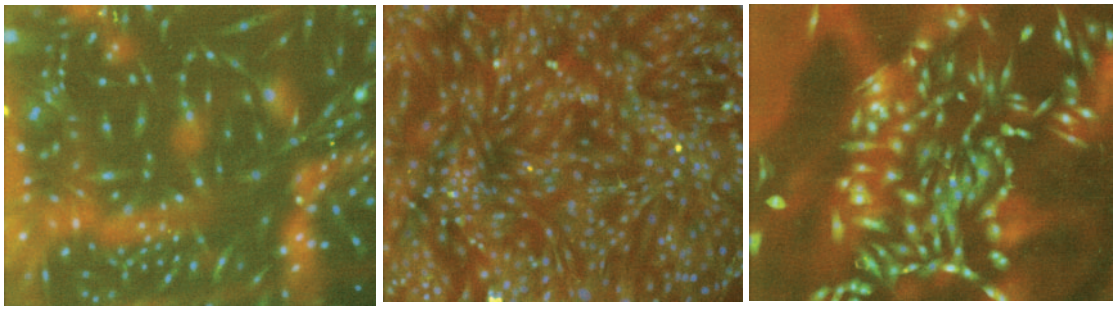

Control **+ Insulin** **+ Insulin + GFAT + DON**

Figure 37. GFAT over-expression in the presence of DON (lower magnification-20x). Note the increase in green fluorescence intensity, which signifying increased GLUT4 translocation.

4. Measuring the degree of O-link GlcNAcylation

To test whether the HBP was indeed activated/deactivated in response to experimental manipulations, cells were probed with a primary O-GlcNAc antiboby coupled to FITC (green colour). In parallel, the nucleus was stained with DAPI (blue colour). The degree of GlcNAcylation was then assessed using immunofluorescence microscopy (Figs. 38 – 41). We found that the overall degree of O-GlcNAcylation markedly increased under high glucose conditions (Fig. 38).

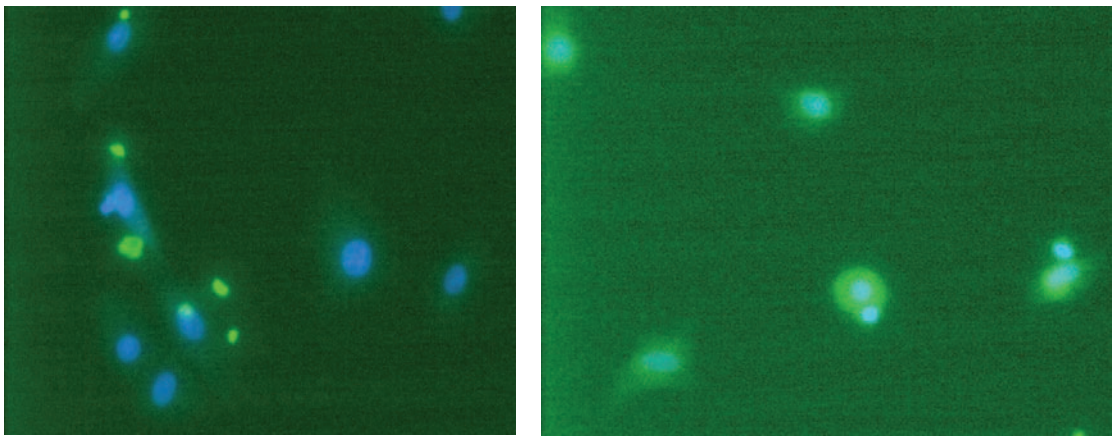

5 mM Glucose **25 mM Glucose**

Figure 38. Increased O-GlcNAcylation in response to high glucose treatments. The bright green spots observed for 5 mM glucose is a result of crystal formation and was not included for comparison purposes.

A) B)

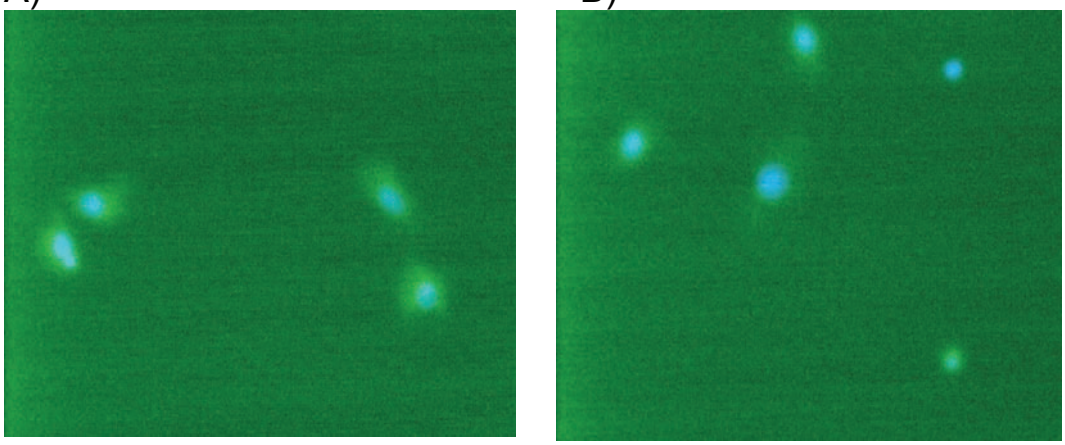

PUGNAc (HBP activator) **DON (HBP inhibitor)**

Figure 39. Degree of overall O-GlcNAcylation in response to HBP modulation. PUGNAc increased the fluorescence intensity, while DON resulted in an opposite effect. A) – FITC-labeled O-GlcNAc ± 50 μM PUGNAc; B) – FITC-labeled O-GlcNAc ± 40 μM DON.

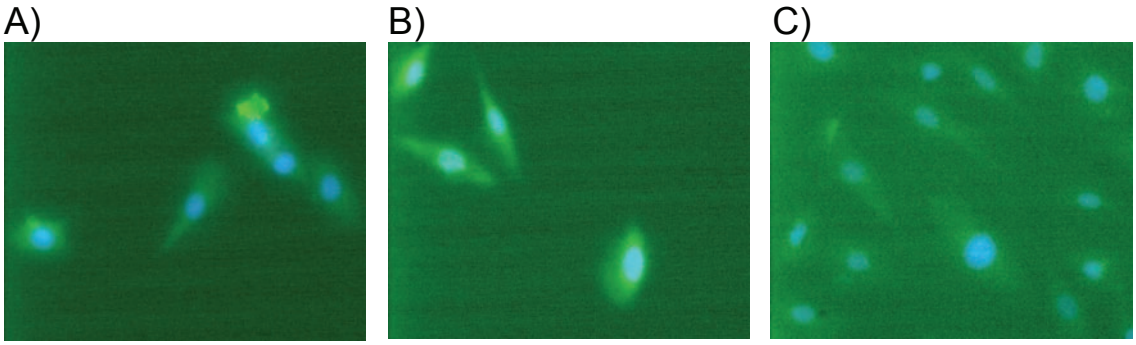

Figure 40. Degree of O-GlcNAcylation in response to GFAT and dnGFAT expression. GFAT increased the fluorescence intensity, while dnGFAT resulted in an opposite effect. A) – C) – FITC-labeled O-GlcNAc + GFAT + dnGFAT.

When PUGNAc was administered, bright green fluorescence staining of cells was observed (Fig. 39). However, DON administration resulted in an opposite effect, i.e. reduced green staining. The high incidence of background staining (green) does make analysis of the pictures rather difficult. Likewise, we tested the overall degree of O-GlcNAcylation with GFAT over-expression. Here GFAT over-expression caused cells to glow quite brightly while this effect was blunted in the presence of DON and dnGFAT (Figs. 40 and 41). GFAT in the presence of PUGNAc and DON caused an increase and decrease, respectively of O-GlcNAcylation (Fig. 41).

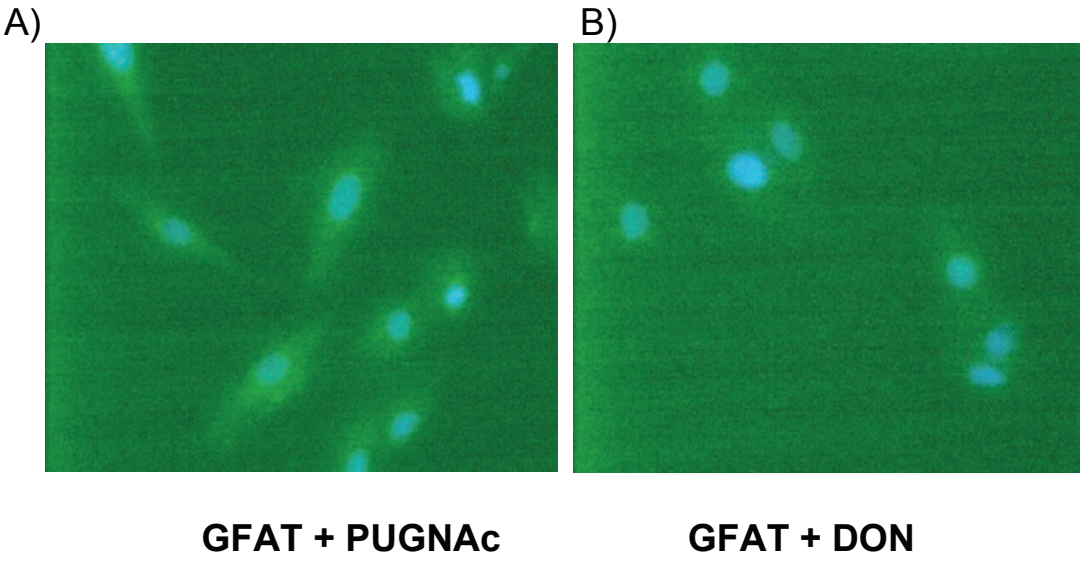

Figure 41. Overall degree of O-GlcNAcylation with GFAT over-expression in the presence of PUGNAc or DON, respectively. A) – B) – FITC-labeled O-GlcNAc ± 50 µM PUGNAc ± 40 µM DON

Chapter 4

Discussion

4. Introduction

It is estimated that the global prevalence of type diabetes will reach ~ 300 million cases by 2025 (Zimmet *et al.,* 2001). Insulin resistance is a major characteristic of type 2 diabetes and obesity (Kolterman *et al.,* 1981; Hollenbeck *et al.,* 1984). However, the mechanisms whereby insulin resistance develops remain, by and large, unclear. The uptake of glucose is a crucial step in myocardial glucose metabolism and is regulated by glucose transporters (GLUT1 and GLUT4). In light of this, we hypothesized that greater HBP flux impairs myocardial GLUT4 translocation to the sarcolemma. The key findings of this study are: 1) Establishment of an *in vitro* experimental system to assay myocardial GLUT4 translocation and 2) Increased activation of the HBP impairs myocardial GLUT4 translocation.

4.1 Establishment of an in vitro experimental system to assay myocardial GLUT4 translocation

Our first aim was to establish a workable *in vitro* experimental system to assess myocardial GLUT4 translocation. We employed rat cardiac-derived H9c2 myoblasts since it is an easy cell line to culture and generate results in a rapid and reproducible fashion. To confirm the validity of our choice we also tested our protocol using different cell lines. Here C2C12 myoblasts, L6 myoblasts, differentiated L6 myoblasts, and CV1 fibroblasts displayed a poor response in terms of GLUT4 translocation. These data therefore support H9c2 myoblasts as our cell line of choice, since it responded best upon insulin stimulation as will be discussed below.

We first tried to determine the optimal insulin concentration and peak response time, i.e. length of time required for GLUT4 vesicles to migrate from intracellular locations to the sarcolemma. Our data clearly show that 100 nM insulin is the optimal concentration in our experimental system. This is in agreement with other studies which reported similar findings for different cell lines (Holman *et al.,* 1994; Pak *et al.,* 2005). However, we spent considerable time and effort to determine the peak response time for our model. Here we initially tried a 14-hour insulin stimulation period, and also serum-starvation studies for long (24 hours) and shorter duration (5-30 minutes). These studies did, however, not yield useful data regarding peak response time.

Interestingly, these studies revealed that with longer insulin stimulation times GLUT4 constitutively cycles from intracellular sites to the sarcolemma and the reverse. This probably occurs through slow exocytosis and fast endocytosis as reported by others (Satoh *et al.,* 1993; Li *et al.,* 2001). Secondly, we also learnt that myocardial GLUT4 storage vesicles (GSV) clearly are located within the perinuclear region of the cell. Our data are in agreement with microscopy studies that localized GSVs within the perinuclear region and as distinct foci throughout the cytosol (Slot *et al.,* 1991; Malide *et al.,* 2000). Moreover, others show that perinuclear GSVs colocalize with markers of the endosomal recycling compartment (ERC), the Golgi complex and the *trans*-Golgi network (TGN; Bryant *et al.,* 2002; Plough and Rolstan 2002). Moreover, insulin-mediated glucose uptake and redistribution of GLUT4 vesicles to the sarcolemma also requires an intact microtubule cytoskeleton (Emoto *et al.,* 2001; Olson *et al.,* 2001; Patki *et al.,* 2001). Together these data show a dynamic system whereby GLUT4 vesicles recycle within specific intracellular compartments and are closely inter-linked with other organelles to ensure rapid cycling upon insulin stimulation.

Our last set of experiments (β-dystroglycan and different GLUT4 antibodies) finally confirmed a peak response for insulin-mediated GLUT4 translocation, i.e. after 5 minutes (with 100 nM insulin). We employed two different GLUT4 antibodies i.e. an intracellular-bound GLUT4 antibody that is directed to the N-terminus of the intracellular GLUT4, and a membrane-bound antibody that is directed to the exofacial loop of the membrane GLUT4. This procedure also allowed us to employ a quantification methodology, i.e. using co-localization analysis of both intracellular-bound GLUT4 and membrane-bound GLUT4 (producing a yellow colour). This dual antibody method became our experimental system of choice for assessing GLUT4 translocation and can now be exploited for various research foci explored within our laboratory, including ischemia-reperfusion, hypertrophy, hypoxia, and AMPK activation. The method is a rapid, accurate, sensitive and reasonably cost-effective when compared to the cost of transfections or radio-nucleotide reagents employed to measure glucose uptake. For example, we also assessed myocardial GLUT4 translocation in real-time by using immunofluorescence microscopy and flow cytometry-based studies. Although these methods are relatively accurate for assessing GLUT4 translocation (Bogan *et al.,* 2001; Czech *et al.,* 2002), they are time consuming and expensive.

4.2 Increased activation of the HBP impairs myocardial GLUT4 translocation

As the prevalence in diabetes increases, morbidity/mortality due to diabetic cardiomyopathies (86) have also been increasingly documented (Spralka *et al.,* 1991; Nielsen *et al.,* 1997; Hirayama *et al.,* 2000; Abel *et al.,* 2007). Both functional (Shapiro *et al.,* 1981) and structural abnormalities have been described (van Hoeven and Factor 1990). However the, etiology of this cardiac pathology remains unclear. Several mechanisms have been proposed that show manipulation of nutrient supply to the heart results in changes in cardiac morphology (Litwin *et al.,* 1990; Bressler and Goldman 1993). Although the heart predominantly metabolises fat, human studies have shown that glucose metabolism becomes essential when there are higher energy demands, for e.g. with exercise (Gertz *et al.,* 1988).

Cardiac glucose uptake is mediated by GLUT1 and most importantly by the insulin–responsive GLUT4 (Kraegen *et al.,* 1993). Both insulin and exercise increase cardiac glucose uptake by triggering intracellular signalling mechanisms leading to the translocation of GLUT4 to the sarcolemma (Slot *et al.,* 1991). However, a reduction in GLUT4 expression is linked to the diabetic cardiomyopathy (Garvey *et al.,* 1993). Furthermore, over-expression of GLUT4 prevented cardiac dysfunction in db/db mice (Semeniuk *et al.,* 2002; Belke *et al.,* 2000). Interestingly, muscle-specific insulin receptor knockout mice did not exhibit insulin resistance, suggesting that the insulin signaling defect possibly occurs further downstream (Michael *et al.,* 1999). On the other hand, GLUT4 knock-out mice displayed insulin resistance, with impaired glucose tolerance and mild hyperinsulinemia (Kim *et al.,* 2005; Stephen and Pilch 1995; Zisman *et al.,* 1999). Together these studies strongly indicate that impaired cardiac GLUT4 translocation and/or reduced expression levels are likely candidates for the onset of myocardial insulin resistance and ultimately significant contributory factors to the diabetic cardiomyopathy.

Several studies show that a marked decrease in AKT/PKB levels is also associated with insulin resistance (Pak *et al.,* 2005). Decreased AKT activity may be due to the disruption of the actin cytoskeleton (Olson *et al.,* 2001). Since GLUT4 is a downstream target of AKT/PKB, this may be a potential mechanism whereby GLUT4 levels are decreased with insulin resistance.

Our laboratory proposed that diminished myocardial GLUT4 translocation is due to increased HBP flux during the insulin resistant state. Our preliminary results demonstrated that insulin resistant db/db mice displayed greater GFAT peptide levels. The db/db mouse possesses a “diabetic” gene (db), which encoding a G-to-T point mutation of the leptin receptor thereby leading to abnormal splicing and defective leptin signaling. This makes the animal hyperphagic and results in hyperinsulinemia, hyperleptinema and insulin resistance (Wyse and Dulin 1970; Coleman and Hummel 1974). Our GFAT expression data are in agreement with others, i.e. reporting that increased GFAT activity is associated with insulin resistance (Donald A. McClain 1995; Yki-Jarvinen *et al.,* 1996; Balasubramanyam *et al.,* 2007). However, as far as we are aware, our data are the first to report this finding for the heart.

Our *in vitro* data strongly support our hypothesis, i.e. the increased HBP flux impairs myocardial GLUT4 translocation. We make this statement based on several key findings in our study: 1) Both high glucose treatment and HBP activation resulted in a marked reduction of insulin-mediated myocardial GLUT4 translocation to the sarcolemma. Conversely, high glucose treatment and HBP inhibition restores insulin-mediated myocardial GLUT4 translocation to the sarcolemma. This is in agreement with several other studies using skeletal muscle and adipose tissue (Marshall *et al.,* 1991; Rossetti *et al.,* 1990; Hazel *et al.,* 2004; Arias *et al.,* 2004). 2) Increasing glucosamine administration caused a marked decrease in myocardial GLUT4 translocation to the sarcolemma. This is in agreement with others reporting similar results (Maria G. Buse 2000; Marshall *et al.,* 1991). 3) Over-expression of the HBP rate limiting enzyme (GFAT) led to an attenuation of myocardial GLUT4 translocation. To correct for transfection efficiency, we first observed the fluorescence intensity under lower magnification (20x).

We also selected individual cells under high magnification (60x) and quantified our results using co-localization analysis. We further strengthened our results by synergistically activated HBP, i.e. GFAT over-expression and PUGNAc (HBP activator) treatment. To verify that GFAT was actually the rate limiting enzyme of HBP, we co-transfected our cells with a dominant negative GFAT construct and observed a marked increase in GLUT4 translocation. However, PUGNAc treatment with GFAT over-expression did not further decrease GLUT4 translocation. We

propose that GFAT over-expression leads to increased UDP-GlcNAc, the obligatory donor substrate of OGT, resulting in increased in O-GlcNAcylation of target proteins. The down stream target for increased O-GlcNAcylation due to PUGNAc administration is therefore secondary to GFAT over-expression.

Despite the discovery of O-GlcNAcylation ~ 24 years ago (Torres and Hart. 1984), some researchers are unsure regarding the role of O-GlcNAcylation in the pathogenesis of insulin resistance (Rordorf-Nikolic *et al.,* 1995; Federici *et al.,* 2002; Patti *et al.,* 2002). However, in this study we observed increased O-GlcNAcylation in response to high glucose, PUGNAc administration and GFAT over-expression. Conversely, decreased O-GlcNAcylation was observed with DON administration and transfection studies using a dominant negative GFAT construct. Our data are therefore in agreement with others that have also provided substantial evidence regarding increased O-GlcNAcylation in the pathogenesis of insulin resistance (Maria G. Buse 2000). Furthermore, decreased O-GlcNAc modification improved both the contractile function and intracellular calcium levels in the diabetic myocardium (Hu *et al.,* 2005).

4.3 Conclusion

Our first aim was to establish an *in vitro* fluorescence microscopy- and flow cytometry-based model for visualization and assessment of myocardial GLUT4 translocation using H9c2 cardiac-derived myoblasts. This study successfully established a model for measuring myocardial GLUT4 translocation (fluorescence microscopy) and our experimental system can now be used for multiple studies that assess GLUT4 translocation.

Our second aim was to employ our successfully established *in vitro*-based model to investigate the role of the HBP in myocardial GLUT4 translocation to the sarcolemma. Here we found that high glucose, glucosamine administration and GFAT over-expression all attenuated myocardial GLUT4 translocation. Furthermore, transfection of H9c2 cardiac-derived myoblasts with a dominant negative GFAT construct restores myocardial GLUT4 translocation. Employment of pharmacological HBP modulators underscores these findings. Future studies in our laboratory will now investigate the potential molecular targets involved in diabetic cardiomyopathy. Here

we propose that members of the insulin signaling pathway, e.g. IRS1/IRS2, PI-3 kinase, AKT/PKB, and Munc 18c are all likely candidates to explain attenuated myocardial GLUT4 translocation observed and especially since all of these proteins may be O-GlcNAcylated (Rordorf-Nikolic *et al.,* 1995; Patti *et al.,* 1999; Boehmelt *et al.,* 2000; Federici *et al.,* 2002).

In summary, our study shows that under conditions of nutrient excess (e.g. hyperglycemia, hyperlipidemia) the HBP is chronically activated and that this may have serious consequences for the host organism. It is likely that the HBP becomes dysregulated during the pre-diabetic/early diabetic state and that O-GlcNAcylation of members of the insulin signaling pathway occurs during this stage. This will lead to myocardial insulin resistance, and in the long term, will contribute to the onset of the diabetic cardiomyopathy. Investigations to find unique inhibitors of this maladaptive pathway should therefore result in the development of novel therapeutic agents that will lead to a reduction in the growing global burden of disease for type 2 diabetes and associated cardiovascular diseases.

4.4. References

Abel ED. and Boudina S. (2007) Diabetic cardiomyopathy revisited. Circulation. 2007;115:3213-3223

Arias EB., Kim J. and Cartee GD. (2004) Prolonged incubation in PUGNAc results in increased protein O-linked glycosylation and insulin resitance in rat skeletal muscle. Diabetes, 53, 921-930

Balasubramanyam M., Faooq S., Srinivasan V., Sandhya N., Sampathkumar R. and Mohan V. (2007) Glutamine fructose-6-phosphate amidotransferase (GFAT) gene expression and activity in patient with type 2 diabetes: inter-relationships with hyperglycaemia and oxidative stress. Clinical biochemistry 40(13-14):952-7

Belke DD., Larsen TS., Gibbs EM., Severson DL. Altered metabolism causes cardiac dysfunction in perfused hearts from diabetic (db/db) mice. Am J Physiol Endocrinol Metab 2000;279:E1113

Boehmelt G., Wakeham A., Elia A., Sasaki T., Plyte S., Potter J., Yang Y., Tsang E., Ruland J., Iscove NN., Dennis JW., Mak TW.. Decreased UDP-GlcNAc levels abrogate proliferation control in EMeg32-deficient cells. *EMBO J*. 2000 Oct 2;19(19):5092-104.

Bogan JS., Mckee AE. and Lodish HE. (2001) Insulin-responsive compartments containing GLUT4 in 3T3-L1 and CHO cells: regulation by amino acid concentrations. Mol. Cell. Biol. 21:4785-4806

Bressler R. and Goldman S. (1993) *Cardioscience* 4, 133−142

Bryant NJ., Govers R. and James DE. (2002) Regulated transport of the glucose transporter GLUT4. Nat.Rev.Mol.Cell Biol.3,267-277

Buse MG., Nelson BA. and Robinson KA. (2000) High glucose and glucosamine induce insulin resistance via different mechanisms in 3T3-L1 adipocytes. Diabetes 49(6):981-91

Coleman DL.: Diabetes-obesity syndrome in mice. *Diabetes* 31 (Suppl. 1): 1-6, 1982

Czech MP., Jiang ZY., Chalwa A., Bose A. and Way M. (2002) A Phosphatidylinositol 3-Kinase-independent insulin signaling pathway to N-WASP/Arp2/3/F-actin required for GLUT4 transporter recycling *J. Biol. Chem*, Vol. 277, Issue1, 509-515

DeFronzo RA., Simonson D., Ferranni E. Hepatic and peripheral insulin resistance: a common feature of type 2 (non-insulin –dependant) and type- 1(insulin-dependent) diabetes melitus. *Diabetologia* 23:313-319, 1982

Emoto M., Langille SE. and Czech MP. (2001) A role for kinesin in insulin-stimulated GLUT4 glucose transporter translocation in3T3-L1 adipocytes. *J Biol Chem* 276(14):10677-10682

Federici M., Menghini R., Mauriello A., Hribal ML., Ferrelli F., Lauro D., Sbraccia P., Spagnoli LG., Sesti G., Lauro R. Insulin-dependent activation of endothelial nitric oxide synthase is impaired by O-linked glycosylation modification of signaling proteins in human coronary endothelial cells. *Circulation*. *2002;106:466*

Garvey WT., Hardin D., Juhaszova M. and Dominguez JH. (1993) *Am. J. Physiol.* **264**, H837−H844

Garvey WT., Hardin ED., Juhaszova M., Dominguez JH. (1993) Effects of diabetes on myocardial glucose transport system in rats: implications for diabetic cardiomyopathy. *Am J Physiol* 264:H837–H844

Gertz EW., Wisneski JA., Stanley WC., and Neese RA. (1988) Myocardial substrate utilization during exercise in humans. Dual carbon-labeled carbohydrate isotope experiments. *J Clin Invest* 82: 2017–2025,

Hazel M., Cooksey RC., Jones D., Parker G., Neidigh JL., Witherbee B., Gulve EA., McClain DA. (2004) Activation of the hexosamine signaling pathway in adipose tissue results in decreased serum adiponectin and skeletal muscle insulin resistance. *Endocrinology* 145:2118-2128

Hirayama H., Sugano M., Abe N., Yonemoch H., Makino N. (2001) Troglitazone, an antidiabetic drug, improves left ventricular mass and diastolic function in normotensive diabetic patients. *Int J Cardiol* 77:75–79

Hollenbeck CB., Chen YI., Reaven GM. (1984) A Comparison of the relative effects of obesity and non-insulin-dependent diabetes mellitus on in vivo insulin-stimulated glucose utilizaion. *Diabetes* 33:622-626

Holman GD., Clark JF., Young PW., Yonezawa K. and Kasuga M. (1994) Inhibition of the translocation of GLUT1 and GLUT4 in 3T3-L1 cells by the PI 3-kinase inhibitor, Wortmannin. *Biochem. J*. 300, 631-635

Hu Y., Belke D., Suarez J., Swanson E., Clark R., Hoshijima M., Dillmann WH. Adenovirus mediated overexpression of O-GlcNAcase improves contractile function in the diabetic heart. *Circ Res.* 2005; 96: 1006–1013.

Kim JH., Stewart TP., Zhang W., Kim HY., Nishina PM. and Naggert JK. (2005) Type 2 diabetes mouse model TallyHo carries an obesity gene on chromosome 6 that exaggerates dietary obesity. *Physiological Genomics* **22** 171–181

Kolterman OG., Gray RS., Griffin J., Burstein P., Insel J., Scarlett JA., Olefsky JM. Receptor and postreceptor defects contribute to the insulin resistance in non-insulin-dependent diabetes mellitus. *J Clin Invest* 68:957-969, 1981

Kraegen EW., Sowden JA., Halstead MB, Clark PW., Rodnick KJ, Chisholm DJ. and D.E James DE. (1993) Glucose transporters and in vivo glucose uptake in skeletal and cardiac muscle: fasting, insulin stimulation and immunoisolation studies of GLUT1 and GLUT4. *Biochem J* 295: 287–293,

Li D., Randhawa VK., Patel N., Hayashi M. and Klip A. (2001) Hyper-osmolarity reduces GLUT4 endocytosis and increases its exocytosis from a VAMP2-independent pool in 16 muscle cells. *J Biol Chem* 276:22883-22891

Litwin SE., Raya TE., Anderson PG., Daugherty S., Goldman S. Abnormal cardiac function in the streptozotocin-diabetic rat. Changes in active and passive properties of the left ventricle. *J Clin Invest* 1990, 86(2)**:**481-488.

Malide D., Ramm G., Cushman SW. and Slot JW. Immunoelectron microscopic evidence that GLUT4 translocation explains the stimulation of glucose transport in isolated rat white adipose cells. *J Cell Sci*. 2000;113:4203-4210.

Marshall S., Bacote V., Traxinger R.R. Discovery of a metabolic pathway mediating glucose-induced desensitization of the glucose transport system. Role of hexosamine biosynthesis in the induction of insulin resistance. *J Biol Chem* (1991) 266:4706–4712.

McClain DA. Hexosamines as mediators of nutrient sensing and regulation in diabetes. *J Diabetes Complications* 16: 72–80, 2002

McClain DA., Zhou J., Neidigh JL., Espinosa R, Lebeau MM. (1995) Human glutamine:fructose-6-phosphate amidotransferase: Characterization of mRNA and chromosomal assignment to 2p13. *Human Genetics* 1995:96(1):99-101

Michael MD., Winnay JN., Curtus SE., et al: Liver –specific insulin receptor knockout mice are several insulin resistant [Abstract 0040]. 59th Annual Scientific Session of American Diabetes Association, San Diego, CA, 1999.

Nielsen TT., Botker HE., Moller N., Bagger JP. and Schmitz O. (1997) Myocardial insulin resistance in patience with syndrome X. *J Clin Invest*. 1997; 100(8): 1919-1927

Olson AL., Trumbly AR., and Gibson GV. (2001) Insulin-mediated GLUT4 translocation is dependent on the microtubule network. *J Biol Chem* 276: 10706-10714

Pak Y. and Ha H. (2005) Modulation of the caveolin-3 and Akt status in caveolae by insulin resistance in H9c2 cardiomyoblasts. *Experimental and Molecular Medicine*. Vol 37. No. 3, 169-178

Patki V., Buxton J., Chalwa A., Lifshitz L., Fogarty K., Carrington W., Tuft R. and Corvera S. (2001) Insulin action on GLUT4 traffic visualized in single 3T3-L1 adipocytes by using ultra-fast microscopy. *Mol. Biol. Chem* 12:129-141

Patti ME. Nutrient modulation of cellular insulin action. *Ann N Y Acad Sci*. 1999 Nov 18;892:187-203.

Ralston E. and Ploug T. (2002) Exploring the whereabouts of GLUT4 in skeletal muscle (review). *Mol.Membr.Biol* 19, 39-49

Rordorf-Nikolic T., Van Horn DJ., Chen D., White MF., Backer JM. Regulation of phosphatidylinositol 3'-kinase by tyrosyl phosphoproteins. Full activation requires occupancy of both SH2 domains in the 85-kDa regulatory subunit. *J Biol Chem*. 1995 Feb 24;270(8):3662-6.

Rossetti L, Giaccari A, DeFronzo RA. Glucose toxicity. *Diabetes Care* 13: 610–630, 1990

Satoh S., Nishimura H., Clark AE., Kozka IJ., Vannucci SJ., Simpson IA., Quon MJ., Cushman SW. and Holman GD. (1993) Use of bis-Mannose photolabel to elucidate insulin-regulated GLUT4 subcellular trafficking kinetics in rat adipose cells: Evidence that exocytosis is a critical site of hormone action, *J. Biol. Chem.* 268, pp. 17820–17829.

Semeniuk LM., Kryski AJ., Severson DL. Echocardiographic assessment of cardiac function in diabetic db/db and transgenic db/db-hGLUT4 mice. *Am J Physiol Heart Circ Physiol*. 2002;283:H976-H982.

Shapiro LM., Howat AP., Calter MM. Left ventricular function in diabetes mellitus. I: Methodology, and prevalence and spectrum of abnormalities. *Br Heart J.* 1981 Feb;45(2):122–128

Slot JW., Geuze HJ., Gigengack S., Lienhard GE. and James DE. (1991) Immuno-localization of the insulin regulatable glucose transporter in brown adipose tissue of the rat. *J. Cell Biol*. 113, 123-135

Stephens, JM; Pilch, PF. The metabolic regulation and vesicular transport of GLUT4, the major insulin-responsive glucose transporter. *Endocr Rev.* 1995 Aug;16(4):529–546.

Torres C., Hart GW. Topography and polypeptide distribution of terminal N-acetylglucosamine residues on the surfaces of intact lymphocytes. Evidence for O-linked GlcNAc. *J Biol Chem.* 1984; 259: 3308–3317

Van Hoeven KH. and Factor SM. A comparison of the pathological spectrum of hypertensive, diabetic, and hypertensive-diabetic heart disease. *Circulation* **82**, 848−855 (1990).

Wyse BM, Dulin WE: The influence of age and dietary conditions diabetes in the db mouse. *Diabetologia* 6:268-273, 1970

Zimmet P., Alberti KG. and Shaw J. (2001) Global and societal implications of the diabetic epidemic. *Nature*. 414: 782-787

Zisman A., Peroni OD., Abel ED et al: Muscle specific knock-out of GLUT-4 results in glucose intolerance and insulin resistance [Abstract 0043]. 59th Annual Scientific Session of American Diabetes Association, San Diego, CA, 1999